MEASUREMENT OF OPERATIONAL VARIABLES
IN A HYDROCYCLONE

MEASUREMENT OF OPERATIONAL VARIABLES

IN A HYDROCYCLONE

by

W. O. Witbeck, B.A.Sc.

A Project Report

Submitted to The Faculty Of Graduate Studies
In Partial Fulfillment Of The Requirements
For The Degree
Master Of Engineering

McMASTER UNIVERSITY

OCTOBER 1972

ACKNOWLEDGEMENTS

I would like to express my thanks to Dr. D.R. Woods who gave most generously of his time and whose enthusiasm and helpful suggestions were never exhausted.

The invaluable advice of T.E. Pollock, Dr. J. McGregor and A.J.S. Liem are gratefully acknowledged.

My thanks are also due to the financial assistance from an N.R.C. grant.

Lastly, the long hours and patience afforded by my typist and wife, Dinny, are sincerely appreciated.

Wayne Witbeck

W. O. Witbeck

Hamilton, October 1972.

ii

MASTER OF ENGINEERING
(Chemical Engineering)

TITLE: Measurement of Operational Variables in a Hydrocyclone

AUTHOR: W. O. Witbeck, B.A. Sc. (University of Toronto)

SUPERVISOR: Dr. D. R. Woods

NUMBER OF PAGES: 74

SCOPE AND CONTENTS:

Energy loss was measured across a 3.0 inch hydrocyclone operating with and without an air core.

The separational efficiency, as indicated by the $(Dp)50$ diameter, was measured as a function of feed concentration, feed flow rate and volume split.

This $(Dp)50$ "cut size" was obtained from mass balances on the total solids and particle size distributions for the feed, overflow and underflow.

TABLE OF CONTENTS

LIST OF FIGURES

LIST OF TABLES

CHAPTER 1

INTRODUCTION

1.1 BACKGROUND

The gas cyclone has been used in industry for many decades for separating particulate matter from gaseous streams. Its inherant economy of design and relatively maintenance free operation have earned an easily spotted place of prominence on many a manufacturer's roof.

Although its "effluent", in many cases, is not as pure as future air quality standards are likely to demand, it might well survive for quite some time as an inexpensive "primary purifier".

The liquid cyclone, or "hydrocyclone" did not really gain any mentionable industrial use until the late 1930's when its use at the Dutch State Mines gained for it a permanent place as a process tool. This first extensive application was the separation of small pieces of coal from shale by use of a "heavy medium" slurry of water and sand.

As one would expect, the present day understanding of hydro-cyclone design has grown from almost nil in the late thirties to some reasonably complete design procedures advanced by Rietema (1961) and Lilgé (1962).

In the process of developing the modern hydrocyclone theory, researchers discovered that its great advantage of being physically simple was not balanced by simple behavioural analysis. Predicting the performance of the hydrocyclone can still be classed as a rather "grey" area.

The reasons for this lack of complete theoretical correlation, which is necessary to predict physical separation efficiency from known operational quantities, are twofold. One, paradoxically, lies in its own

simplicity of operation. A feed to be separated is forced to enter the cyclone (in this paper synonymous with hydrocyclone) tangentially and hence the fluid mixture is forced into a spiral motion about the axial axis. (see Figure 1.) Since the circular cross-sectional area decreases from feed inlet to the underflow outlet, the law of conservation of angular momentum demands that the tangential velocity must greatly increase as a smaller and smaller diameter is encountered. This fast spinning motion creates a high centripetal force on all elements of fluid and heavier particulates in the cyclone, the latter being preferentially thrown to the cyclone wall where downward bulk motion eventually carries them out the underflow. To build up a reliable theoretical understanding requires extensive knowledge of this internal three dimensional flow pattern; the measurement of this pattern has proven to be a difficult, time consuming task. Large discrepancies among results still exist.

A second reason for the lack of complete theoretical design and operational efficiency correlations is that the cyclone is most often called upon to separate distributions of particulates. These distributions in themselves are very difficult to characterize by their size and their properties in a fluid, the latter owing to variations in shape, size, surface properties and density. If, indeed, a set of parameters is generated to characterize all the above particulate properties of some input distribution, we are further required to develop a general "transfer function model" for the standard shapes of hydrocyclones to completely forecast which particles will appear at the overflow and which ones at the underflow. Such a model might be mechanistic but unlikely. Its elements would be comprised of physical cyclone dimensions, inlet and outlet velocities and fluid properties. When the feed characterization model is substituted into the cyclone transfer function model, the complete characterization

2

model for both output streams would result. This has been impossible so far and such a general model will likely never be developed without extensive empirical evaluation of a host of operational factors. Some of the present day empirical design methods, such as those advanced by Lilgé (1962), do permit the optimization of a cyclone shape, but only for the range of conditions under which the correlations were derived.

1.2 HOW CLOSE HAS PRESENT RESEARCH COME TO THIS IDEAL CASE?

Researchers have long looked toward a sound knowledge of the equations of motion as being the key to a fundamental understanding of operation design. Rietema (1962) has formulated theoretical equations from assumptions based on Kelsall's (1952) experimental profiles. This was done for cyclones operating with an aircore and have inherent inconsistancies. Ohasi and Maeda (1958) provide other data which contradict Kelsall's data, in particular the radial velocity profiles.

To eludicate this, and to obtain data for cyclones operating without an air core, Knowles (1971) measured velocity profiles with a high speed cinematic technique.

An objective of the present work is to complement our knowledge of velocity profiles with actual separational efficiency data. This could form the basis for subsequent theoretical analysis.

Traditional research done in an effort to predict a cyclones' efficiency involves the estimation of a parameter called (Dp)50. This being the size of particle which reports 50% to the overflow, and 50% to the underflow. There are at least eight correlations for (Dp)50. Most of these have the general form $(Dp)50 = f(X, n, Q, \sigma, \rho)$

where   X = one or more dimensional parameters

n = kinematic viscosity of feed slurry

3

Q = feed flow rate

σ = density of solids or liquids to be separated

ρ = density of the liquid carrier medium

Four of the eight correlations empirical and four are semi-empirical.

Since Bradley (1957), Kelsall (1952) and Lilgé (1962) represent the expected separation to be that of Figure 2, then (Dp)50 would seem to completely define the performance of any cyclone for which the input feed size distribution, and the (Dp)50 were known.

Three basic theoretical basic methods have been used to arrive at (Dp)50. These will be discussed in the following section.

1.3   DETERMINATION OF (Dp)50 BY EQUILIBRIUM ASSUMPTIONS

A theoretical approach taken by Bradley (1957), Lilgé (1962) and Kelsall (1952) is one of equilibrium envelopes for all feed particle sizes. The necessary assumptions are;

a) turbulance is negligible

b) the velocity in the radial direction is described by Stokes' Law

c) the radial velocity of the fluid, Vr is constant at the locus of zero axial velocity ($V_z=0$)

d) all the particles radial velocities should become zero when the outward centrifugal force is just balanced by an inward Stokes' correlatable drag force caused by the inward bulk fluid flow. Different sized particles should assume different sized equilibrium positions immediately upon entry into the cyclone.

e) there is negligible short circuiting, recycle or hindered discharge, all of these are shown in Figure 3.

4

f) the velocity distributions measured for specific geometrical configurations are generally applicable.

Assumption (c) would seem to be the one with the least proof of validity, although Bradley (1965) does show photographs of dye injection studies where a definite zero axial velocity "mantle" is established. This "mantle", however, only extends from the top of the cyclone to roughly one-third down the conical section, thus maintence of a locus where both $V_z = 0$ and $V_r = \text{CONST}$ are true, is debatable.

Since the velocity profiles in cyclones are not agreed upon (again because they are experimentally hard to measure), the $(Dp)50$ correlations given by different investigators do not agree. For example, Bradley's equation based on Bradley's impression of the location of the zero velocity mantle is:

$$(Dp)50 = 3.2\,(0.43)^n \frac{D_1^2}{\alpha} \left[\frac{\mu\left(1 - \frac{Q_3}{Q_1}\right)\tan\theta/2}{DQ_1\,(\sigma - \rho)} \right]^{.5}$$

D = diameter of cyclone

n = correlating index to describe tangential fluid velocity as a fn. of radial location most often $V_t R^{0.8} = \text{const.}$
when $Re_{inlet} \quad 4.0 \times 10^4$

$\alpha = \dfrac{\text{periferal velocity}}{\text{ave. vel. in inlet}}$

σ = density of bulk fluid

ρ = density of solid or liquid to be separated

μ = dynamic viscosity of bulk fluid

θ = cone angle

Q_1, Q_3 = flow rate of feed, underflow

Lilgé's theoretical equation is given by

$$(Dp)50 = \frac{\varrho}{2(\sigma - \varrho)} \cdot \left[\frac{316.6 \, Q_1}{D.h} \, (1 - Q_3 \, Q_1) \right]^2 \frac{R_m}{V_m} \cdot C_d$$

$$V_m \, R_m^{0.8} = V_e R_e^{0.8}$$

$$V_e = 5.31 \, V_1 \, (\tfrac{A}{A_1}) \, .565$$

A, A_1 is cross sectional area of cyclone, feed

R_e, V_e is radius, velocity at feed centre line

R_m, V_m is radius, velocity of V_r = const. mantle

It is interesting to note that Burrill (1967) has compared the predicted $(Dp)50$ values for six different correlations and for similar operating conditions the above mentioned equation of Bradley predicts a $(Dp)50$ of 54 microns, whereas Lilgé's predicts 10.4 microns. From this, it would seem that a designer would not be able to choose between two very different designs, without having any apriori laboratory knowledge.

1.4 RIETEMA'S DYNAMIC MODEL FOR (Dp)50 CORRELATION

Another semi-empirical derivation that deserves mention is that of Rietema (1962), who proposes a dynamic theory rather than the previous equilibrium envelope theory. In this theory, Rietema reasons that because separation efficiency must be some function of tangential velocity, then it must also be a function of the pressure drop across the cyclone. A fact which one logically accepts since pressure drop and tangential velocity must be related.

Particles with a stability radius smaller than the overflow nozzle radius may very well be separated towards the outer wall before they have reached their stability radius. Note that the reverse of this

6

assumption was necessary to build the previously mentionned stable envelope theory.

Rietema's derivation is based on several assumptions:

a) the turbulent eddy diffusion has a negligible effect on the separation: this Rietema proves in another paper.

b) the Reynolds number as related to the particles separated is so low that Stokes' Law for free terminal velocity applies.

c) the axial velocity of the particles equals the axial fluid velocity and both are constant.

d) the cyclone has no cylinder, it has only a conical section.

e) an air core develops

f) no short circuit, no hindered discharge and no recirculation takes place.

A particle that enters the cyclone on the centreline of the inlet and just reaches the cyclone wall by the time it arrives at the underflow apex (see Figure 4), will be (Dp)50. Any particles of that same size that enters the cyclone nearer the outside wall than the centerline will exit via the underflow. Similar sized particles entering closer to the center axis of the cyclone will leave by the overflow. To identify the size of (Dp)50, Rietema calculates what Stokes' sized particle could just travel a distance of $D_{inlet}/2$ relative to the cyclone wall. The path of such a particle is shown in Figure 4. One weakness in this theory would seem to be that the underflow fluid with its entrained solids exit through an infinitely small annulus. In actual fact, the (Dp)50 particle Rietema describes could still exit through the underflow and have travelled some distance.

$$\frac{D_{inlet}}{2} - U$$

where U is defined as the distance between the cyclone wall and the liquid-

air core interface, where both are measured at the underflow apex. It is likely that U is quite signifigant compared to $D_{in}/2$ thus introducing a possible error.

The derivation is worth reviewing because it introduces Rietema's design parameter Cy50.

If Vr is the outward velocity of a particle in the radial direction relative to the inward radial fluid flow velocity and T is the residence time of (Dp)50 particle entering on the inlet centerline, then,

$$\frac{D_{inlet}}{2} = \int_0^T Vr \cdot dt$$

Stokes' Law defines this velocity of the particle as

$$Vr = \frac{Vt^2}{r} \cdot \frac{(Dp)50 \, (\sigma - \rho)}{18\mu}$$

where Vt is the particle's tangential velocity and since $Va = \frac{dVa}{dt}$, then the axial velocity is assumed constant and equal to the axial fluid velocity.

$$dt = \frac{dVa}{Va}$$

$$dt = \frac{1}{Va} \cdot \frac{L}{R} dr$$

therfore $$\frac{D_{inlet}}{2} = \int_0^R \frac{[(Dp)50]^2 \, (\sigma - \rho)}{18\mu} \cdot \frac{Vt^2}{r} \cdot \frac{1}{Va} \cdot \frac{L}{R} \cdot dr$$

$$= \frac{[(Dp)50]^2 \, (\sigma - \rho) \, L}{18\mu \, Va \, R} \int_0^R \frac{Vt^2}{r} dr$$

and $$\int_0^R \frac{Vt^2}{r} \cdot dr = \frac{\text{static pressure drop}}{\rho}$$

so $$\frac{D_{inlet}}{2} = \frac{[(Dp)50]^2 \, (\sigma - \rho) \, L}{18\mu \, Va \, R} \cdot \frac{\Delta P_{static}}{\rho} \qquad (1)$$

8

Since Rietema also assumes that there are negligible entrance and exit losses, then $\Delta P_{static} = \Delta P$ total; ie. the static pressure difference between inlet and overflow is about the same as the total energy difference between the same two points.

Dividing both sides of equation 1 by the total volumetric flow

yields: $\quad Q_1 = V_1 \dfrac{D_{inlet}^2}{4}$

gives $\dfrac{(Dp)50^2 \Delta \rho L \Delta P \text{ total}}{\mu \cdot \rho \cdot Q_1} = \dfrac{36 \, Va \, R}{\pi \, V_1 \, D_1}$

where the subscript $_1$ equals inlet.

Rietema (1961) asserts that for any cyclone at some operating inlet velocity, the R.H.S. is approximately constant; he terms this Cy50.

Also there is a certain linear relationship between the axial velocity and the inlet velocity such that

$$Va = C_1 V_1 = C_1 \dfrac{4 \, Q}{\pi \, D_1^2}$$

therefore the R.H.S. becomes a function of only cyclone dimensional parameters and the inlet or axial velocity ratio, thus Cy50 is a dimension-less constant for any fixed cyclone.

After numerous experiments of determining Cy50 numbers for several cyclones under different conditions, Rietema found that the best separation efficiency occurred when the Cy50 number was the lowest at approximately 3.5 .

The term Cy50 was determined by measuring the over and underflow solid concentrations along with their respective particle size distributions, the latter being done by a "standard sedimentation analysis". From this information (Dp)50 could be determined and Cy50 found once the pressure drop across the cyclone was measured.

Rietema then developed a design method for cyclone from contours of constant Cy50 as shown in Figure 5. This figure shows what inlet and

overflow to cyclone diameter ratios should be used for optimum performance.

1.5 METHODS OF DETERMINING PARTICLE SIZE DISTRIBUTIONS

An accurate determination of feed overflow and underflow particle size distributions is required to estimate $(Dp)50$ and to predict the removal efficiency of all other sized particles in the feed. There are many standard methods available, only one of which would be used in this study. These include sieving, sedimentation techniques, photo-extinction and optical methods.

a) Sieving

This technique cannot be used for the size range employed in this study (1 - 30 microns).

b) Sedimentation Techniques

i) Hydrometer technique

When a particle is left undisturbed in a fluid medium in a gravitational field, it will sink with increasing velocity until it reaches some limiting terminal velocity. Should the fluid viscosity and the density difference between the particle be such that the particle falls in the viscous flow regime, then Stokes' Law will predict its time rate of fall.

By also timing the rate of decrease in density of the initially quiescent particle-fluid mixture, a cumulative weight under size distribution can be calculated. (see Herdan (1960) for detailed description)

This method was not used in this study because of inherent difficulties in obtaining the required accuracy. Herdan points out that this technique is a "very simple

method of analysis which has some application for rough purposes but is liable to large errors". These errors arise from surface tension at the stem of the hydrometer, particles settling on the shoulder of the bulb, and the considerable length of bulb as compared with the total test column height. Other papers on the hydrometer method are those of Rossi and Baldacci (1951) and Blake (1949).

ii) An improvement on the hydrometer method has been proposed by Berg (1940) who uses small immersable "divers" which indicate a specific density reading at a certain depth. Accuracy is much improved by this method.

iii) The pipette method is probably the most popular and widely used technique. It has been standardized by many laboratories for the routine control of powdered materials. A precision in the order of $\pm$ 1% is a reasonable expectation according to Herdan.

c) The photo-extinction method involves more sophisticated equipment and is not recommended unless large numbers of distributions are to be analysed. Its principle, however, is very simple as the decrease in turbidity with time is used to indicate the mass concentration depletion at a certain level in the sedimentation vessel.

d) Microscopic measurement is a direct observation method which requires the counting of many particles to obtain a representative sample. While it does have the advantage of allowing the experimenter to accurately define the size of a particle, it suffers from one main drawback, that being the minuteness of the field of observation. The usual

procedure is to prepare a slide on which is placed a representative sample of particles. This sample is most conveniently prepared by agitating a mixture of the particles under consideration and some fluid. The difficulty, as Herdan (1960) points out, is that with a very small field of view, comprising only an infinitesimal portion of the total slide area, conditions of perfect mixedness are not likely to exist. As the slide dries the conditions of perfect uniformity are destroyed. It is then almost impossible to create anything close to micro-mixedness by pushing the particles back and forth on the slide.

1.6   THE OBJECTIVES OF THIS STUDY

The laboratory measurement of (Dp)50 is vitally important to Rietema's design ratios $\frac{e}{D}$ and $\frac{b}{D}$. Equally, it is essential in the estimation of extraction efficiency, Cy50 and in the production of a reduced efficiency curve such as proposed by Yoshioka and Hotta (1955).

Neither Dahlstrom, (1949) using a hydrometer technique, nor Rietema, who employs a standard sedimentation method, have clearly defined what error they expect in their respective (Dp)50 calculations.

The purpose of this work is to:

1) Measure - (Dp)50

> - removal efficiency (as defined by Rietema and Tengbergen-1961)
> - energy loss across cyclone

as a function of feed flow rate and volume split in a cyclone operating with and without an air core.

2) Compare energy losses with those of Rietema (1962)

3) Evaluate the existing $(Dp)50$ correlations by their ability to predict the values obtained experimentally in this study.

4) Obtain separational efficiency data for the same conditions Knowles (1971) used when he measured velocity profiles.

overflow (stream 2)

feed (stream 1)

underflow (stream 3)

Axis Subscripts

r (radial)

t (tangential)

z or a (axial)

14
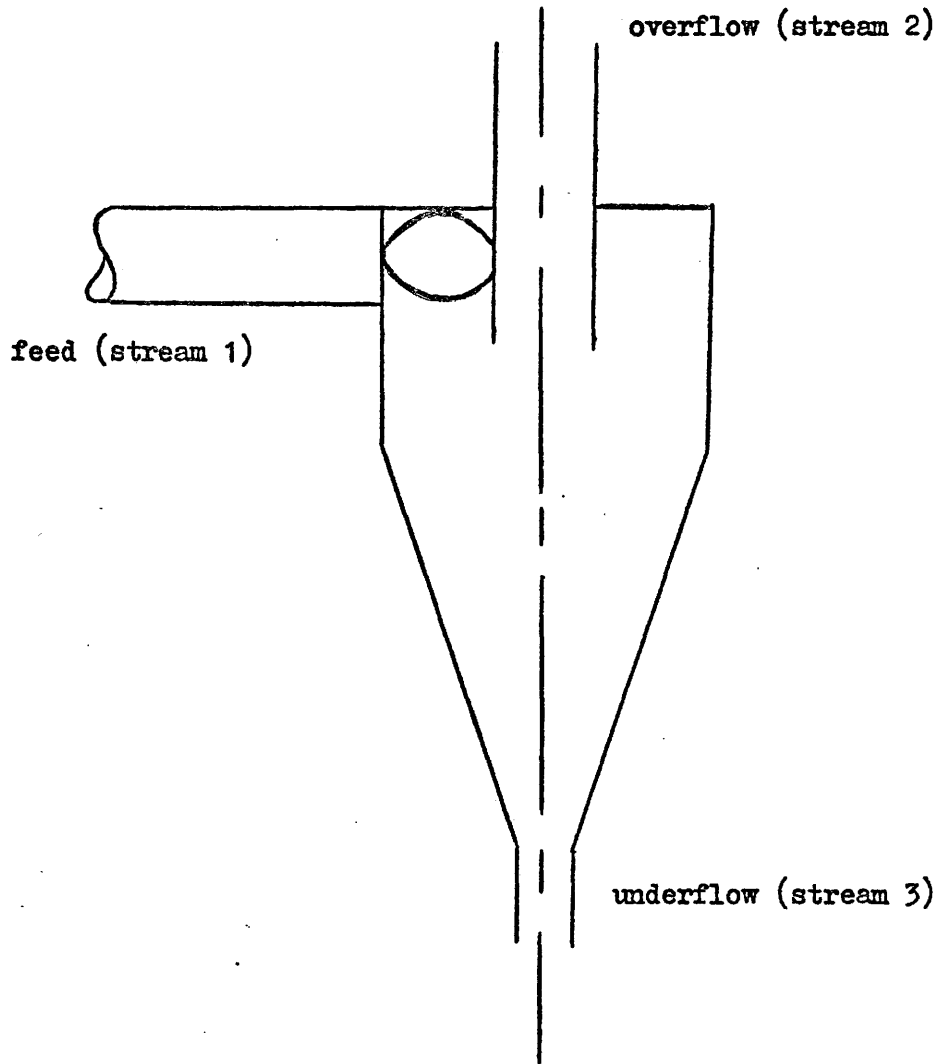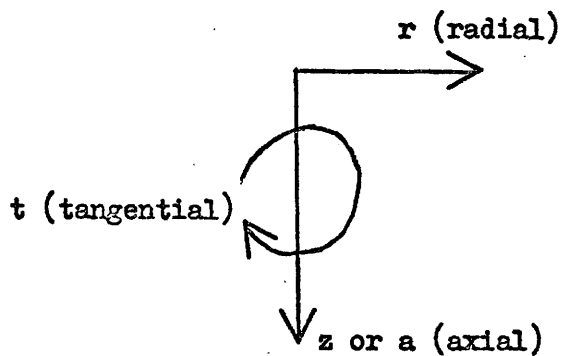
Figure 1-2

Expected and Observed Particle Size Classification
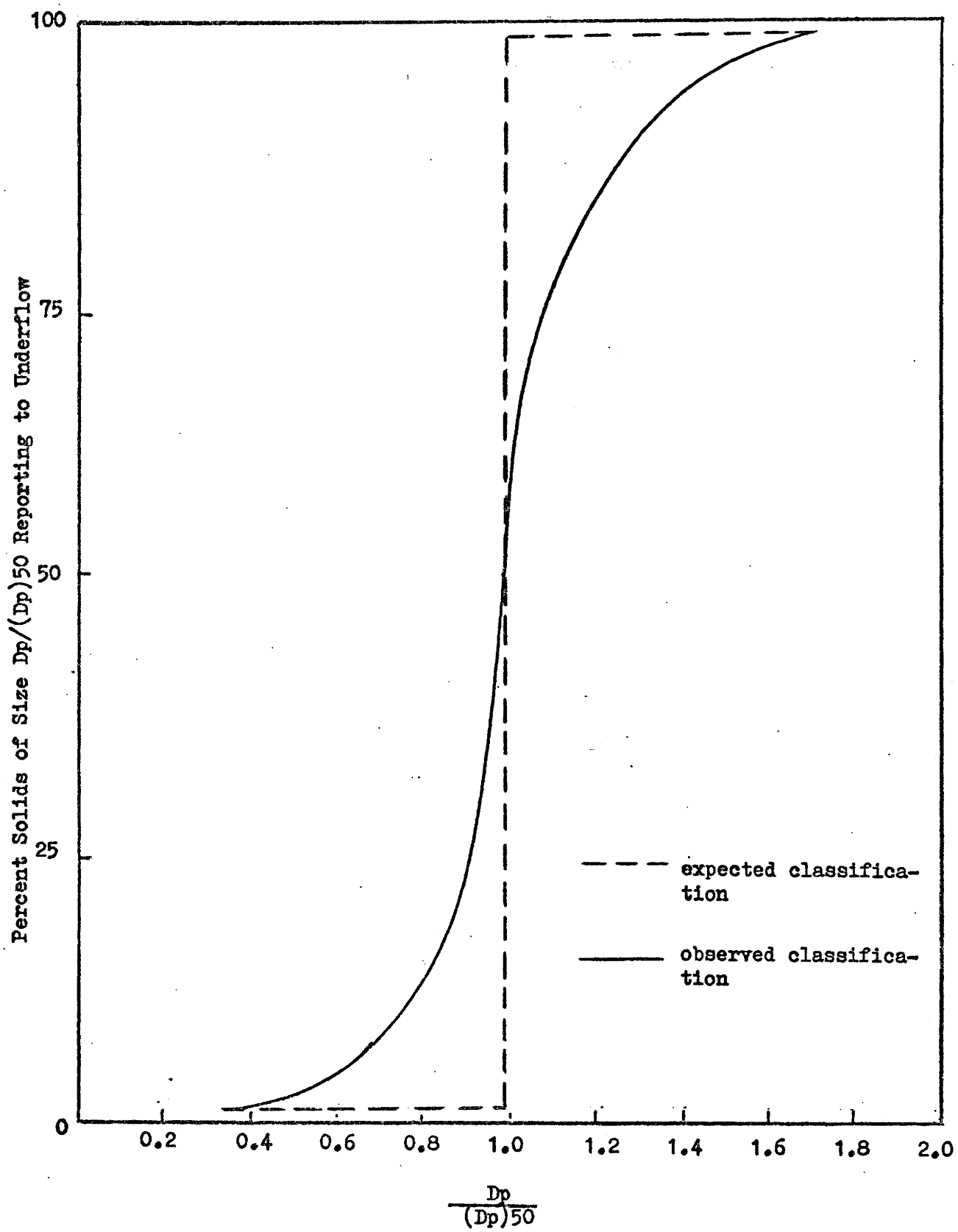
Figure 1-3

Mechanisms in a Hydrocyclone
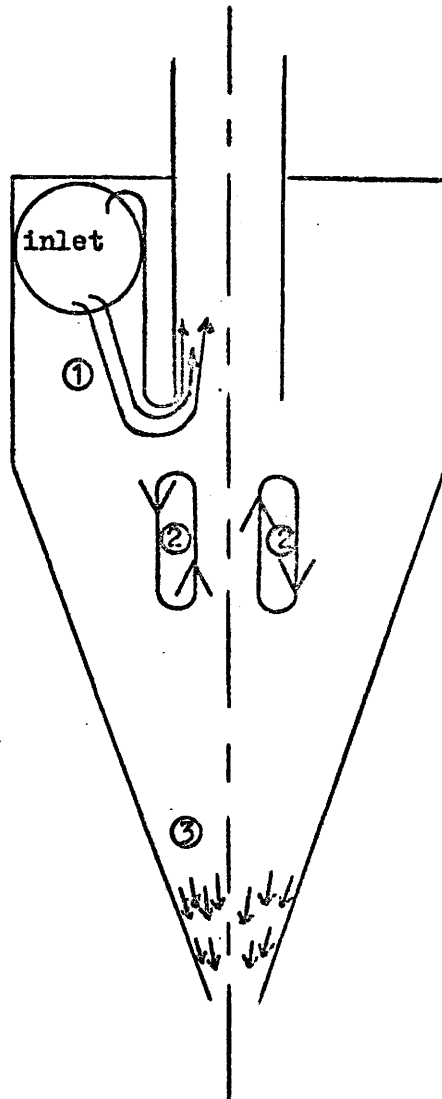
① short circuiting
② recirculation
③ hindered discharge

Figure 1-4

Mathematical Model Proposed

by Rietema (1961) for (Dp)50 to underflow
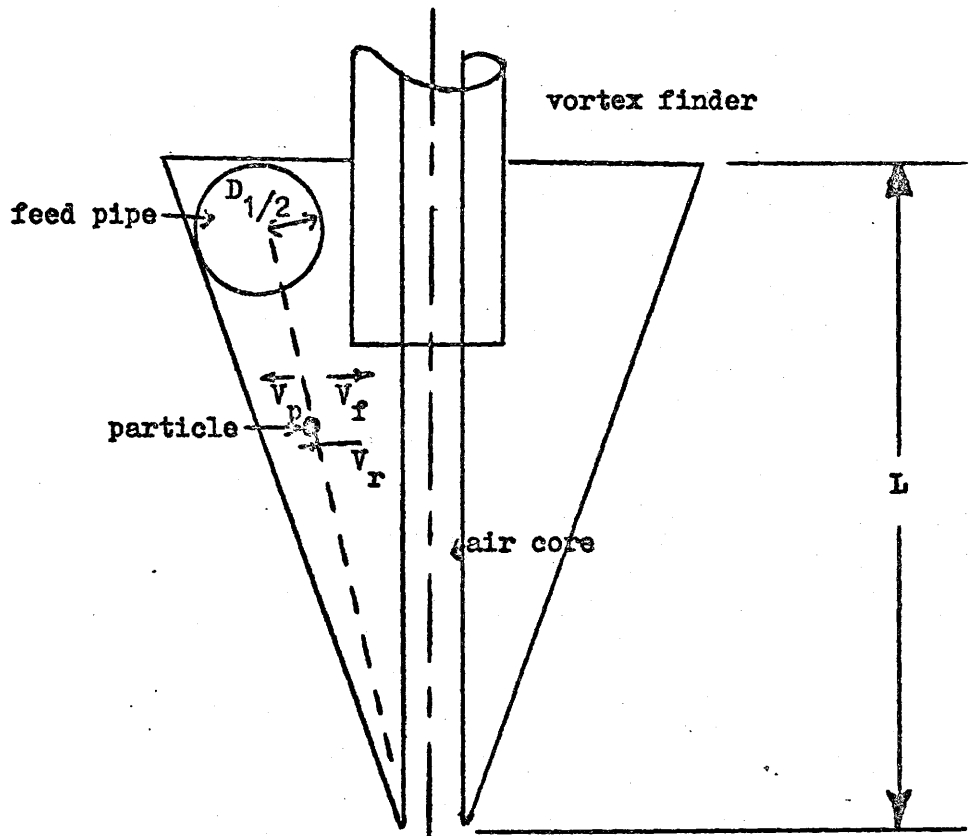
V_f = inward radial velocity of fluid

V_p = outward velocity of particle relative to cyclone wall

V_r = relative outward velocity of particle to fluid

17

Figure 1-5

Contours of Constant Cy_{50} for $L/D = 5$

from Rietema (1961)

b = inlet diameter
e = overflow diameter
D = cyclone diameter

18
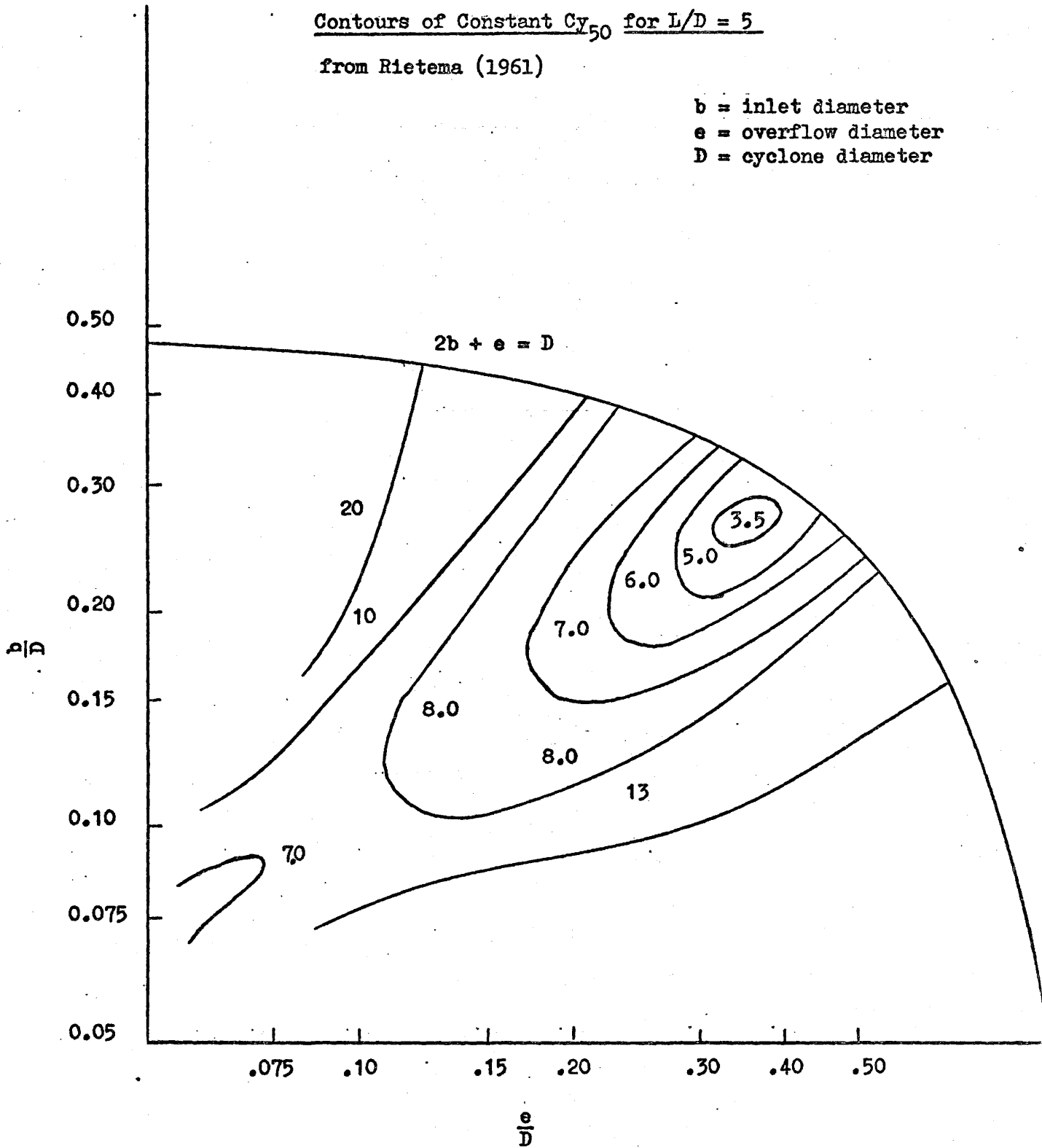
EXPERIMENTAL

The variables studied are listed. The apparatus used, the calibration and measurement techniques, and procedure are discussed. During the preliminary screening runs, some measurement techniques were found to be inappropriate, and hence the equipment was changed.

2.1 Variables Studied

Table 21 lists the dependent and independent variables studied. The range of variables was selected to agree with those chosen by Knowles (1971) in his measurement of velocity profiles and to take advantage of the flexibility of the apparatus.

TABLE 2-1

VARIABLES STUDIED IN THIS WORK						
Dependent Variables \ Independent Variables	WITH AIR CORE			WITHOUT CORE		
	Feed Flow (Reinlet)	Volume Split (V/S)	Feed Concentration	Feed Flow	Volume Split	Feed Conc.
Energy per unit mass ($\Delta E/M$)	3 - 13 USGPM	*	*	range 3 - 13 USGPM	range 1 : 1 to 4 : 1	
Separation Efficiency Indicator $(Dp)50$	*	*	*	range 7-10 USGPM	range 2.4:1 6.2:1	range 850 ppm 2265 ppm
* Limited experimentation was possible. See Chapter 3 for details.						

The feed slurry was maintained at room temperature, which was $20^{o}C \pm 2C^{o}$ for the energy loss studies and $29^{o}C \pm 2C^{o}$ for the (Dp)50 correlations which were performed later in the summer.

2.2 Apparatus Used

The schematic diagram of overall layout is shown in Figure 2-2. The overall system has three sections: the cyclone, the feed preparation and recycle system. A three inch glass cyclone, designed and used by Knowles (1971), is shown in Figure 2-1.

In the feed preparation system, two high speed propeller mixers were so located to give uniform particle concentration in the feed. The feed flowrate was metered through a calibrated rotameter. Samples could be taken from the reservoir, from a tee in the feed line or from combining in one sample the overflow and underflow streams.

The feed pressure was maintained at a fairly constant 30 P.S.I.G. by the two 3450 R.P.M., 1 H.P. centrifugal pumps connected in series.

Tap water at room temperature was used. The glass beads have a reported specific gravity of 2.65 and are available from the Minnesota Mining and Manufacturing Co., St. Paul, Minnesota. Special procedures were required for insertion of these beads into the feed water, details are given in the appendix.

Nearly complete mixedness was maintained in the 50 U.S. gallon resevoir by two 1725 R.P.M., $\frac{1}{4}$ H.P., high speed mixers.

Mass measurements were performed with a Sartorius balance, model 2642, which afforded a digital readout of weight accurate to one ten-thousandth of a gram.

Figure 2-1

Cyclone Dimensions *

Plan View

0.49   1.02

Vertical Section

0.84

1.20   2.00   15.0
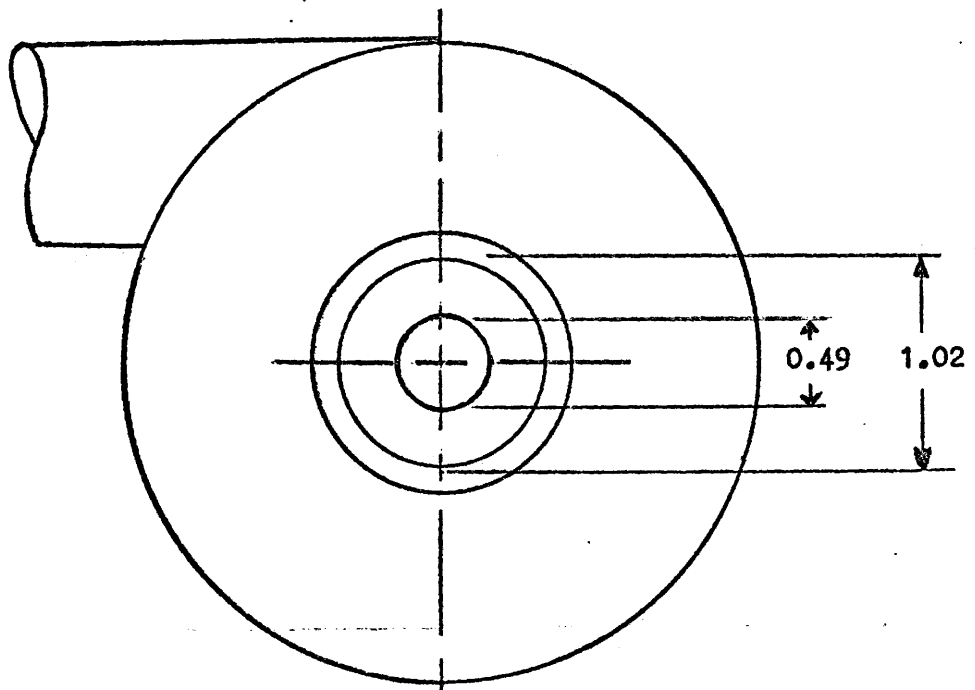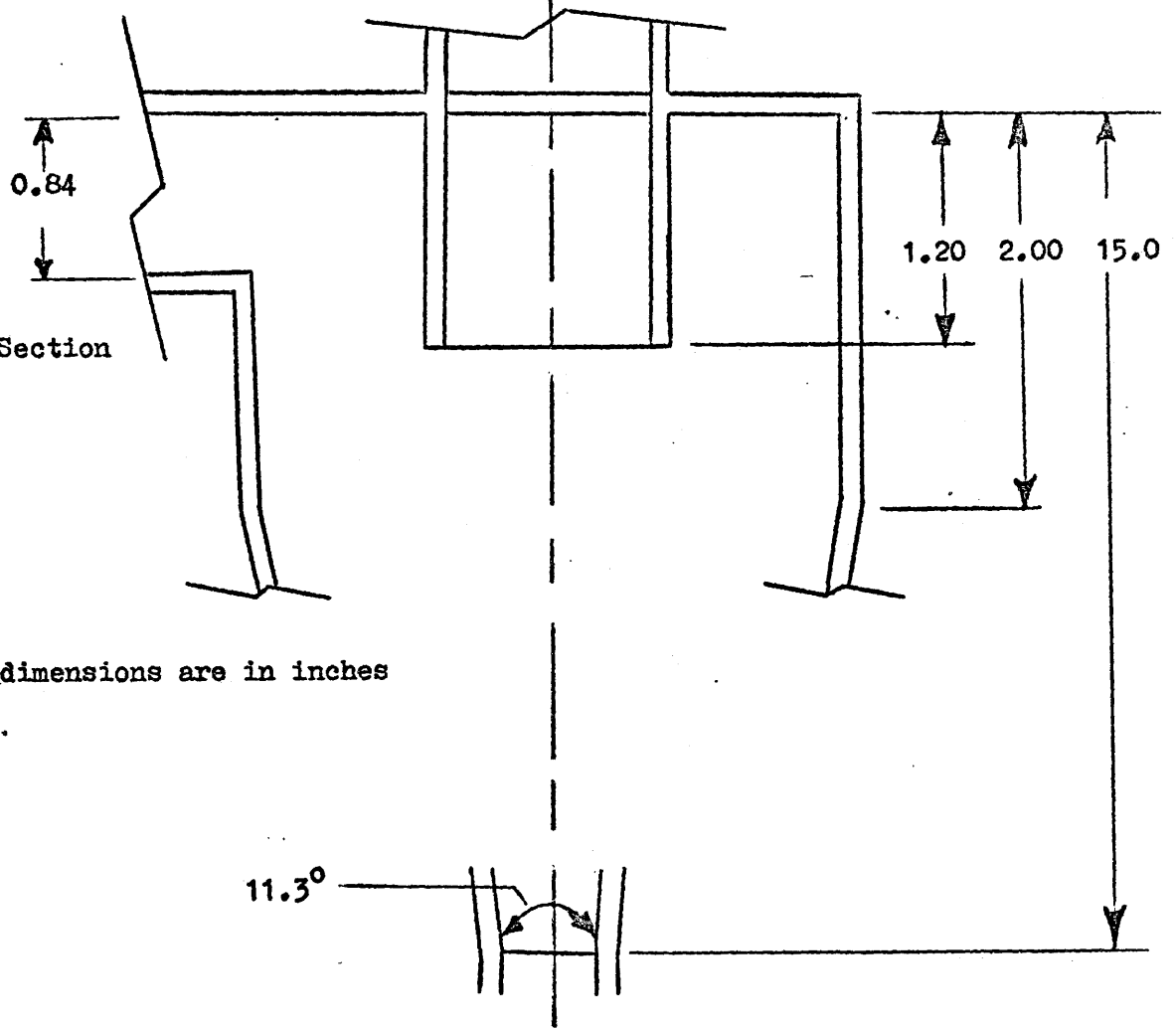
* all dimensions are in inches

11.3°

Figure 2-2   SCHEMATIC DIAGRAM OF OVERALL LAYOUT

quick adjust
discharges

high speed stirrers

underflow line

22

6 gallon measuring buckets

overflow
rotameters

50 gallon reservoir

P1

P3

P

feed line

manometer

centrifugal pumps
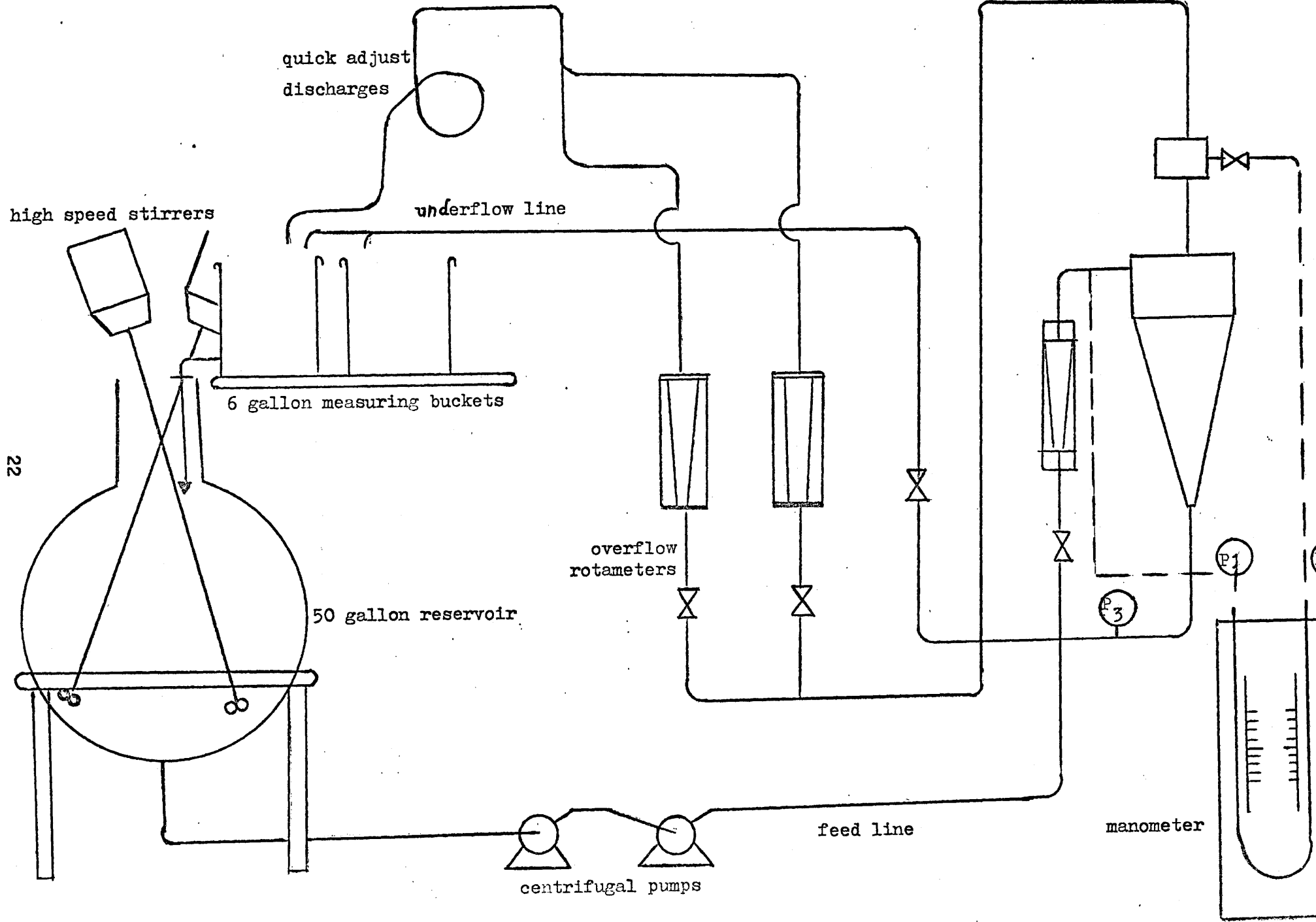
Particle size photographs were taken by use of a Ashahi Pentax reflex camera (without lens) mounted on an Olympus metallurgical microscope, model MR 200009. This was fitted with a 100 x magnification objective lens. Photographic enlargements were used with a Zeiss particle counter model TGZ - 3 to obtain cumulative-linear size distributions of the feed, overflow and underflow particulates.

For photographic work, Kodak or equivalent high contrast single weight paper was used; double weight is too opaque to use on the Zeiss counter. Pan Plus x (ASA 125) black and white film was used throughout. No difficulties were encountered with this medium resolution film.

2.3 CALIBRATION and MEASUREMENT

2.3.1 Flow Control and Measurement

The feed, underflow and overflow were controlled by a gate valve installed in each line. To minimize pressure losses external to the cyclone itself, the overflow was divided into two streams, each with its own control valve and rotameter (see Figure 2-2).

All rotameters were checked for accuracy by measuring the time to accumulate a known volume. This was done for water at $20^{o}C$ (see calibrations pg. A 7,8), and were accurate to 5 to 10%. "Bucket and stopwatch" measurements were used in place of these rotameters when greater accuracy was required.

The maintenance of a constant feed flow was extremely difficult as small fluctuations were present to some degree throughout the study. No practical means of damping out these fluctuations could be found as part of the problem was the fault of uncontrollable variations in the line voltage to the induction motor driven pump.

23

2.3.2 Pressure Measurement

For energy loss calculations, particularly at low flows, the Bourdon tube pressure guages could not give reproducible results. This fact was discovered in preliminary screening runs where pressure drop between feed and overflow was measured at four volume split levels, for each of 13 flow levels. When the same measurements were performed in reverse, the results were not compatable as is shown in Table 2-2. For this reason a mercury differential manometer was installed between the feed and overflow lines with the connecting conduit being filled with water. This gave reproducible results to within 1.5 m.m. Hg. A Bourdon guage was left to measure the underflow pressure since energy loss is relatively insensitive to underflow pressure changes.(see Figure 2-3)

Rietema (1961 pt.II) found a sizable error in pressure loss measurements when pressure ties were not located very close to the cyclone. For this reason, it was thought that pressure in the feed and overflow conduit may be significant in this study, hence the pressure tees were relocated from their original position of roughly three feet from the cyclone to within eight inches. There was a significant difference between the two results.

2.3.3 Weight Measurement

To measure the mass concentration of solids, a mixed sample must be taken in large enough quantity to allow an accurate determination of the solids it contains. Through preliminary runs, it was found that 500 mls. and 1000 mls. were reasonable volumes for the underflow and overflow respectively. It was necessary to take duplicate samples of both streams in order to appreciate the statistical error in identifying a mass concentration.

One mass balance data set consisted of a volumetric flow reading for the underflow and overflow (the feed flow was assumed to be their sum,

Figure 2-3   VARIATION IN PREDICTED ENERGY LOSS
CAUSED BY ERROR IN PRESSURE MEASUREMENT

— Upper limit caused by a +ve 1.5 PSI $p_1 - p_2$ measurement
○ Predicted energy loss
— Lower limit caused by a +ve 1.2 PSI error in P_3 measurement

Δ E/M (FEET H2O)
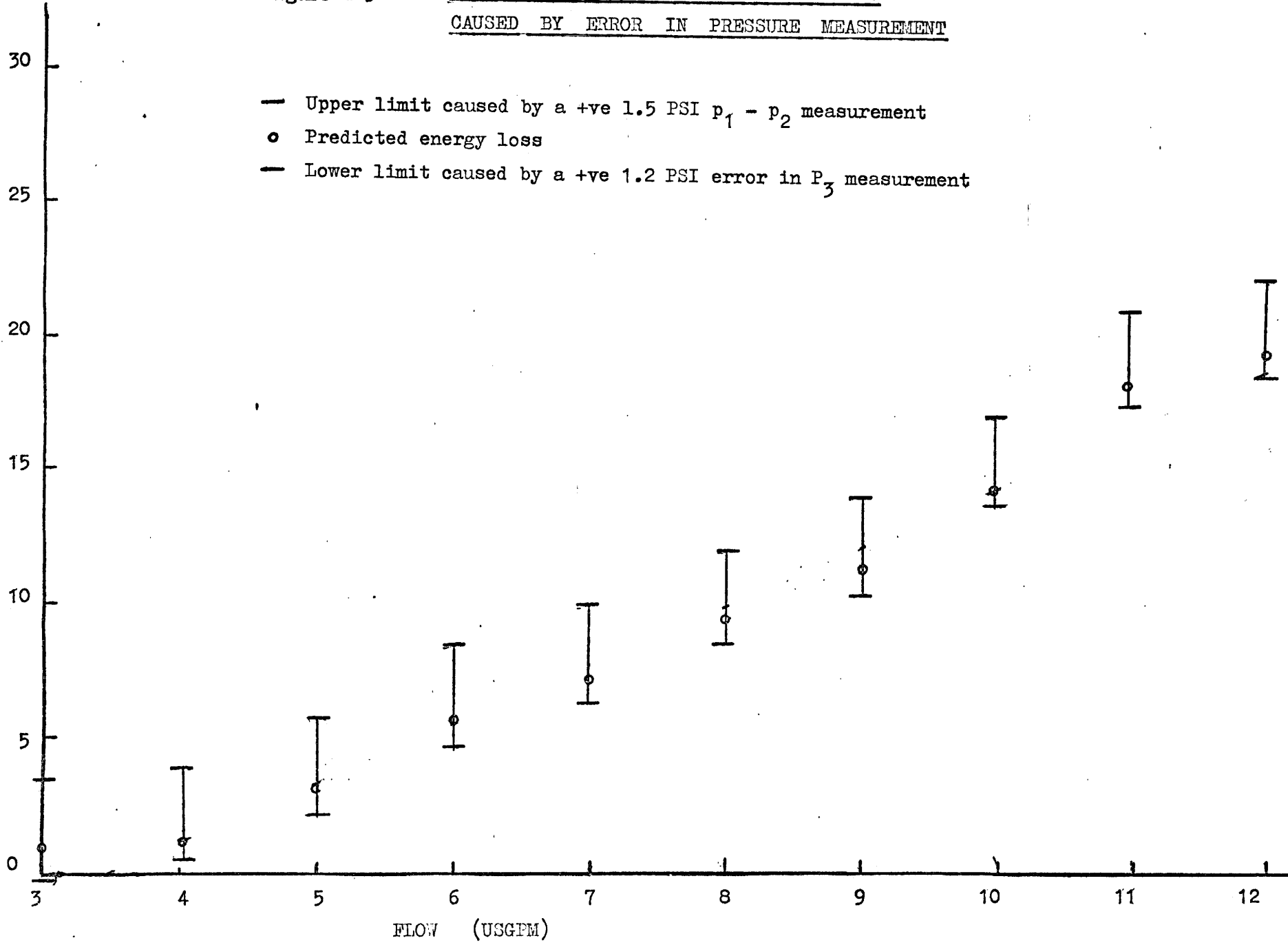
FLOW (USGPM)

TABLE   2-2

VARIABILITY   IN P_s AS   MEASURED   BY   BOURDON   GUAGES

FEED FLOW (USGPM)	ΔP_s (P.S.I.)	ΔP_s (P.S.I.)	ΔP_s (P.S.I.)
2	0	0	0
3	0	0	0
4	1.0	1.0	1.1
5	1.7	1.65	1.8
6	2.6	2.4	2.5
7	3.25	4.0	3.7
8	5.0	5.0	5.3
9	6.3	6.5	6.3
10	9.0	8.3	8.3
11	10.2	10.1	9.8
12	11.9	12.1	12.2
13	14.6	14.4	14.3
14	off scale of Bourdon guages		

order in which data was taken.

since the rotameter reading gave only the order of magnitude values of the flow and based on the rotameter reading the overall balance was within 10%), and duplicate concentration values for feed, under and overflow. Here, the flow rate must be measured accurately, thus the timed known volume approach was used.

Because of inherent drift in the flow in all fluid streams, the duplicate concentration samples had to be taken immediately before the flow in that respective stream was measured. Naturally the flow rate could not be taken before the samples were withdrawn since this would disturb the feed concentration entering the cyclone and hence both exit streams. Because of the varying flow, a flow measurement sample could not be added back into the system fast enough to ensure no flow change occurred before the mass sample was taken. Also, the system must be allowed to regain its equilibrium which is disturbed by the extraction of the first sample before a second sample can be taken and a correction applied (once the first sample has been analysed for liquid and solid content).

It is important to note that this is a closed system and hence any sample removed from the cyclone discharge streams will quickly affect the feed conditions.

Cohen et al (1966) report solids residence times for a 15 cm. diameter cyclone as a "total accumulation ratio", the ratio between the absolute concentration of a size fraction in the contents of the cyclone to that in the feed. For the range of feed flow and volume split investigated in his paper, the accumulation ratio varied from 0.56 to 1.29. This means there was no extreme deviation from plug flow although some backmixing does occur. This backmix element will be assumed neglible because of the far greater volume of the inlet and outlet conduit which is, for our purposes, assumed plug flow.

In deciding how two replicate samples can best be extracted from a fluid stream in the present system, it is quickly appreciated that all six samples for one mass balance data set must be taken without any means of replacing a known quantity of solids in between samples. It, therefore, is mandatory to predict the effect of taking one sample out on all subsequent samples. Since very dilute feed concentrations were used in this work, the effect of a small change in feed concentration (never larger than 10%) was assumed to result in a linear change to the mass concentrations of both the underflow and overflow. This means we are assuming dilute systems to have the property that a change in inlet feed concentration does not effect the probability of any sized feed particle going to the underflow. This assumption provides a basis from which all corrections can be made. If the system is allowed to return to equilibrium before a subsequent replicate sample is taken, a correction can be applied to the second sample as soon as the water and solids content of the first are analysed.

It would be difficult to correct a second sample taken some time "T" after an initial sample, where $T < \bar{t}$, the plug flow residence time for the system. Here we assume plug flow even though we conclude from Cohen et al (1966) that the cyclone has some backmixing. Again, this assumption is likely valid since the cyclone's volume was 0.9 litres while the total of the feed conduit and over-underflow lines was approximately 4.0 litres.

The shortest sampling time possible will be closely given by the larger of the two assumed plug flow residence times $\bar{t}_1$ and $\bar{t}_2$,

where $\bar{t}_1 = \dfrac{\text{volume of feed conduit}}{\text{feed flow}} + \dfrac{\text{volume of overflow conduit}}{\text{overflow rate}}$

$\bar{t}_2 = \dfrac{\text{feed conduit volume}}{\text{feed flow}} + \dfrac{\text{underflow conduit volume}}{\text{underflow rate}}$

The longest residence time that occurred over the range of variables measured was in the feed-underflow stream with the volume split and feed rate set at 6:1 and 7 USGPM respectively.

At these conditions

$$\bar{t}_2 = \frac{0.51 \text{ gallons}}{7.0 \text{ USGPM}} + \frac{0.201 \text{ gallons}}{1.16 \text{ USGPM}}$$

$$= 0.246 \text{ minutes}$$

$$= 14.7 \text{ seconds.}$$

From this it was concluded that all second replicate samples could safely be taken 14.7 seconds after the first. Any further delay would increase the chances of taking the second replicate under different flow rate conditions. The overall accuracy of a mass balance would be seriously affected by a very small change in the underflow rate (see Figure 2-5). For a 0.05 USGPM error in the underflow rate, the mass balance will be out 2.5%.

Other investigators have not normally been concerned with such calculations because much higher solids concentrations were used. Rarely is less than 1% by weight used in the feed slurry and more often 5 to 10% is employed. The highest feed concentration used in this study was 0.2%.

With higher concentrations, the accepted method has involved the collection of relatively large known volumes of underflow and overflow (several gallons) over a timed period. Good solids concentration accuracy is afforded by weigh ing the total mass collected.

A complete schedule of a mass balance is shown in the appendix along with a sample calculation which illustrates how linear corrections are applied.

To allow for settling of the smallest particles in a mass balance sample, an impractical length of time would be required. It would be desirable to collect all particle sizes down to and including 1 micron. This size of particle, however, with a S.G. of 2.65 and settling at Stokes' velocity would take approximately 100 hours to fall the height of a

Figure 2-5 ERROR ANALYSIS IN HYDROCYCLONE MASS BALANCE

Note: — % error defined as $\left[\dfrac{\text{MASS IN} - \text{MASS OUT}}{\text{MASS IN}}\right]$ X 100

— taken for overflow conc. = $\dfrac{\text{UNDERFLOW CONC.}}{40}$

and V/S = 4 : 1

— shaded area is error inherant with reading a rotameter

% ERROR IN MASS BALANCE

ERROR IN MEASURING UNDERFLOW RATE (%)
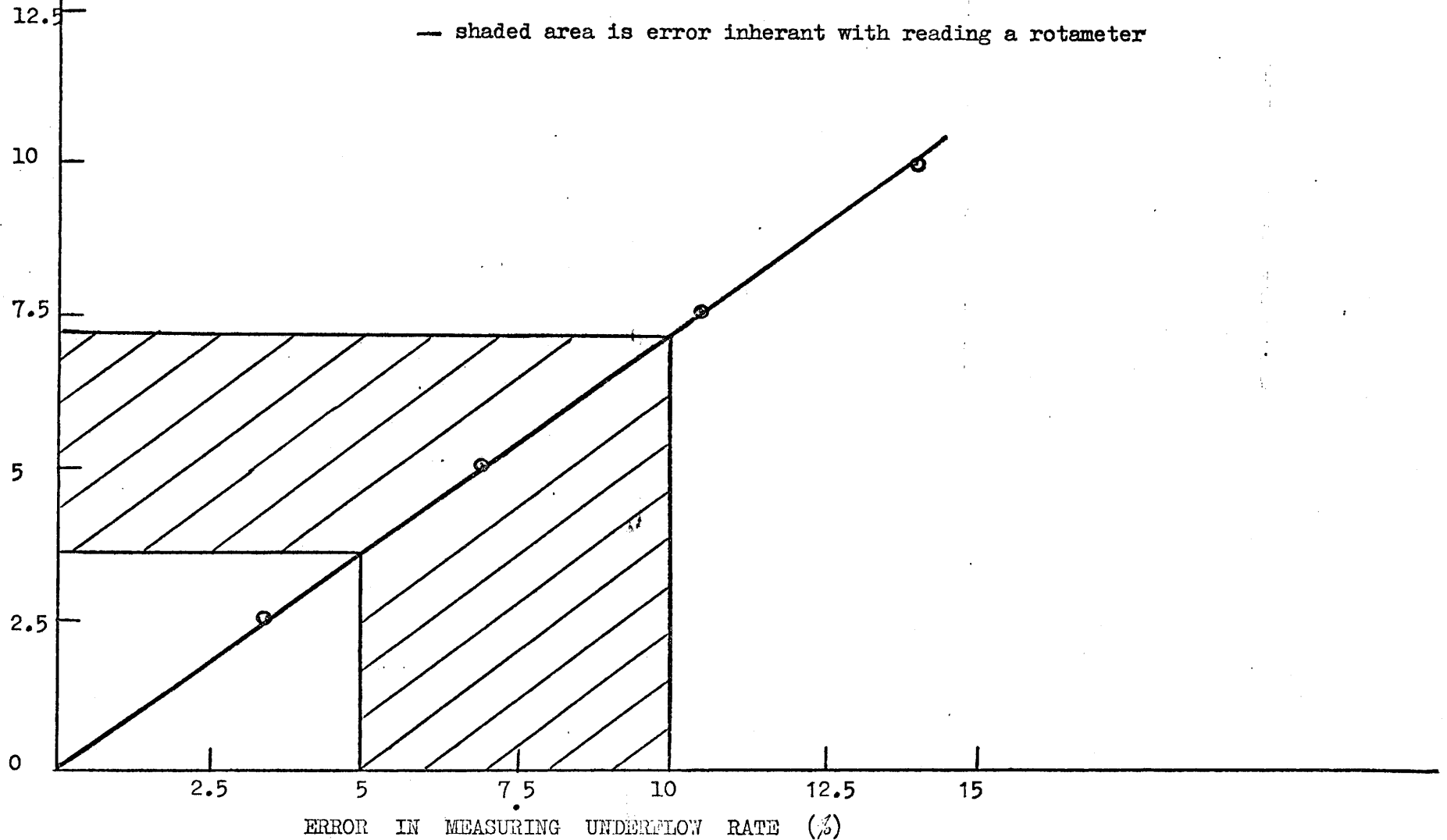
graduated cyclinder (about 1.0 ft.). Since, in this study, the mass samples were only allowed to settle for 18 - 24 hours, we could only expect a portion of 1.0 and 2.0 micron particles to be collected and all of those 3.0 microns or larger. This would in no way affect mass calculations but $(Dp)50$ values would not be correct if they were very close to the 1 - 2 micron range.

With one day delay between actually collecting a sample and the analysis for solids weight, it was necessary to take a second and third set of samples without having replaced the first. This dictated a linear correction on all of the second and third sample set elements. No further correction was required since the first sample was replaced before the fourth sample set was taken. The maximum correction required was about 10%.

2.3.4 Particle Size Measurement

For the slight drift flow conditions of these experiments, the sample taken for mass balance purposes was also considered to be the best representation for particle size analysis.

From the 50 ml. samples used for mass concentration analysis (see appendix for detailed procedure), about 30 mls were carefully decanted and the remainder was agitated. A few drops of this mixture were withdrawn through the wide end of an eyedropper glass, with a reduced agitation still being applied. The inverted eyedropper was emptied very rapidly onto a clean microscope slide and dried over a bunsen burner. Inspection of this slide with a 100 x objective lens revealed that the beads were not lying in a single thickness plane, but were stacked five to ten deep. Since a small bead could not be seen if it lay directly beneath a larger one, a spreading technique was adopted in an effort to allow all sized beads to be seen with equal ease. The narrow depth of field of this microscope system

30

meant that particles in the extremes in size could not both be in focus. This necessitated two pictures at different focal planes for each sample. Great care was needed to prevent double counting. Despite these precautions, piles of particles could be seen. See Figures A-3 and A-4.

A series of photographs were then taken in an ordered pattern (see Figure 2-6). Each photograph contained between 100 - 150 particles; ten pictures were ample to allow a total of 625 beads to be counted for each distribution. One photograph of a 1 m.m. scale marked off in 10 micron divisions was used for monitoring the total effective magnification (from bead to photographic enlargement).

The Zeiss counter reports size in different windows, labelled 1 to 48, with 1 being the smallest and 48 being the largest. By adjusting the film negative:photographic paper magnification, each Zeiss window number took on the units of microns. When a total of 625 particles had been counted, the individual window totals were recorded.

Figure 2-6

Microscope-Camera Optical Setup
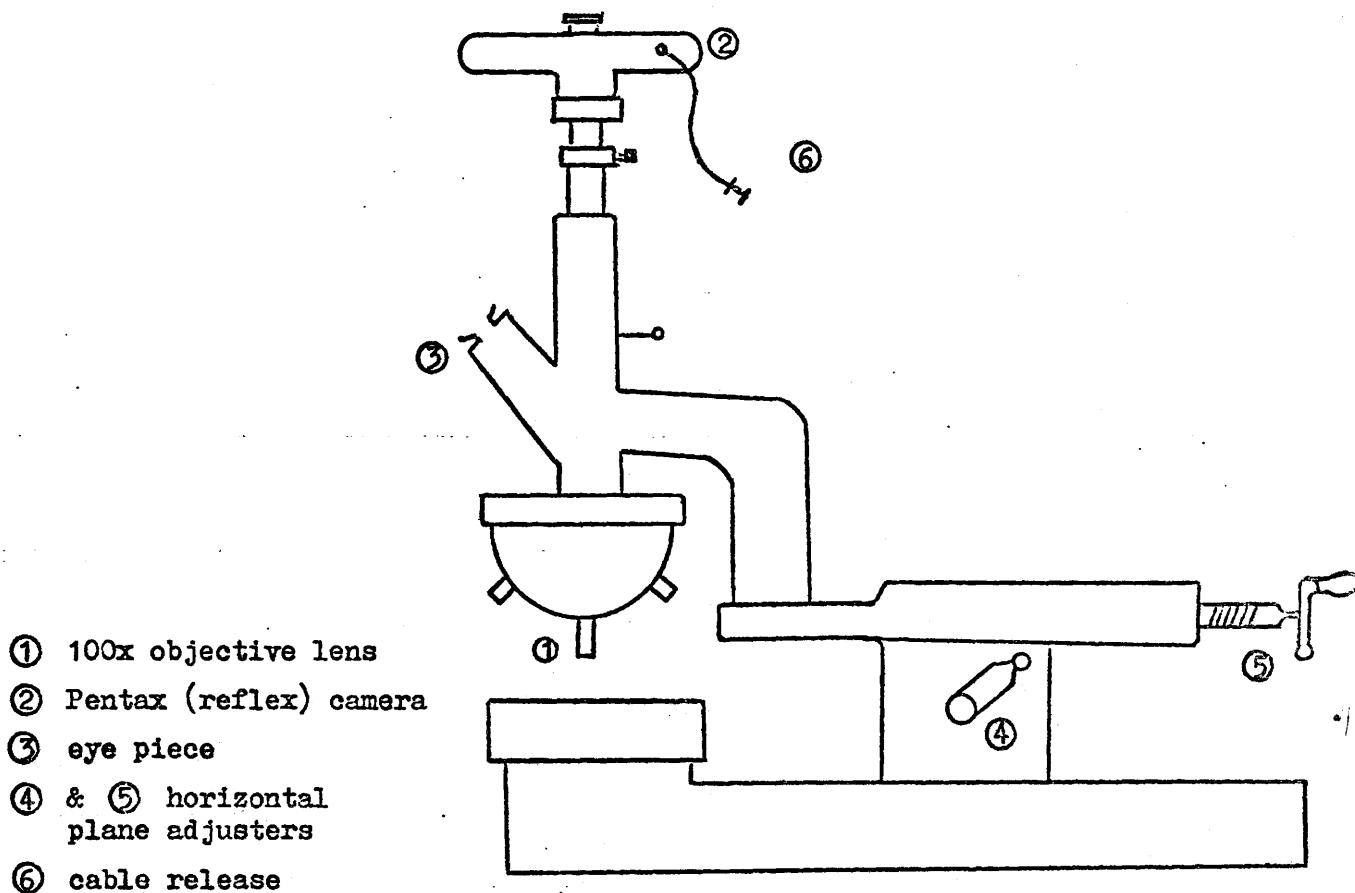
① 100x objective lens
② Pentax (reflex) camera
③ eye piece
④ & ⑤ horizontal
   plane adjusters
⑥ cable release

Microscope Slide
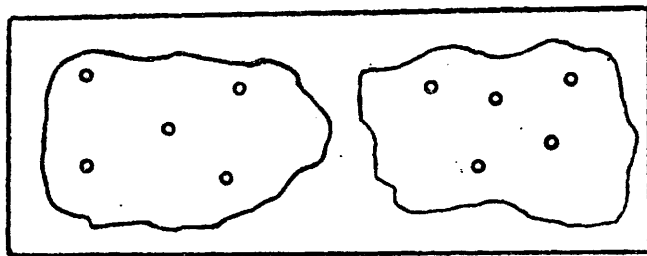
underflow sample   overflow sample

O = approximate position and size of field for two differently focussed pictures

CHAPTER 3

RESULTS AND DISCUSSION

3.1 ENERGY LOSS MEASUREMENT

The results are shown in Tables 3-1 and 3-2 for the cyclone operating with and without an air core respectively.

Although this cyclone was built using Rietema's design ratios, see Figure 3-1, it could not operate reliably, with an air core, unless the underflow valve was partly closed. When the underflow was allowed to discharge freely, no overflow occurred until the feed flow rate reached 12 USGPM. Despite attempts to lower the overflow pressure by pumping and syphoning, no overflow could be maintained because of excessive air bubbles in the overflow line.

The only solution was to restrict the underflow diameter by placing an insert at the cyclone apex. To obtain a reasonable volume split (1:1 or more) required a large reduction in the underflow diameter, too large to be of interest for this work.

3.1.1 UNITS OF REPORTING RESULTS

Rietema (1961), Dahlstrom (1949) and most other researchers report energy loss/unit mass as a pressure drop between feed and overflow. This method is acceptable when the underflow discharges directly to atmosphere such as for air-core operation. However, the problem is more complicated when no air core is present. Then the complete Bernoulli equation is needed.

Table 3-1

Results of Pressure Drop Measurement

Cyclone Operating With Air

Core

Feed Flow (USGPM)	Feed Press. (P.S.I.)	Overflow Press.	Underflow Pressure	ΔP_s (P.S.I.)
3	.2	+	0.0	.2
4	.6	+	0.0	.6
5	.9	+	0.0	.9
6	1.4	+	0.0	1.4
7	2.3	+	0.0	2.3
8	5.2	+	0.0	3.3
9	6.4	+	0.0	4.4
10	7.8	+	0.0	5.2
11	6.4	+	0.0	6.4
12	7.3	.5	0.0	7.8
13	8.5	.8	0.0	9.3

+   slightly positive pressure (0 to .3 P.S.I.) which fluctuated making measurement difficult

*   allowed to discharge freely at atmospheric pressure

Figure 3-1

Reynolds' Dependence on Cyclone Pressure Drop

partly from Rietema (1961)

$\dfrac{b}{D} = .266$

$\dfrac{e}{D} = .133$

$\dfrac{u}{D} = .066$

$\dfrac{b}{D} = .34$

$\dfrac{e}{D} = .28$

$\dfrac{u}{D} = .163$

$\dfrac{b}{D} = .266$

$\dfrac{e}{D} = .266$

$\dfrac{u}{D} = .133$

Design recommended
by Rietema

$\dfrac{b}{D} = .133$

$\dfrac{e}{D} = .133$

$\dfrac{u}{D} = .066$

$\dfrac{b}{D} = .133$

$\dfrac{e}{D} = .266$

$\dfrac{u}{D} = .133$

⊙ data from this study (no air core)

$\dfrac{(\Delta P)\text{ static}}{\frac{1}{2}\rho \langle v\rangle^2}$

$\text{Re}_{\text{inlet}} = \dfrac{\rho \langle v\rangle_1 D_1}{\mu}$
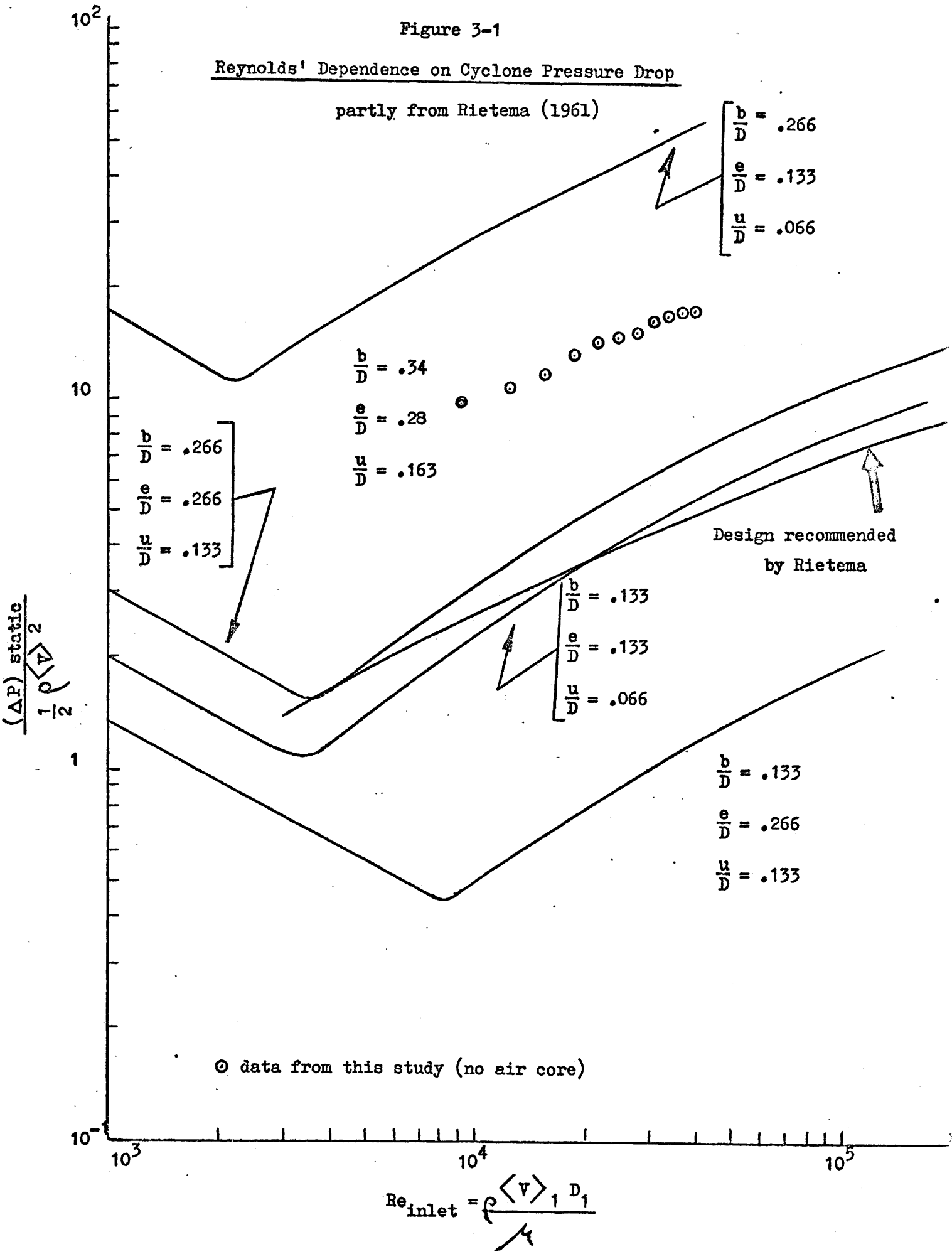
Table 3-2

Results of Pressure Drop Measurement

Cyclone Operating Without Air Core

(1) Volume Split = 1:1

Feed Flow (USGPM)	Feed Pressure P.S.I.	Overflow Pressure+ P.S.I.	Underflow Pressure⊗ P.S.I.	ΔP_s P.S.I.	ΔP_s Ft (H_2O)	$\Delta E/M$ $\frac{Ft - Lb_f}{Lb_m}$
3	1.75	1.418	1.8	.332	.8	.1
4	1.75	1.058	1.7	.692	1.6	1.4
5	3.6	2.42	2.4	1.18	2.7	3.1
6	6.0	4.2	3.5	1.8	4.2	4.5
7	8.2	5.66	5.1	2.54	5.9	6.3
8	9.9	6.47	5.9	3.43	7.9	8.8
9	12.3	8.3	4.2	4.0	9.7	10.8
10	17	12.0	5.2	5.0	12.0	12.2
11	15	8.45	6.3	6.55	14.5	16.3
12	unobtainable					
13	unobtainable					

+ calculated from feed pressure (Bourdon guage) minus mercury manometer reading

⊗ calculated from Bourdon guage

Table 3-2 cont.

(ii) Volume Split = 2:1

Feed Flow (USGPM)	Feed Pressure P.S.I.	Overflow Press.$^+$ P.S.I.	Underflow Press.$^\otimes$ P.S.I.	ΔP_s P.S.I.	ΔP_s Ft (H$_2$0)	$\Delta E/M$ $\frac{Ft\text{-}Lb_f}{Lb_m}$
3	0.139*	-.349	0.7	.390	.9	.6
4	2.0	1.259	2.0	.741	1.7	1.2
5	5.0	3.700	3.0	1.30	3.0	2.8
6	7.5	5.550	4.9	1.95	4.5	4.2
7	10.5	7.770	7.8	2.73	6.3	6.1
8	13.3	9.620	9.3	3.68	8.5	8.3
9	17	12.95	12.25	4.2	9.7	10.4
10	9.7	4.4	3.75	5.3	12.2	12.8
11	11.6	4.8	4.15	6.8	17.6	16.7
12	13.0	5.1	4.4	8.2	18.9	19.8
13	11.0	4.6	-	10.1	23.3	23.6

* calculated from water manometer

Table 3-2 cont.

(iii) Volume Split = 3:1

Feed Flow (USGPM)	Feed Pressure P.S.I.	Overflow Press.+ P.S.I.	Underflow Press.@ P.S.I.	ΔP_s P.S.I.	ΔP_s Ft (H_2O)	$\Delta E/M$ Ft-Lb$_f$ / Lb$_m$
3	2.2	1.772	2.25	.428	1.0	.52
4	3.9	3.082	3.6	.818	1.9	1.5
5	6.4	5.055	5.6	1.345	3.1	2.7
6	8.9	6.9	7.3	2.0	4.6	4.3
7	12.3	9.46	9.75	2.84	6.5	6.4
8	16.25	12.45	12.75	3.8	8.8	8.6
9	13.3	9.75	8.75	4.55	10.5	10.6
10	17.0	11.3	11.3	5.7	13.2	13.4
11	5.65	-1.27	0.0	6.92	16.0	15.3
12	7.4	-1.03	0.0	8.43	19.5	19.0
13	9.75	-0.57	0.0	10.32	23.8	23.8

Table 3-2 cont.

(iv) Volume Split = 4:1

Feed Flow (USGPM)	Feed Pressure P.S.I.	Overflow Press.+ P.S.I.	Underflow ⊗ Press. P.S.I.	ΔP_s P.S.I.	ΔP_s Ft (H_2O)	$\Delta E/M$ Ft-Lb$_f$ / Lb$_m$
3	2.4	1.962	1.7	.438	1.0	1.1
4	4.4	3.582	3.9	.818	1.9	1.7
5	7.5	5.155	6.6	1.345	3.1	2.9
6	10.0	7.95	8.6	2.05	4.7	4.4
7	14.0	13.08	11.3	2.92	6.7	6.4
8	17.9	14.0	14.9	3.9	9.0	8.6
9	15.6	11.0	11.7	4.6	10.6	10.4
10	5.7	-.25	1.25	5.95	13.7	13.1
11	8.1	.75	1.95	7.35	17.0	16.6
12	12.4	4.07	.6	8.33	19.2	21.6
13	8.4	-2.06	2.0	10.46	24.1	22.3

If the elevational components are negligible, the equation is

$$\frac{\Delta E}{M} = \frac{M_1\left[\frac{P_1}{\rho} + \frac{V_1^2}{2g_c}\right] - \left[M_2\left(\frac{P_2}{\rho} + \frac{V_2^2}{2g_c}\right) + M_3\left(\frac{P_3}{\rho} + \frac{V_3^2}{2g_c}\right)\right]}{M_1}$$

in units of $\dfrac{Ft - Lbs_f}{Lb_m}$

If the $V_1^2 \simeq V_2^2 \simeq V_3^2$

then

$$\frac{\Delta E}{M} = \frac{\frac{M_1 P_1}{\rho} - \frac{M_2 P_2}{\rho} - \frac{M_3 P_3}{\rho}}{M_1}$$

If $\dfrac{M_3 P_3}{\rho}$ is small, relative to other terms and $M_1 \simeq M_2$,

then

$$\frac{\Delta E}{M} \simeq \frac{M_1}{M_1 \rho}\left[P_1 - P_2\right] \simeq \left[P_1 - P_2\right] \simeq P_s$$

where $M_{1,2,3}$ is the mass flow rate at the feed, overflow and underflow.
Table 3-2 compares the energy loss as reported by ΔP_s and $\Delta E/M$.
The $\Delta E/M$ representation depends on two flow and three pressure measurements. It is, therefore, subject to more error than ΔP_s which depends on only one pressure measurement. This pressure is, of course, influenced by the metering of two other flows.

It would appear that the values obtained by the two methods are indistinguishable as measured in this experiment. This follows from

an inherent 5 to 10% error in a rotameter measured flow. For this reason, the ΔP_s values will be subsequently used as the indicator of energy loss across the cyclone.

Rietema (1961) reports energy loss by the dimensionless parameter

$$\frac{\Delta P_s}{\frac{1}{2}\rho \langle \bar{v} \rangle_1^2}$$

which has a unique value for each inlet Reynolds number. Figure 3-1 shows both the experimental values for the cyclone used in this study and Rietema's findings for four different cyclone shapes. He also found that the pressure drop ΔP_s was higher in a cyclone operating without a core as compared to the same cyclone under similar conditions, but with an air core. Rietema quotes a factor of 2 in this comparison. Table 3-3 lists pressure drop ratios calculated from air core/non air core operation. Similar conditions of volume split were unobtainable but this may not be important since pressure drop was insensitive to volume split in the non air core mode.

The pressure measurements for the air core mode were subject to some error because of a fluctuating manometer level. This was caused by a pulsating surge of water in the overflow conduit which extended 4 - 8 inches above the cyclone.

The unsatisfactory air core mode operation of this cyclone is because the underflow exit was too large to operate without a valve, and with the valve arrangement the air core did not form readily. However, the studies were to be done on the existing hydrocyclone with its "large" underflow to provide data consistent with that of Knowles.

40

Table 3-3

Pressure Loss Ratio for Non-Air core/Air Core Operation

Feed Flow (USGPM)	$\dfrac{(\Delta P_s)\ \text{No Core}}{(\Delta P_s)\ \text{Air Core*}}$
3	1.65
4	1.24
5	1.44
6	1.40
7	1.19
8	1.12
9	0.955
10	1.02
11	1.06
12	1.05
13	1.09

* Here ΔP_s is measured between feed and underflow since no fluid exited via the overflow until the feed flow was 12 USGPM.

Dahlstrom (1949) uses a term $Q/\sqrt{F}$, the capacity ratio, to predict the expected energy loss in the cyclone. Here Q and F are in units of flow and total pressure drop respectively. Dahlstrom claims that the basic expression "$Q//\sqrt{F}$ = constant" has been found applicable to most flow apparatus. Equations for pressure loss, ΔP_s, and the horsepower required could both be generally defined as follows,

since $\dfrac{Q}{\sqrt{F}}$ = K_1 = constant

then $F = K_2 Q^2$

or, in units of P.S.I.

$$\Delta P_s = K_3 Q^2 \tag{2}$$

Figure 3-2 shows the experimental values found in the present work give the relationship

$$\Delta P_s = 0.0488 Q^{2.14}$$

where Q is in U.S.G.P.M. Theoretically n should be $\leqslant 2$
The general expression for power usage in a cyclone using our nomenclature is:

$$POWER = \rho \cdot Q \cdot \Delta P_s$$

with equation (2) this becomes

$$POWER = K_3 \rho \cdot Q^3$$

and with suitable units for Q this can be written

$$\text{Horsepower (H.P.)} = K_4 \rho \cdot Q^3 \tag{3}$$
$$= K_5 Q^3$$

Figure 3-2

Pressure Drop, ΔP_s, as a
Function of Feed Flow
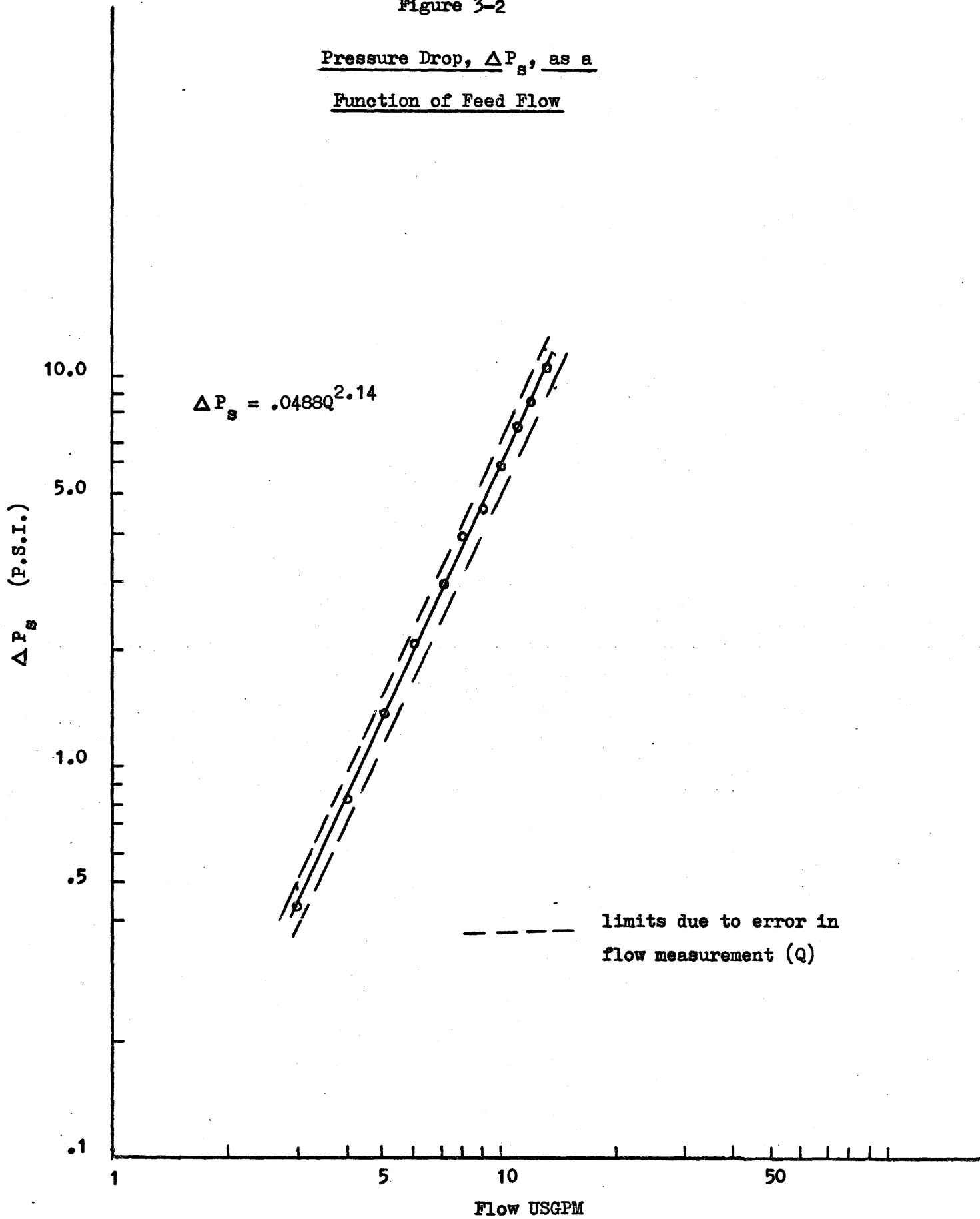
$\Delta P_s = .0488Q^{2.14}$

_ _ _ _ _ limits due to error in
flow measurement (Q)

43

Figure 3-3

HORSEPOWER REQUIREMENTS FOR THE

HYDROCYCLONE AS CALCULATED FROM ΔP_S

$$HP = .0266Q^{3.11}$$

$$1 \text{ H.P.} = \frac{Ft - Lb_f}{Min.} \Big/ 33,000$$

FEED FLOW – USGPM
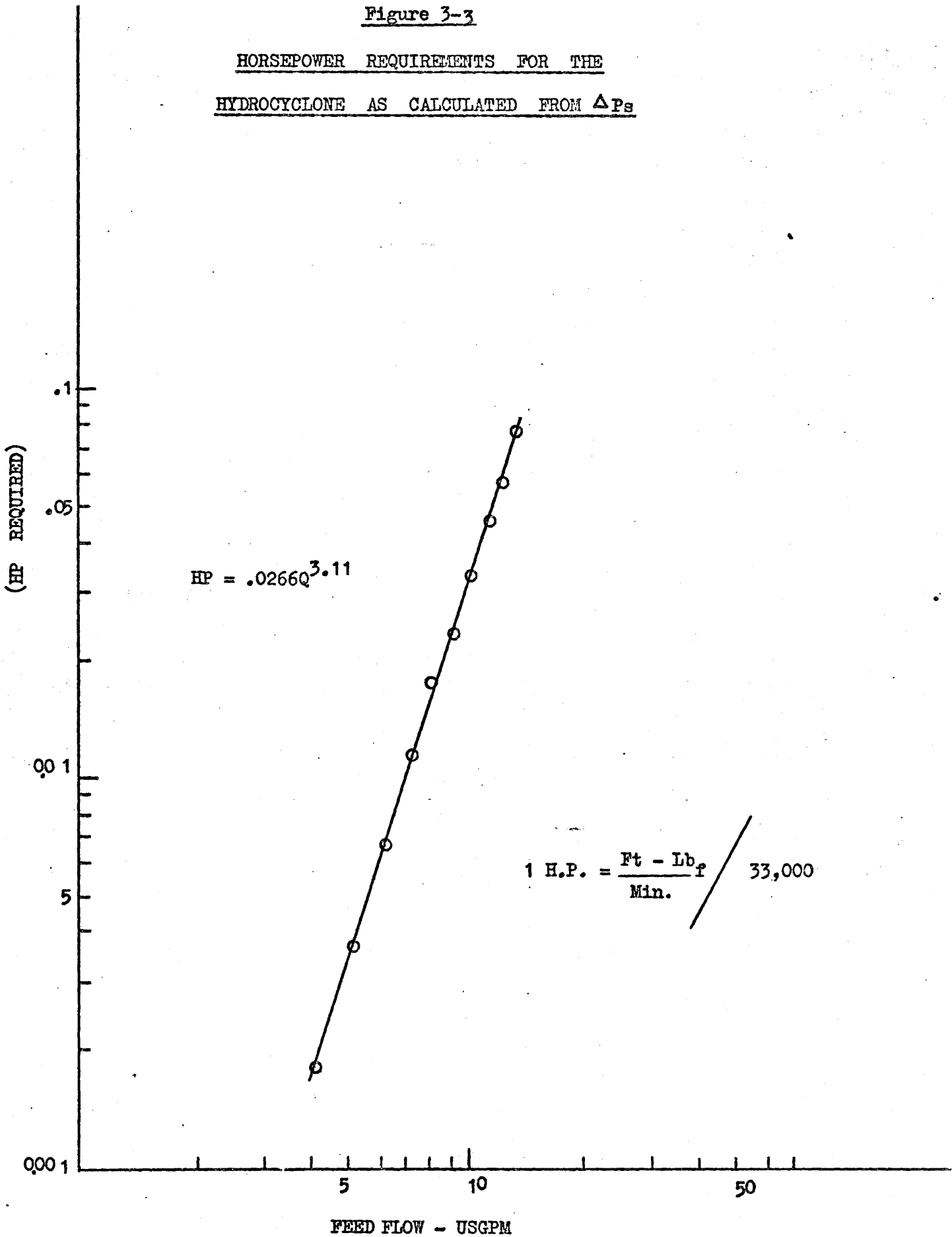
Figure 3-3 shows the horsepower required for the present cyclone as calculated from ΔP_s measurements.

The resulting equation is;

$$H.P. = 0.0266Q^{3.11}$$

where Q is in U.S.G.P.M.

The exponentials 3.11 and 2.14 should differ by 1.0 but there is some error estimating slopes from the data points. The constant capacity ratio for this cyclone in the range of variables studied is;

$$Q/(F)^{0.47}$$

which is in good agreement with the previous results of Dahlstrom for a fixed shape of a hydrocyclone.

3.2 CONSISTENCY CHECKS

The mass liquid balances over the system are a consistency check for the data. The results of the material balances on the total solids over the system are shown in table 3-4. Actual feed, overflow and underflow solids concentrations are shown in table 3-5. This table also gives the percent difference for the two underflow and two overflow replicates. These mass balances show that extremely consistent results were obtained except perhaps for run 13 where the mass balance closed within 6%. Mass balances on individual cut ranges are shown on pg.A-10

3.2.1 CORRELATING THE SEPARATION EFFICIENCY

Separation efficiency can be calculated from Rietema and Tenghergen's (1961) formula where

TABLE 3-4

Balance on Total Solids over System

All mass values are for 1.0 litre total mixed feed entering cyclone

	Mass in (gms) $= C_1Q_1$	Mass out		% Error
		Over (gms) $= C_2Q_2$	Under (gms) $= C_3Q_3$	
1	2.265	1.873	.343	2.16
2	"	1.9075	.303	2.40
3	"	1.929	.296	1.76
4	"	1.959	.350	0.01
5	"	1.915	.340	0.44
6	"	2.088	.214	1.62
7	"	2.092	.230	2.50
8	"	2.080	.182	0.13
9	"	2.098	.162	0.27
10	"	2.092	.175	0.09
11	"	2.119	.162	0.70
12	"	2.034	.179	2.30
13	"	1.828	.294	6.05
14	"	2.085	.163	0.75
15	"	2.069	.190	0.25
16	"	2.059	.2325	1.20

TABLE 3-5

RESULTS OF MASS BALANCES

M.B.	UNDERFLOW[i] CONC.(PPM)	ERROR[ii] (%)	OVERFLOW[i] CONC.(PPM)	ERROR[ii] (%)	ERROR IN MASS BALANCE (%)
1	9,565	0.2	436	3.6	2.16
2	10,460	0.5	381	*	2.4
3	9,630	*	377	2.7	1.76
4	9,725	0.267	369	2.54	0.01
5	10,525	1.0	372	*	0.44
6	10,860	1.0	265	12.4	1.62
7	14,430	1.28	260	7.25	2.47
8	7,060	0.21	258	4.66	0.13
9	10,600	*	220	15.0	0.26
10	9,770	1.44	220	0.01	0.09
11	10,900	0.905	198	0.75	0.73
12	10,770	0.01	227	3.33	2.33
13	14,220	+	346	(+)	6.05
14	6,540	+	217	+	0.75
15	14,870	+	219	+	0.25
16	10,770	+	227	+	1.00

* one of two replicates was spoiled

+ only one sample taken

(+) only one sample taken, portion of solids lost

i - Arithmetic average of Replicates (PPM)

ii-% deviation of replicates from each other

$$n = \text{efficiency} = \left[\frac{c_3 Q_3}{c_1 Q_1} - \frac{\rho_3 Q_3 - c_3 Q_3}{\rho_1 Q_1 - c_1 Q_1} \right]$$
$$\text{(A)} \qquad\qquad \text{(B)}$$

$$= \frac{Q_3}{Q_1} \left[\frac{c_3}{c_1} - \frac{\rho_3 - c_3}{\rho_1 - c_1} \right]$$

Term (A) is the fraction of feed solids that goes out the underflow.

Term (B) is the fraction of liquid that goes out the underflow. The efficiencies are shown in Figure 3-4 which shows the experimental levels used in a single level statistical design, with replicates on the face center (o, $\pm$1) instead of at the center 00. Experimental values of coded levels are also shown in table 3-6.

Table 3-6

Coded and Uncoded Levels For Two Independent Variables,

Volume Split and Feed Flow Rate

Level	Feed Rate (USGPM) $x1$	Volume Split $x2$
-1	7.0	2.4:1
0	—	4.25:1
+1	10.0	6.1:1

The run numbers and their respective concentration levels are shown on pages A-11 and A-12.

Figure 3-4

Geometric Description of Experimental Design

All efficiencies shown in %

Volume Split

X_2

X_1

Feed Flow USGPM

49
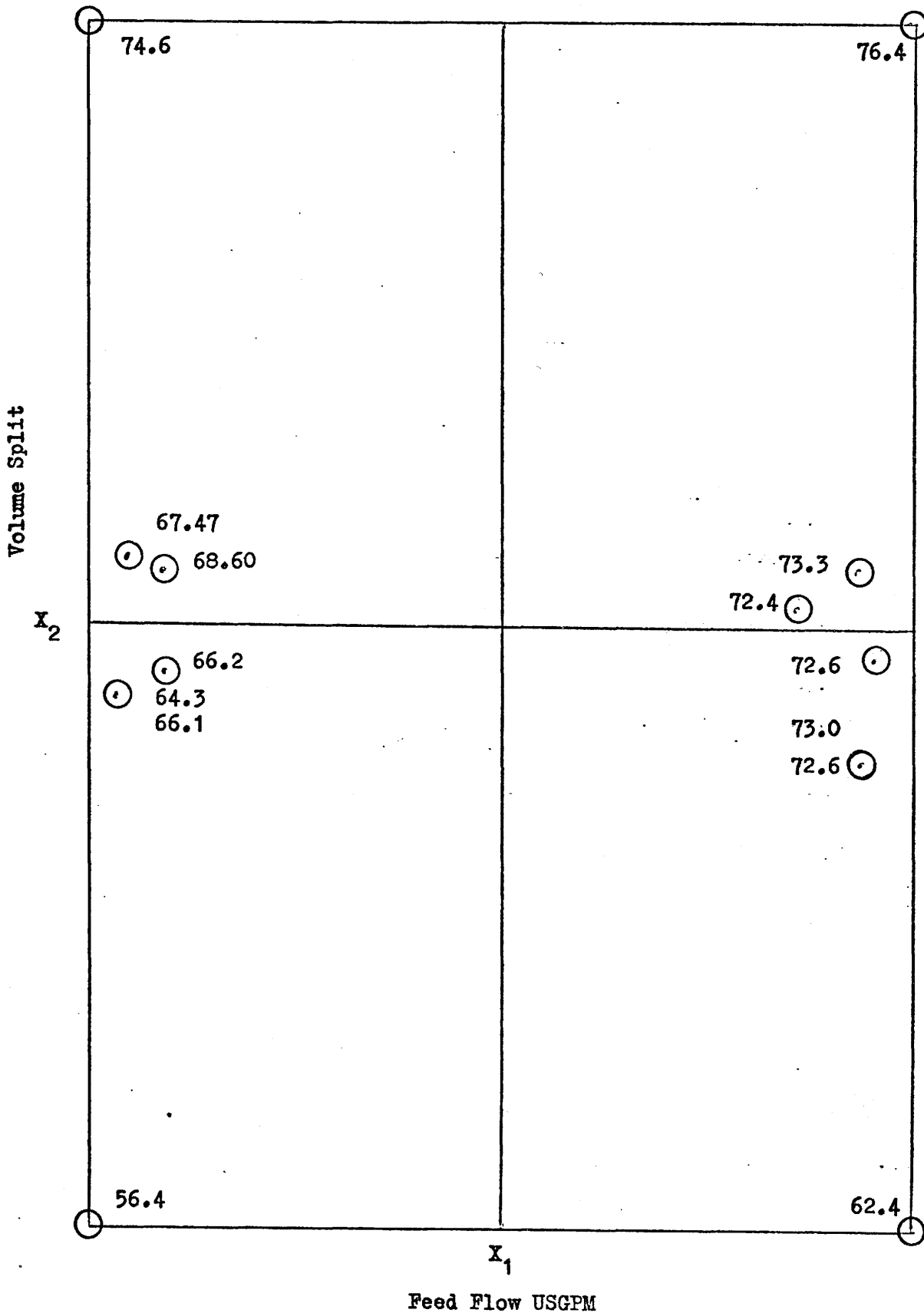
The parameters in the efficiency correlation were evaluated by multiple regression for the trial expression;

$$\text{Efficiency} = B_1 + B_2 X_1 + B_3 X_2 + B_4 X_2^2 + B_5 X_1 X_2$$

where X_1 is feed flow rate

$\quad\quad X_2$ is volume split

The results of this regression, in coded form, are:

$$\text{Efficiency} = 70.41 + 2.09 X_1 + 8.05 X_2 - 2.9 X_2^2 - 1.05 X_1 X_2$$

with a $(X^1 X)^{-1} S^2$ matrix as shown in Table 3-7.

Table 3-7

Variance – Covariance Matrix for Single Level Experimental

Design With Two Independent Variables

.224	0	0	-.224	0
0	.075	0	0	0
0	0	.112	0	0
-.224	0	0	.335	0
0	0	0	0	.112

A Covariance appears between the constant term, B_1 and B_4, the parameter for X_2^2 because their respective columns in the X matrix were very similar. See table 3-8.

Table 3-8

X and Y Matrixes

b_0	x_1	x_2	x_2^2	$x_1 x_2$		Y
+1.0	−1.0	+1.0	+1.0	−1.0		74.6
+1.0	−1.0	0.0	0.0	0.0		68.0
+1.0	−1.0	−1.0	+1.0	+1.0		56.4
+1.0	+1.0	1.0	+1.0	+1.0		76.4
+1.0	+1.0	0.0	0.0	0.0		72.8
+1.0	+1.0	−1.0	+1.0	−1.0		62.4

Since replicates were not taken at the centre point of the design, only single averaged values for Y could be used in the X matrix to avoid a biased weighting of these replicated points. These replicates, shown on Figure 3-4, were used to obtain an outside error estimate of σ^2. This was calculated to be $S^2 = 0.477$ and was obtained from completely different runs that were at least partly randomized in time.

Four other proposed models were evaluated in exactly the same way as just described. The five models considered are shown in Table 3-9. The residual sum of squares is shown opposite each model.

Table 3-9

Models Proposed for Efficiency Correlation

Model	Residual SS
$b_0 + b_1 x_1 + b_2 x_2$	16.3
$b_0 + b_1 x_1 + b_2 x_2 + b_3 x_2^2$	4.64
$b_0 + b_1 x_1 + b_2 x_2 + b_3 x_2^2 + b_4 x_1^2$	*
$b_0 + b_1 x_1 + b_2 x_2 + b_5 x_1 x_2$	11.9
$b_0 + b_1 x_1 + b_2 x_2 + b_3 x_2^2 + b_5 x_1 x_2$	0.235

* impossible to evaluate with the design used since x_1^2 column in x matrix is the same as b_0 column.

The best model is that which removes the greatest amount of sums of squares (S.S.) but does not remove any S.S. that is associated with the measurement of any Y value.

From the outside error estimate, the additional S.S. removed by adding another term to the model, can be tested by an F test.

Since the S.S. of the model predictions about the experimental points has one degree of freedom and the error estimate had 7 degrees of freedom, we can test if;

$$\frac{\text{decrease in S.S. by adding term}}{\text{error S.S.}} \; > \; F(1, 7, 0.95)$$

Only when the above inequality is true then the term should be kept in the model.

The model with the lowest S.S. has an S.S. of 0.235. To test whether this model is significant as compared with the model that has the second lowest S.S. (which was 4.64), we compute

$$4.64 - 0.235 \; = \; 4.405$$

F test $\dfrac{4.405}{0.477} \; = \; 9.25$

This is greater than $F(0.95, 1, 7) = 0.559$ and so all terms should be kept, thus:

$$\text{Efficiency} = 70.41 + 2.09x_1 + 8.05x_2 - 2.9x_2^2 - 1.05x_1x_2$$

From this, we infer that efficiency is a stronger function of volume split than feed flow rate within the range of variables studied.

3.3 MODELING OF DISTRIBUTIONS

To obtain the diameter of the Dp(50) particle, it is necessary to have a reliable model representing the particle size distributions of the underflow and overflow.

Cumulative number distributions are obtained from counting 625 particles on the Zeiss counter; a typical result is shown in Figure 3-5. By differentiating such a cumulative curve, the discrete frequency distribution can be created, as shown in Figure 3-6. The solution for the Dp(50) particle size is given by the intersection of the overflow and underflow discrete curves or the point of equal slopes on the cumulative frequencies. Before solving from either type of curve, a correction must be applied to the overflow or underflow distribution so that the total number of particles from both is in the same ratio as actually exited from the cyclone. To make this correction, the total relative weight of both distributions must be known along with the actual mass flow of solids out of the cyclone. If the overflow is to be corrected, each particle size in the distribution must be multiplied by x; where x is given by;

$$x = \frac{(\text{mass of solids out overflow})}{(\text{mass of solids out underflow})} \cdot \frac{(\text{integrated underflow wt. dist.})}{(\text{integrated overflow wt. dist.})}$$

The procedure of finding Dp(50) would be simple if there was no uncertainty associated with any counted distribution. The raw data could be integrated, corrected, and the value of Dp(50) calculated directly. Unfortunately this was not possible since replicate determinations of feed, overflow and underflow distributions indicated a fairly high variance for most particle sizes. These variances are shown in Figures 3-7 and 3-8. These variances could originate from several

53

Figure 3-5

TYPICAL CUMULATIVE

FREQUENCY PLOT

(M.B.#9-2)

△ UNDERFLOW DISTRIBUTION
O OVERFLOW DISTRIBUTION

CUMULATIVE FREQUENCY (NUMBER)

PARTICLE DIAMETER (MICRONS)
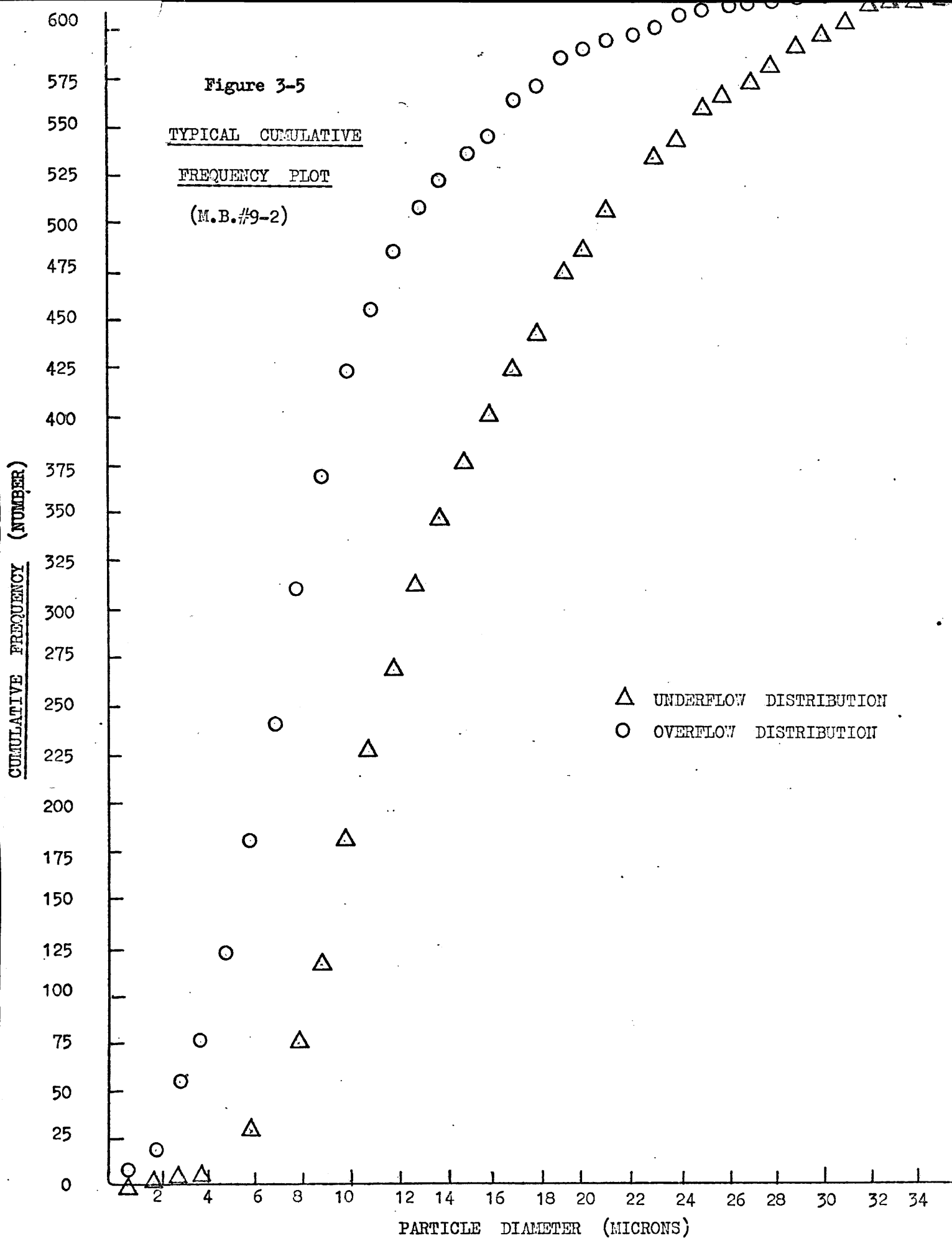
Figure 3-6   DISCRETE FREQUENCY PLOT FOR

MASS   BALANCE   #9-2

△ UNDERFLOW DISTRIBUTION
○ OVERFLOW DISTRIBUTION
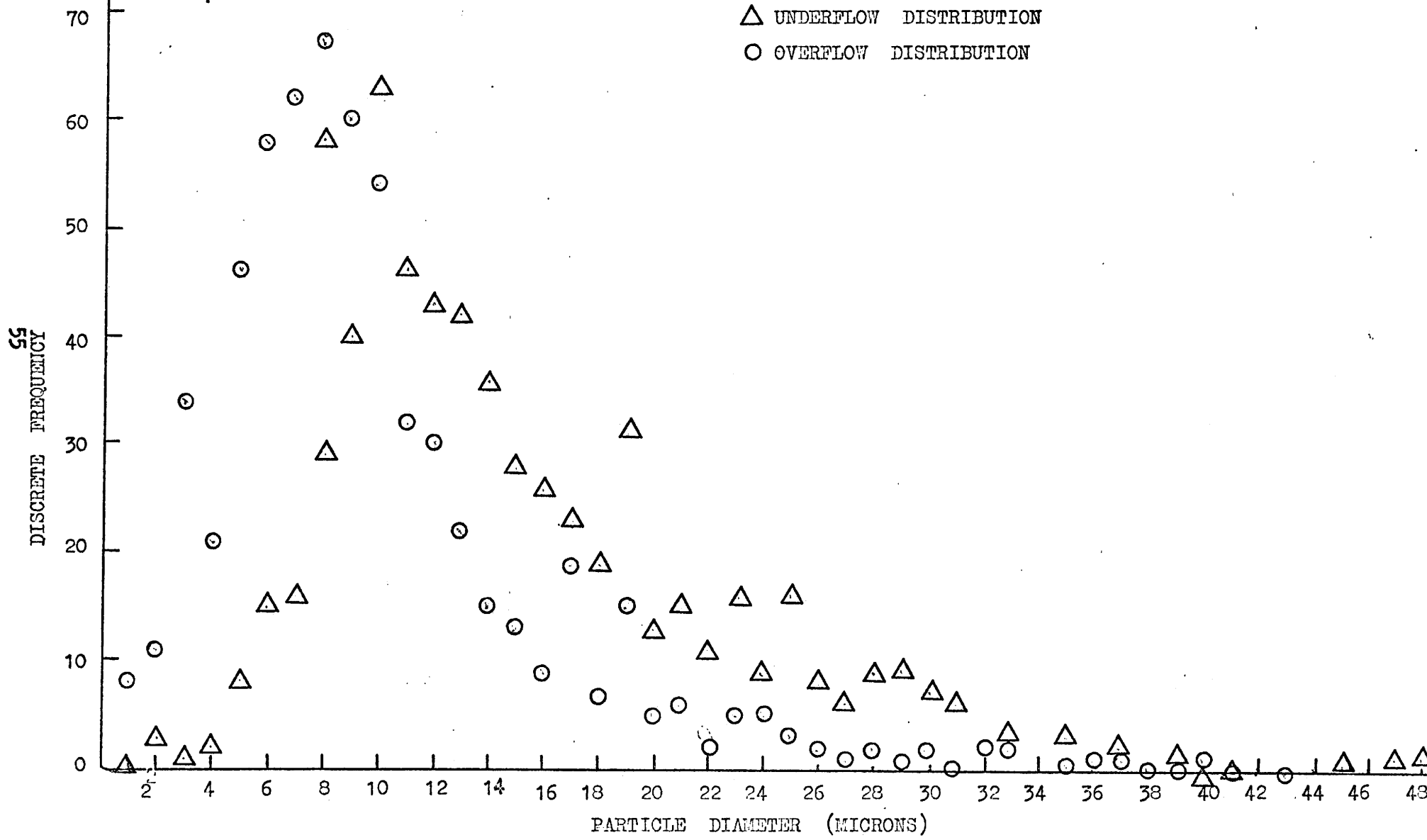
Figure 3-7 VARIANCE OF FIVE FEED DISTRIBUTIONS
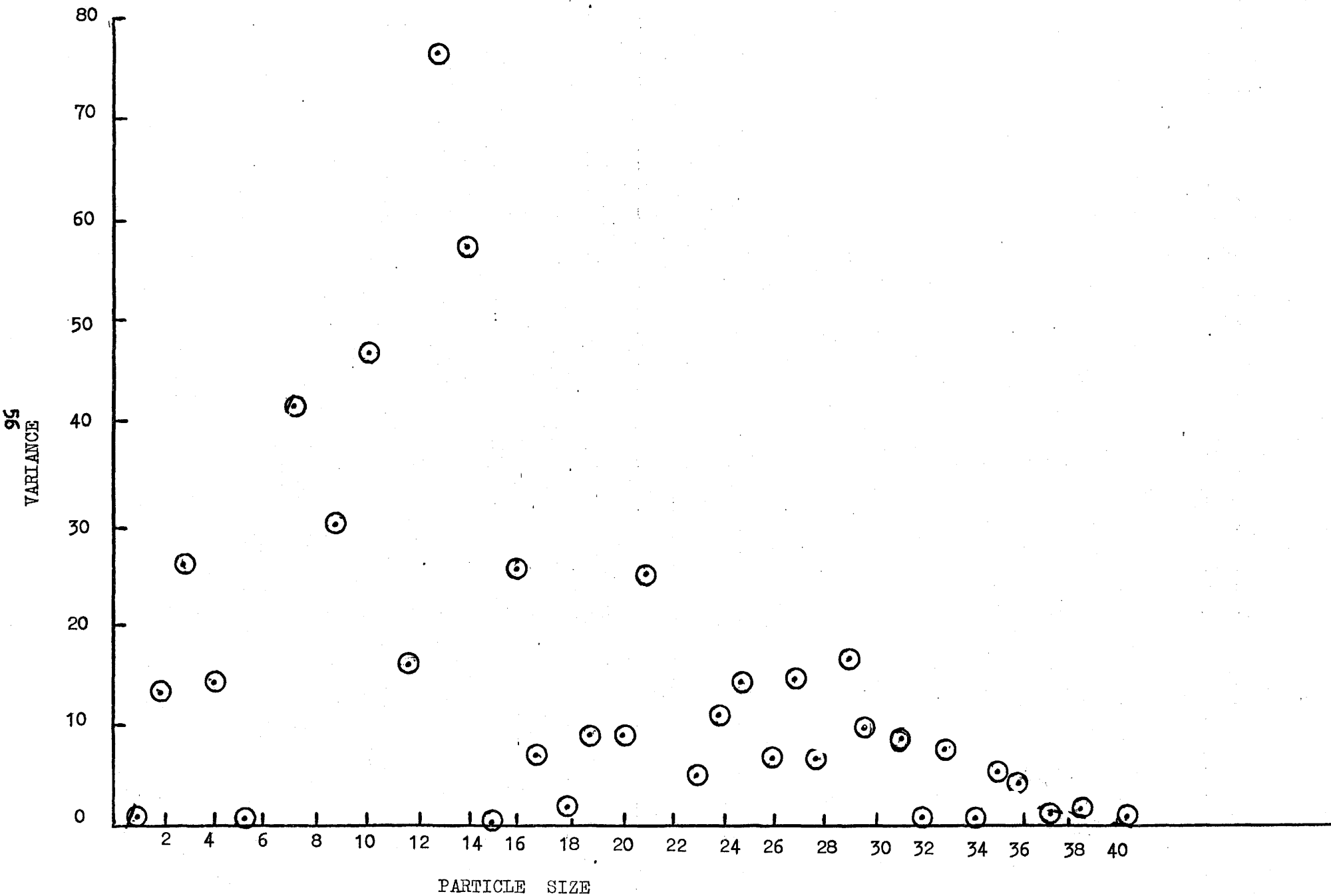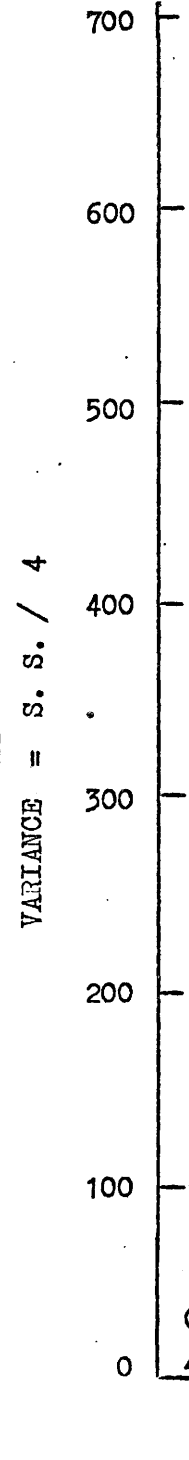
Figure 3-8 VARIANCE FROM FOUR REPLICATE DISTRIBUTIONS

Note: Variance is calculated from pairs of discrete frequencies
ie: the frequencies of 1 & 2 micron particles are added to give
one frequency of a 2 micron particle.

O   Overflow

△   Underflow

See pg. A-13 for a log. probability representation of the 5 feed
replicates.
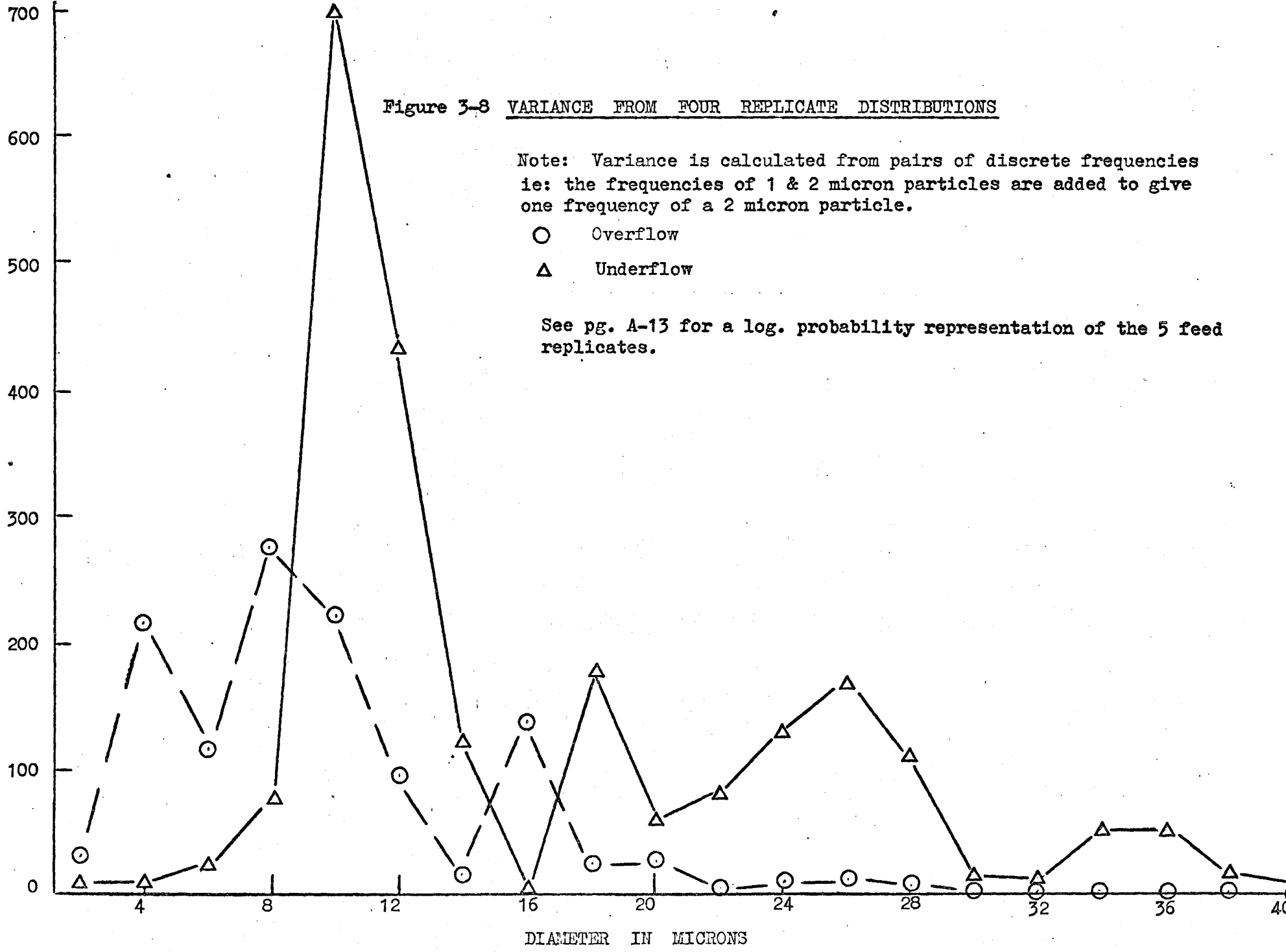
sources of error.

  1) Taking samples that contain different distributions-
   due to changing conditions in any flow stream.

  2) Inclusion of non representative particles in the limited
   number of photographs taken.

  3) Inability to accurately identify the size of any one
   particle.

The first two effects are indistinguishable in this study. Figure 3-9
gives some idea of the relative contribution of the third effect to the
overall variance. This Figure shows a polynomial fit to three sets
of underflow confidence limits, where confidence number = $(\sqrt{\text{var}})(t_{n=4} ,90\%)$
obtained from grouping only one, two or three adjacent particle sizes.
A noticable reduction in variance is obtained by grouping by twos, but
no further improvement occurs when three particle sizes are added together
to calculate one variance. This would indicate two things; that the
variance is mostly due to effects 1 or 2 or both, and the accuracy on
estimating any one particle size is about $Dp \pm .5$ microns.

  With some uncertainty in the distributions, suitable modeling
techniques must be used to minimize the error in

  1) obtaining an integrated weight value

  2) solving for $Dp(50)$ from a set of underflow and corrected
   overflow curves.

It is highly probable that no one model can simultaneously be the best
for both objectives. This is because the best model for criterion 1
would have to follow the higher weight frequencies closely and the best
model for criterion 2 would have to follow only a few points on either
side of the $Dp(50)$ diameter. Preliminary examination of the raw data,

Figure 3-9 LEAST SQUARES POLYNOMIAL FITS FOR 90% CONFIDENCE LEVELS OF OVER AND UNDERFLOW DISTRIBUTIONS

△ 10th order poly. R.M.S. = 22.6
○ 10th order poly. R.M.S. = 11.2
□ 9th order poly. R.M.S. = 4.5
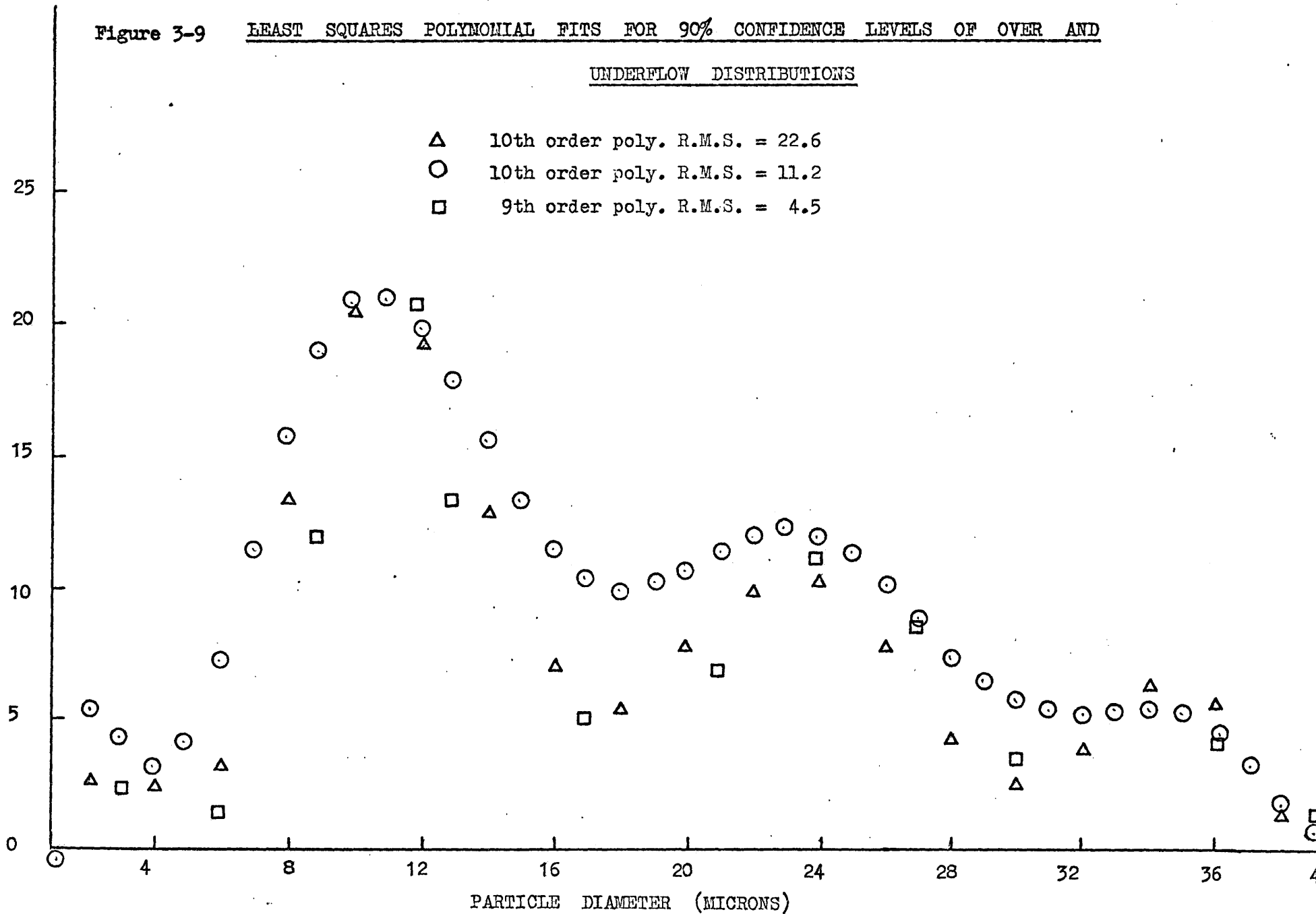
corrected by an estimated weighting factor, indicated that Dp(50) lay in the smaller size end of the distribution. It was then apparent that a model that was weighted to fit the heavy end of the distribution would likely not provide the best possible fit for the frequencies in the region of Dp(50).

3.3.1 FINDING THE BEST WEIGHT MODEL

Computer programs were written to integrate all the raw discrete curves. That is to evaluate the term:

$$\sum_{i=1}^{40} D_i^3 \cdot f_i$$

where 40 was the largest diameter found, and f_i is the number of particles counted of size D_i.

Polynomials were also fit to the discrete distributions, ignoring for the moment that the variance was not the same for all particle sizes. The order of polynomial used was the one which provided the lowest residual mean square (usually about seventh order). In all cases, the ratios of "total underflow weight to total overflow weight" given by the integrated raw data, and the integrated polynomial predictions of the discrete frequencies were almost equal. The maximum difference was only 1% which would be insignificant in these calculations.

The reason for this striking similarity was the ability of the polynomial to follow the high weight frequencies very closely, see Figure 3-19 No other methods of modeling a distribution for

60

Figure 3-10   TYPICAL GAUSSIAN AND POLYNOMIAL MODELS

OF A FEED DISTRIBUTION

⊙ 7th ORDER POLY (R.M.S.=31.7)   D.O.F.=32
□ DISCRETE FREQUENCY VALUES   D.O.F.=40
△ GAUSSIAN LOG TRANSFORMED (R.M.S.=89.2)   D.O.F.=38
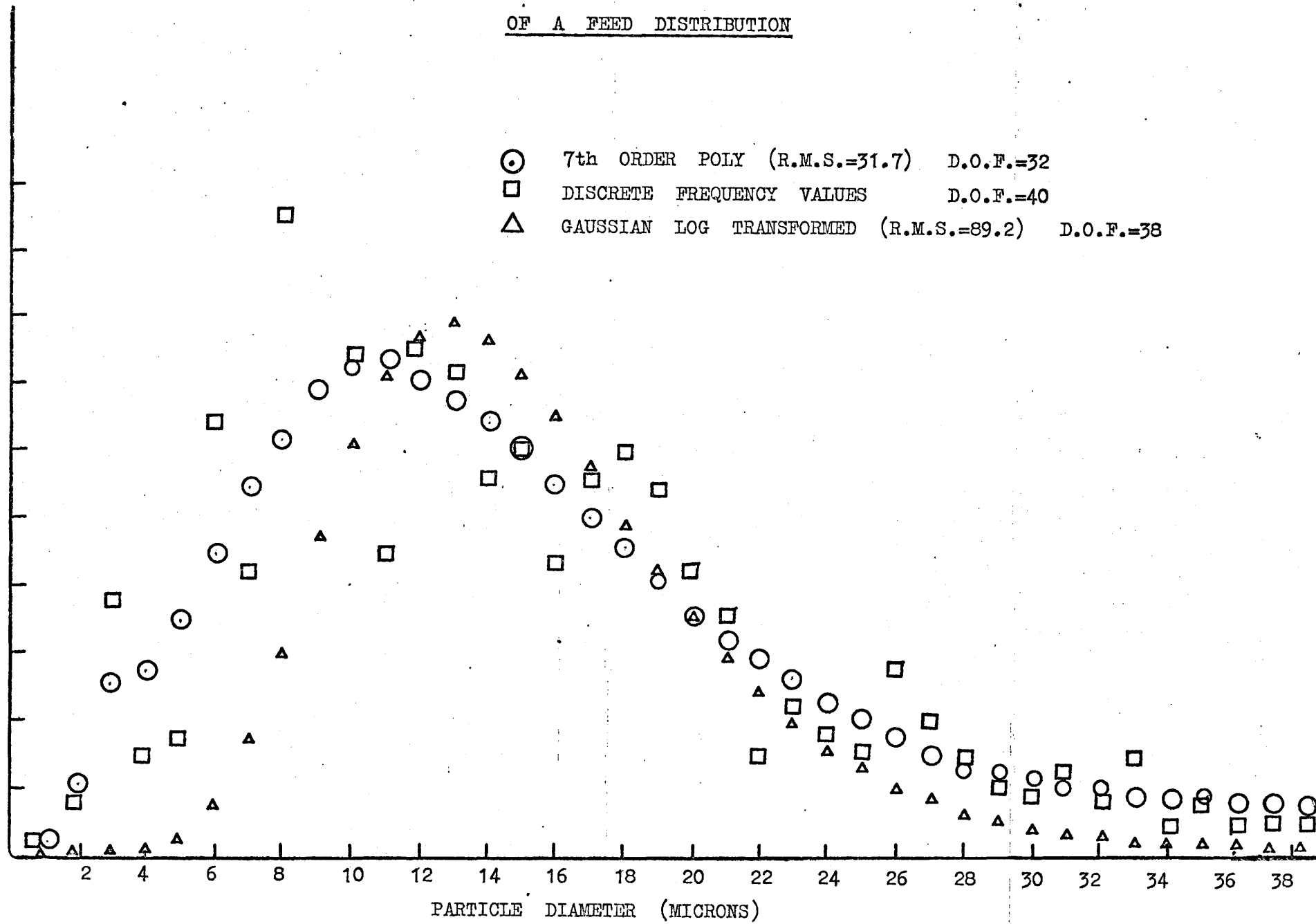
weight needed to be considered. It was later found that none of the models used for (Dp)50 solution gave a good approximation of the distribution weight.

3.3.2 FINDING THE BEST MODEL FOR THE SOLUTION OF (Dp)50

Many distributions of ground and otherwise manufactured particles can be represented by a log-normal distribution. A typical underflow – overflow set of data are plotted on log probability paper as shown on Figure 3-11 and also on a square root probability plot as shown in Figure 3-12. It appears that most of the underflow experimental frequencies follow a square root probability model while the underflow and feed distributions follow (closely) a log-normal distribution. In general, one is satisfied if the data follow a straight line between 10 and 90% limits.

To compare the square root and log-probability models with a polynomial model, one feed distribution, which was closely log-normal, was fitted by a non weighted least squares polynomial of order 7. This order gave the lowest R.M.S. (31.7) as compared to all other orders tried.

The variance and mean of the actual discrete data values were calculated and used as parameters in the Gaussian equation

$$F = A \exp - \left[(x - \mu)^2 / 2\sigma \right]$$

μ = mean diameter
σ = std. deviation

where F is the discrete frequency and A is a constant equal to the peak of the normal distribution. The same programs searched for that value of A which would minimize the R.M.S. between the actual data points and the proposed Gaussian model. The best fit had an R.M.S. of 89.2

Figure 3-11 LEAST SQUARES FIT FOR BEST

STRAIGHT LINE MODEL

△ UNDERFLOW DISTRIBUTION (R.M.S.=89.19)

○ OVERFLOW DISTRIBUTION

DIAMETER (LOG SCALE)

63

CUMULATIVE PROBABILITY (%)
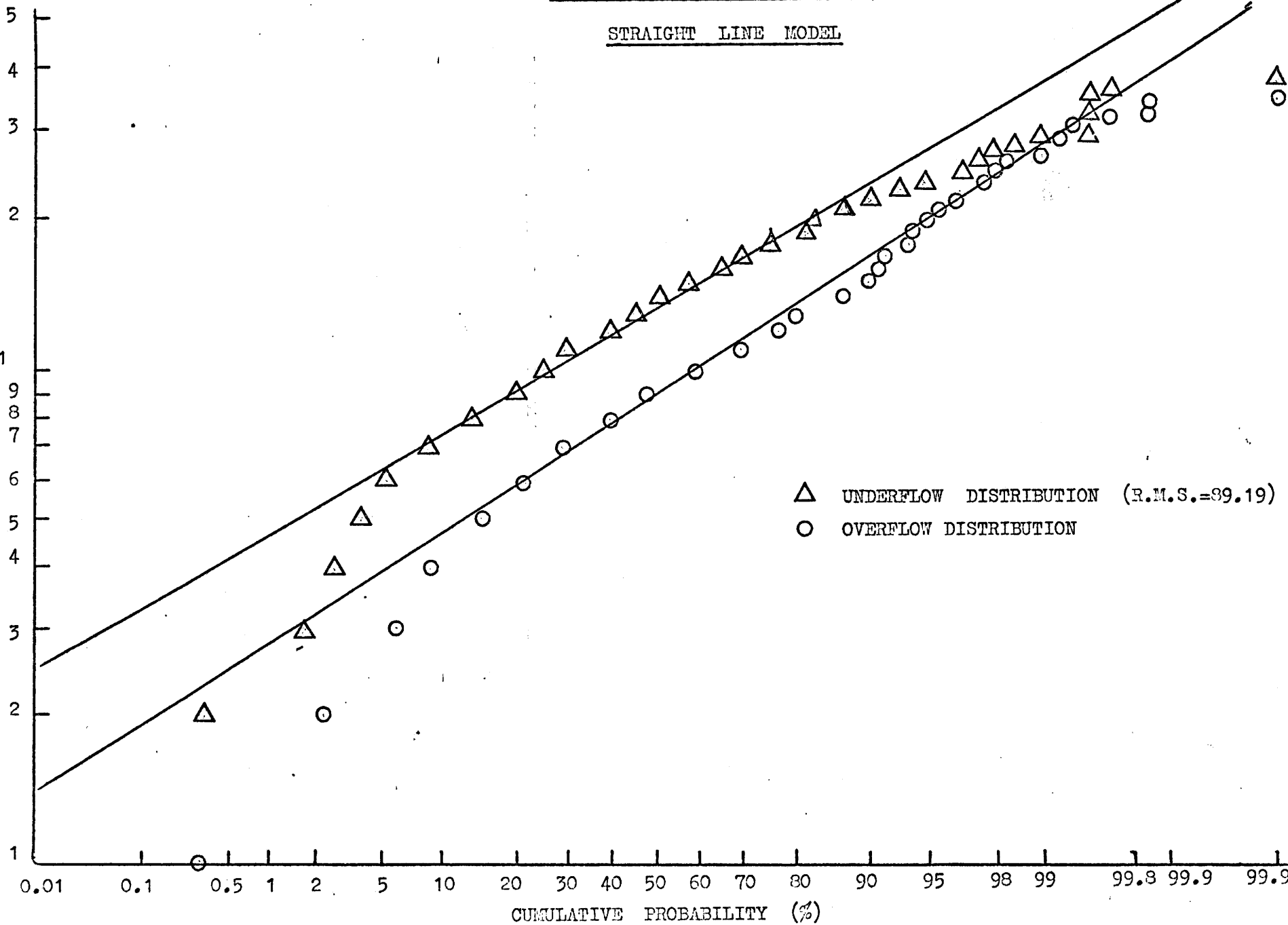
Figure 3-12 <u>LEAST SQUARES FIT FOR BEST</u>

<u>STRAIGHT LINE MODEL</u>

△ UNDERFLOW DISTRIBUTION (R.M.S.≈119.0)

O OVERFLOW DISTRIBUTION
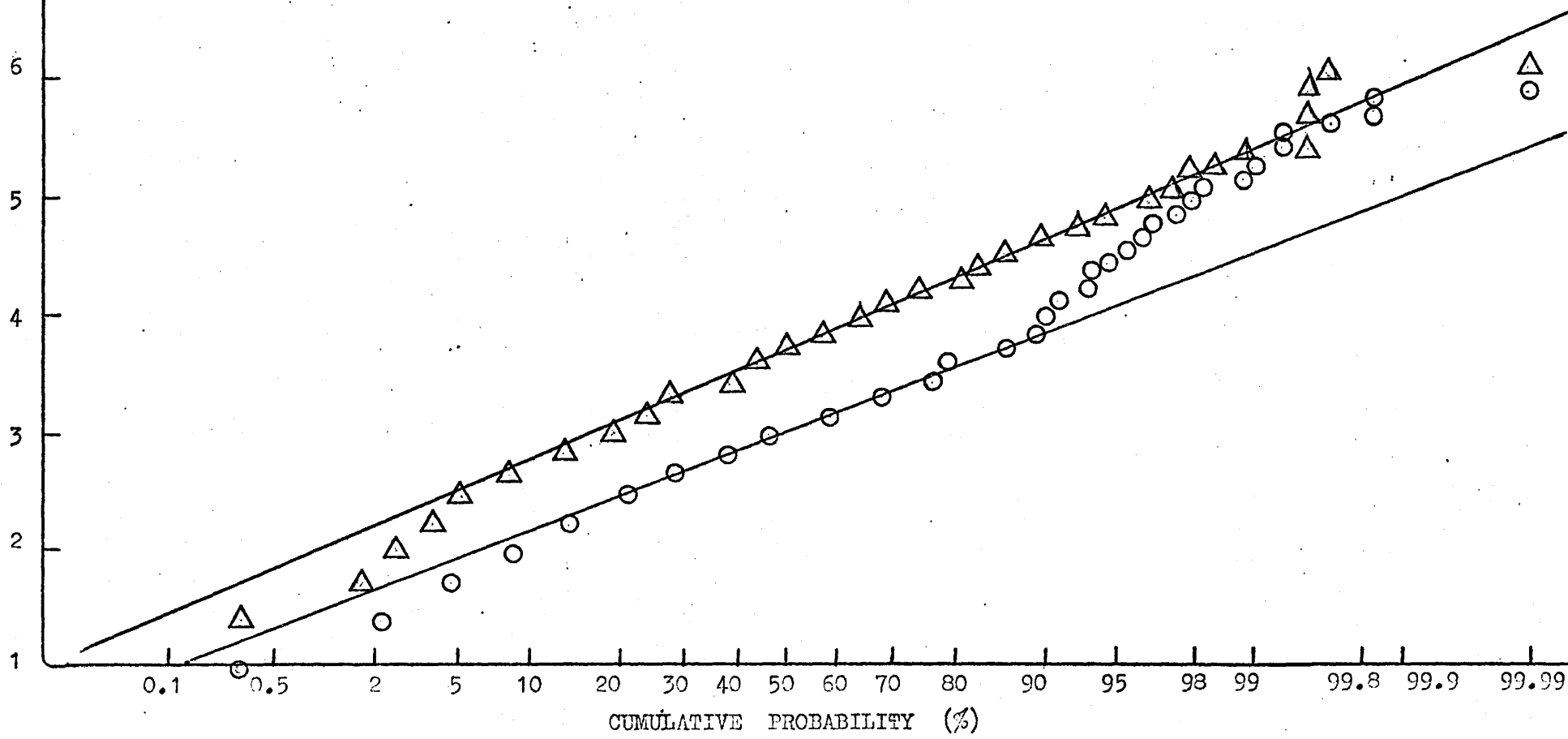
and is shown in Figure3-10. The distributions on this figure do
not appear normal since they have been transformed back from the log-
domain after the best fit was obtained. From this it appeared unwise
to use the usually employed log-normal distribution. Similar tests
were made on a square root normal distribution model with the polynomial,
understandably yielding a significantly lower R.M.S.

At this point it might be argued that the polynomial is not
necessarily the best model to use just because it can more closely
follow the experimental data. One could defend the log normal-model
or more complicated standard models, by stating that between the
20 to 80 % points the feed and underflow are very closely a straight
line and that the points deviate at each end because of errors in
sampling and in measurement are greatest in the tails of any distribution.
The dilemma could be solved if there was some easy method of determining
what total error is involved in identifying frequencies in the tails of
the distribution; this error can only be eludicated by some independent
means of determing the distribution which has the same relative accuracy
throughout all sizes (it is doubtful that any such procedure exists).
The chosen method would inevitably involve counting many more particles
than those counted in this study. Since this is a highly impractical
solution to the present problem, one must decide from the available
data which model to use.

The polynomial was chosen to represent the data because
all points in the tails of replicate samples deviated from a straight
line in roughly the same manner, and the only evidence that the log-
normal distribution is correct is that in many cases it is a convenient
model that appears to be close to that actually measured.

The error in describing the frequency of any diameter D_i

as F_i is assumed to be normally distributed, hence we calculate the variance of any observed frequency F_i as being

$$\frac{\sum_{i=1}^{x} (F_i - \overline{F})^2}{x - 1}$$

where x is the number of replicates measured and $\overline{F}$ is the mean of x frequencies.

The variances of the underflow and overflow distributions are shown in the previously mentioned Figure 3-8. Because the fitted curve of these variances indicates a varying variance-diameter relationship, we cannot justify fitting a non-weighted least squares polynomial. There are two solutions to this. One would be to use a weighted least squares, where $1/S^2$ is the weighting factor for each diameter in the data; the other is to search for a transform of the discrete data which has a roughly constant variance. The latter would allow the fitting of a non weighted polynomial to the transformed frequencies. The transformation method was adopted because of uncertainty in the variances themselves. Several transforms were tried, with log 10 giving the variance with almost no trends in the variance. Figure 3-13 shows the variance of the log 10 transformed data, which is certainly not constant, but has little tendency to either increase or decrease as diameter goes from 1 to 40 microns. We can then assume that the true variance is nearly constant and use a non-weighted least squares library program (LESQ) to fit the data.

A program listed in the appendix fits all underflow data,

66

Figure 3-13   Variance of Log. Transformed Discrete Frequencies
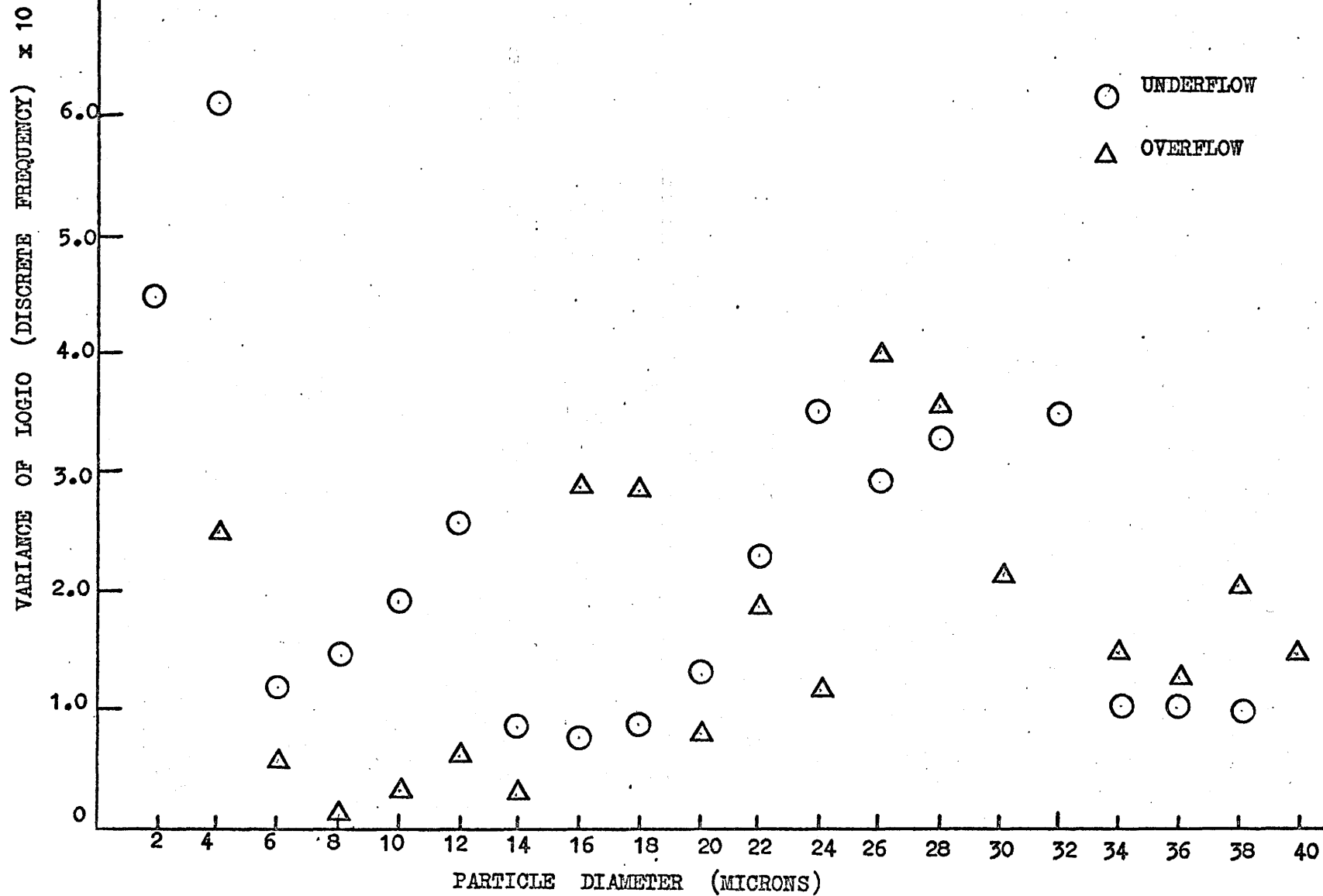
corrects all overflow data and fits it, and then solves the two curves (fig. 3-14)
for a first trial (Dp)50 value. However, this attempts to fit the
data over the whole range. From Figure 3-10 the fit is not
good in the region most critical for the calculation of (Dp)50
although the fit over the whole data range is acceptable. To improve
on the estimate of (Dp)50 the data are fitted just in the region
close to (Dp)50 as determined from the overall curve fit just outlined.

The best pair of curves representing the discrete data in
the region of (Dp)50 is likely given by some lower order polynomial
fitted to only a few points in the area of the first trial.

A second order polynomial was used to fit 6 points in the
area of the initial (Dp)50 solution. Since all initial solutions
lay between 5 and 10 microns, the fit need involve only the logarithms
of the frequencies of particle sizes 5 to 10 microns. The solutions
of this second log. fit were used as a best estimate of (Dp)50. The
results are shown in Figure 3-15. If all the determinations at a feed
flow rate of 10 USGPM are considered to represent several measurements
of the same (Dp)50 size, then (Dp)50 at this flow, is 6.77 microns
± 2.44 at 95% confidence limits.

The effect of feed flow rate on the (Dp)50 size cannot be
calculated since only two determinations were taken at a flow rate of
7 USGPM and the confidence of any such determinations is not high
enough.

There are many semi-empirical correlations for (Dp)50, all
off which assume an air core. The (Dp)50 size predicted by these for
the cyclone used in this study is shown in Table 3-8; a feed flow of
10 USGPM was used throughout.

Figure 3-14 TYPICAL SOLUTION OF Dp50 FROM DISTRIBUTIONS FITTED BY POLYNOMIALS
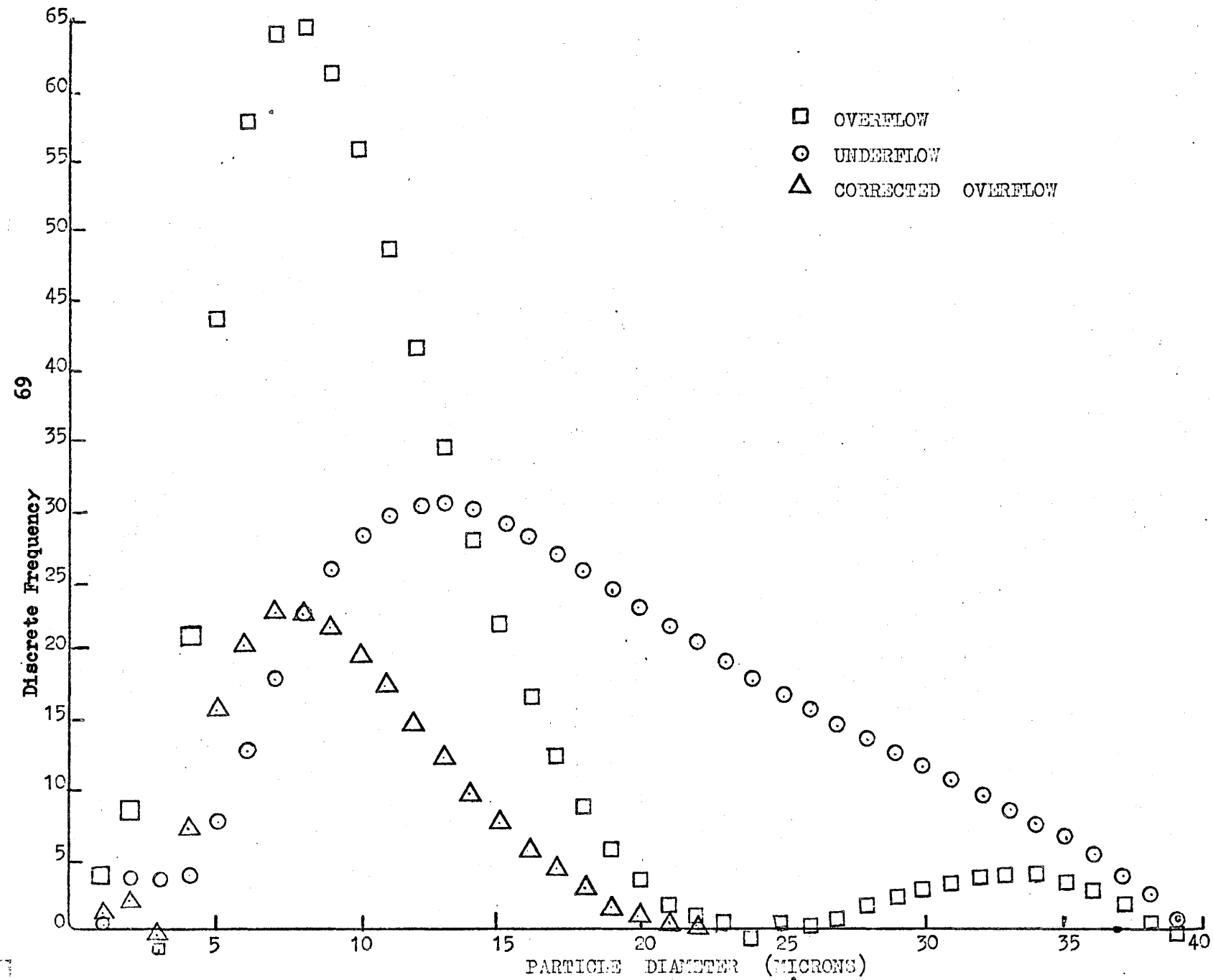
Figure 3-15

MAP OF THE (Dp)50 DIAMETER
REPORTED IN MICRONS
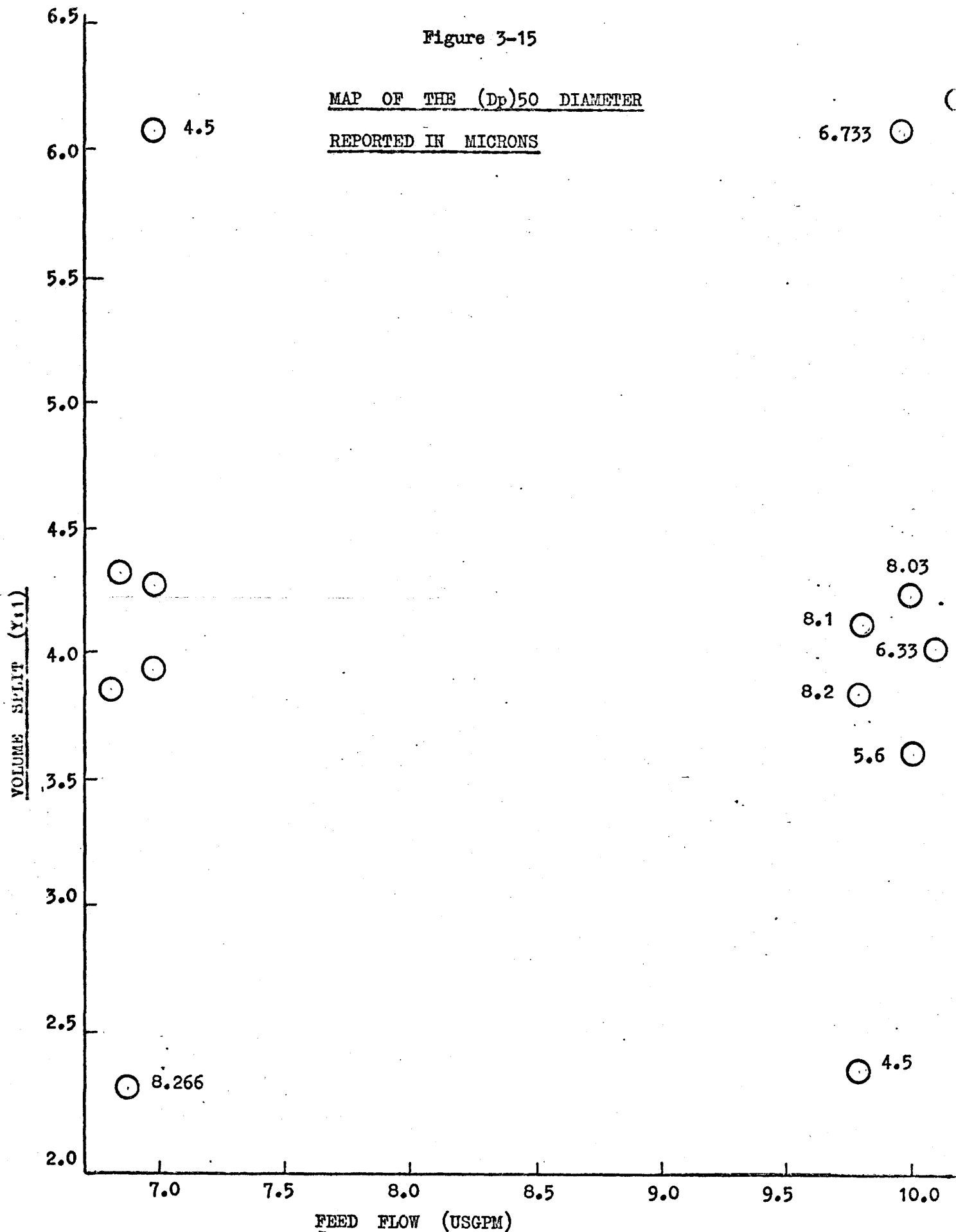
Table 3-10 *

(Dp)50 Size as Predicted by Various Correlations

Researcher	(Dp)50 microns
Dahlstrom	15.40
Yoshioka and Hotta	4.45
Haas	10.20
Rietema	7.60
Lilgé	2.80

* the units and detailed expressions are shown in Bradley (1965) pg. 85

As seen in Table 3-10 only Rietema's prediction of 7.6μ is valid for this study.

A reduced efficiency curve was generated from the polynomial
log. fits/a pair of underflow and overflow distributions. Mass balance
#8 was picked at random for this comparison with the results shown in
Figure 3-16. This figure shows that the separation in our study is
"less sharp" than that found by Yoshioka and Hotta (1955).

Figure 3-16

REDUCED EFFICIENCY CURVE

⊙ YOSHIOKA & HOTTA
△ THIS STUDY
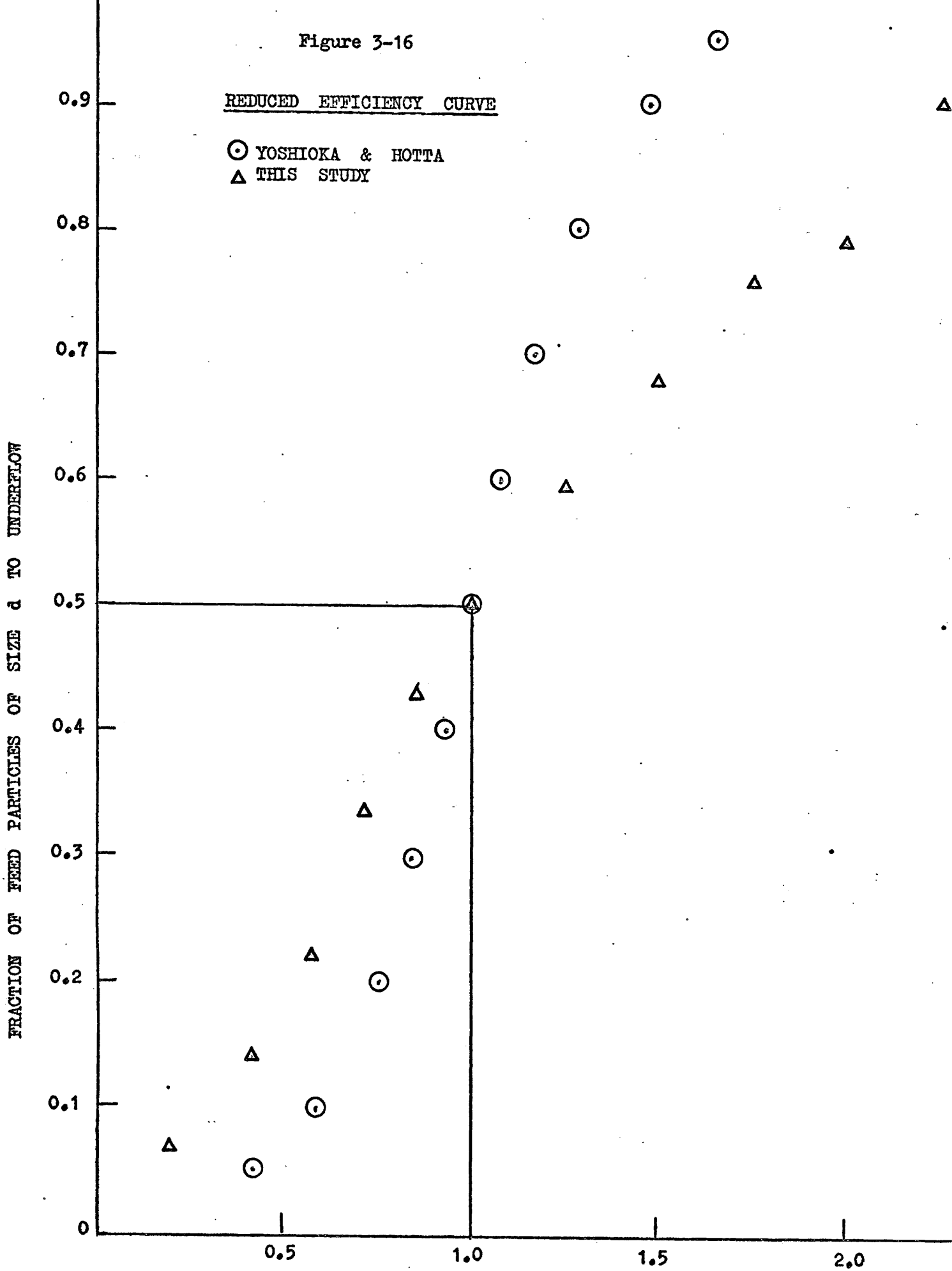
CHAPTER 4

CONCLUSIONS

4.1 New Conclusions

The following are "new conclusions", not discussed in other hydrocyclone literature.

1) The $(Dp)50$ diameter of spherical glass beads for the cyclone in this study, operating with no air core at a feed flow rate of 10 USGPM lies between the limits of 4.3 to 8.2 microns.

2) There is no measurable numerical difference in reporting energy loss as ΔPs or $\Delta E/M$ when similar units are used.

3) Rietema's $(Dp)50$ correlation, based on air core operation, appears to give the best approximation for the non-air core conditions at 10 USGPM used in this study.

4.2 Refute Conclusions

This section deals with the conclusions that are not in agreement with those found in the literature.

1) For the range of inlet Reynold's number studied (1.0×10^4 to 4.3×10^4), the pressure drop, ΔPs, is higher in this cyclone when operating without a core as compared to its operation with an air core. The two differ by a factor ranging from 1.0 to 1.65, depending on the feed flow rate. Rietema suggests this factor is about 2.0 over a range of feed flow rates.

2) The F factors found by Rietema (1961) are significantly lower than

those found in this study for similar conditions of cyclone geometry and inlet Reynolds number.

3) Yoshioka and Hotta's reduced efficiency curve (derived for a 6 inch cyclone operating with an air core) represents a "sharper classification" than was characteristic of the performance of this cyclone (without an air core).

4.3 Conclusions in Agreement with Cyclone Literature

1) The static pressure drop ΔP_s is almost independent of volume split.

2) The separation efficiency, as defined by Rietema and Tenghergen is a much stronger function of Volume split than feed flow rate for the range of variables studied. This was also found by Hsiang(1972).

3) The capacity ratio of $Q/F^{.47}$ found in this study is in good agreement with that of Dahlstrom who gives $Q/F^{.5}$. Indeed the exponent 0.5 falls within the errors in the present determination of the exponent.

REFERENCES

REFERENCES

BERG, S., "Studies on Particle Size Distribution", Danish Acad. of Tech. Science, Ingeniorvidenskabelige Skrifter, Copenhagen, 2, (1940).

BLAKE, P.D., F.Soc. Chem. Ind. 68, (1949), pg. 138.

BRADLEY, D., "A Theoretical Study of the Hydraulic Cyclone", The Industrial Chemist, Sept., (1958), pg. 478.

BRADLEY, D., "The Hydrocyclone", Permagon Press, copyright (1965).

BRADLEY, D. and PULLING, D.J., "Flow patterns in the Hydraulic Cyclone and Their Interpretation in Terms of Performance", Tran. Instn. Chem. Engrs., 37, (1959), pg. 34-45.

BURRILL, K.A., "The Effect of Drop Size Distribution, Feed Concentration, and Volume Split of the Separation of Two Immiscible Liquids in a Hydrocyclone", M. Eng. Thesis, McMaster University, Hamilton, May, (1967).

COHEN, E., et al, "Mineral Processing and Extractive Metallurgy", Instn. of Min. and Metallurgy, 75, (1966).

DAHLSTROM, D.A., "Cyclone Operating Factors and Capacities of Coal and Refuse Slurries", Min. Trans., Sept., (1949), pg. 331-344.

DRAPER, N.R. and SMITH, H., "Applied Regressional Analysis", John Wiley and Sons, New York, (1966).

HAAS, P.A., "Midget Hydrocyclones Remove Micron Particles", Chem. Engineering Progress, 53, (1957), pg. 204.

HSIANG, T.C.H. and WOODS, D.R., "The Influence of Design and Operating Variables on Energy Consumption and Separation Efficiency of a Hydrocyclic Concentrator", The Canadian Journal of Chem. Eng., 50, Oct. (1972).

REFERENCES

HERDAN, G., "Small Particle Statistics", Butterworths, (1960).

KELSALL, D.F., "A Study of the Motion of Solid Particles in a
Hydraulic Cyclone", Tran. Instn. Chem. Engrs., $\underline{30}$, (1952),
pg. 93-99.

KNOWLES, S.R., "Photographic Fluid Velocity Measurement in a
Hydrocyclone", M. Eng. Thesis, McMaster University,
Hamilton, (1971).

LILGE, E.O., "Hydrocyclone Fundamentals", Trans. Inst. Min. and
Metallurgy, $\underline{71}$, (1962), pg. 326-334.

OHASI, H., and MAEDA, S., "Motion of Water in a Hydrocyclone",
Chem. Eng., Japan, $\underline{22}$, (1958), pg. 203-204.

RIETEMA, K.A., "Performance and Design of Hydrocyclones", Parts I,
II, III, and IV, Chem. Eng. Science, $\underline{15}$, (1961).

RIETEMA, K. and TENGHERGEN (1961) in "Cyclones in Industry",
Rietema, K. and Verver, C.G., eds. Elsevier Publishing.

ROSSI, C. and BALDACCI, R., F. Applied Chem., $\underline{1}$, (1951), pg. 446.

YOSHIOKA, N. and HOTTA, Y., "Liquid Cyclone as Hydraulic Classifier",
Chem. Eng., Japan, $\underline{19}$, (1955), pg. 637.

APPENDIX

Detailed Method For Obtaining a Mass Balance

- fill reservoir with water to 20 gallon mark, a level at which complete mixing can be most easily obtained.
- weigh out and add enough particles to approximate a desired concentration.
- check resulting feed concentration by starting stirrers and taking replicate grab samples.
- adjust feed concentration if necessary.
- turn on feed pump
- adjust feed flow to roughly the desired rate
- adjust volume split be simultaineously changing overflow and underflow valves, and at the same time keeping the feed flow at about its proper final level
- when flows are approximately correct in all lines, the "bucket and stop watch" technique should be used to check overflow and underflow rates - the feed rate is assumed equal to their total. The feed rotameter was used to check this assumption.
- further readjustment will likely be necessary; as the system warms up
- when all flows are within reasonable limits of those desired, two 500 ml. grab samples are taken (approximately 15 seconds apart) from the underflow free discharge line
- immediately recheck the underflow rate to ensure that it is the same as it was just prior to taking the sample; if they are not different by more than 2% then the samples were assumed to be taken at a known flow rate and are said to be valid

Note: With this equipment the above procedure will usually need repeating many times since steady state is difficult to achieve.

- when a valid pair of underflow samples have been taken, two 1000 ml.

replicate overflow samples should be taken, followed by a check on the overflow rate. About ten seconds were allowed between replicate overflow samples for the reasons already discussed on underflow sampling.

- turn off feed motor and stirrers

- top up reservoir to 20 gallon mark.

Calculating Solids Concentrations

- allow 18 hours for solids to settle in the four graduated cylinders

- slowly syphon off most of the supernatant water without disturbing the sediment

- wash down the sides of the graduate with a few mls. from a wash bottle

- allow 30 minutes to resettle

- remove as much supernatant as possible with a pipette

- set up a funnel and 50 ml. graduated flask, quickly drain all the contents of the graduate through the funnel

- as this is being done a hard spray of water should be directed up into the cylinder to flush out all solids

- all solids should be in the 50 ml. flask by the time 30 mls. of liquid have been added (otherwise the stopper will contact solids shen it is applied)

- allow at least 18 hours for the 50 ml. flasks to come to thermal equilibrium in the balance room - two reference flasks with no solids should be made up

- fill all flasks as full as possible from a reservoir of small size

- one by one, place a designated stopper on its respective flask making sure it is applied in a consistant orientation and pushed straight on with exactly the same force (about 15 pounds)

- one of the two replicatereference flasks should be weighed first (to the fourth decimal of a gram), the other should be weighed after all other solids containing flasks have been measured
- a dustless type of wiper should be used to dry the exterior of each flask since any dust or moisture of any kind can significantly affect the accuracy
- each flask used in the above procedure must be weighed several times in succession when it contains only water. This will give it a reference weight to be compared with the two replicate calibration flasks.
- the solids concentrations can now be calculated as follows:

Sample Mass Balance Calculation

<u>Primary Data</u> (for Mass Balance #7)

$$\text{underflow} = \frac{2 \text{ gal. x } 60 \text{ seconds}}{85.5} = 1.404 \text{ USGPM}$$

$$\text{overflow} = 4 \text{ gal. x } 60 \text{ seconds} = \underline{8.56} \text{ USGPM}$$

$$\text{feed flow} = \text{total} = 9.964 \text{ USGPM}$$

$$V/S = \frac{8.56}{1.404} : 1 = 6.1 : 1$$

-two previous sample sets (#5 & 6) are missing
- reservoir level set to 20 U.S. gal.
- water temperature at time samples were taken = $27.2^{\circ}C$

Calibration

$$1\text{st replicate wt.} = 84.6990 \text{ grams}$$

$$2\text{nd replicate wt.} = \underline{84.6980} \text{ grams}$$

$$\text{average weight} = 84.6985 \text{ grams}$$

original reference weight = 84.6985 grams

Δ correction = -0.0720 grams

First underflow Calculation

first underflow flask U_1 = 98.4182

minus correction 00.0720

98.4902

subtract ref. wt. of U_1 flask 94.4018

wt. due to solids 4.0884 grams

actual wt. of solids (with S.G. = 2.65) $= 4.0884 \times \dfrac{2.65}{(2.65 - 1.00)}$

correct for only 502 mls. of sample being taken is

$$4.0884 \times \frac{2.65}{1.65} \times \frac{1000}{502} = \text{gms./litre}$$

correct for 14.6266 grams missing (for M.B. #5 & 6) from a total of 185.5 gms. which is total solids being used throughout.

$$4.0884 \times \frac{2.65}{1.65} \times \frac{1000}{502} \times \frac{185.5}{173.6} = 14{,}080 \text{ P.P.M.}$$

Second underflow Calculation

second underflow flask = 97.8602

minus correction 00.0720

97.9322

subtract ref. wt of U_2 flask 93.8516

wt. due to solids 4.0806

actual weight of solids $= 4.0806 \times \dfrac{2.65}{1.65}$

correct flor 198 mls. of samples

$$= 4.0806 \times \frac{2.65}{1.65} \times \frac{1000}{498} \text{ gms/litre}$$

correct for total solids missing   = 14.6266

$$\underline{4.0884}$$

18.7150 gms.

$$= 4.0806 \ \ x \ \frac{2.65}{1.65} \ x \ \frac{1000}{4.98} \ x \ \frac{185.5}{169.5}$$

correct for 498 mls. of water missing from 72.8 litres of total water.

$$= 4.0806 \ \ x \frac{2.65}{1.65} \ x \ \frac{1000}{4.98} \ x \ \frac{185.5}{169.5} \ x \ \frac{72.3}{72.8} \ = 14260 \ \text{P.P.M.}$$

average underflow concentration = 14,170 P.P.M.

First and Second Overflow Calculation

A similar set of calculations produce overflow distributions of 266 and 248 P.P.M. respectively. The average is 256 P.P.M.

Mass Balance

mass in	= conc. x flow	
	= 2,265 x 9.974	= 22,700 mg./min
mass out	1,4170 x 1.404	= 19,900 mg./min
plus	265 x 8.57	= 2,195 mg./min
		22,095 mg./min

error $= \dfrac{22,700 - 22,095}{22,700}$ = 2.64%

PREPARATION OF FEED SLURRY

Many micro-fine powders such as talcs and glass beads require special attention just to get them "wet". This is because their surface properties are often hydrophobic; also entrained air in such a finely divided void space is difficult to dislodge.

Herdan(1960) describes three methods of attacking the problem. These are; a) prolonged agitation

b) boiling the mixture for 20 minutes or longer

c) addition of medium to beads while both are under a partial vacuum.

The method used in the preparation of the 3M beads used in this study presented a fourth alternative. The procedure follows.

Water containing 3 - 4 mls. of liquid soap per litre, is slowly added to a dry container of beads. Here the soap diminishes the hydrophobic problem. The difficulty of air entrapment is solved by the gradual thickening of a water layer around each particle. At first, a thick paste is produced. This gradually changes into a slurry which should be left to stand for one week. Periodically the mixture should be agitated allowing any remaining air to escape.

OVERFLOW ROTAMETER CALIBRATION

(water at 20°C)

Y-axis: SCALE READING

X-axis: ACTUAL FLOW IN USGPM
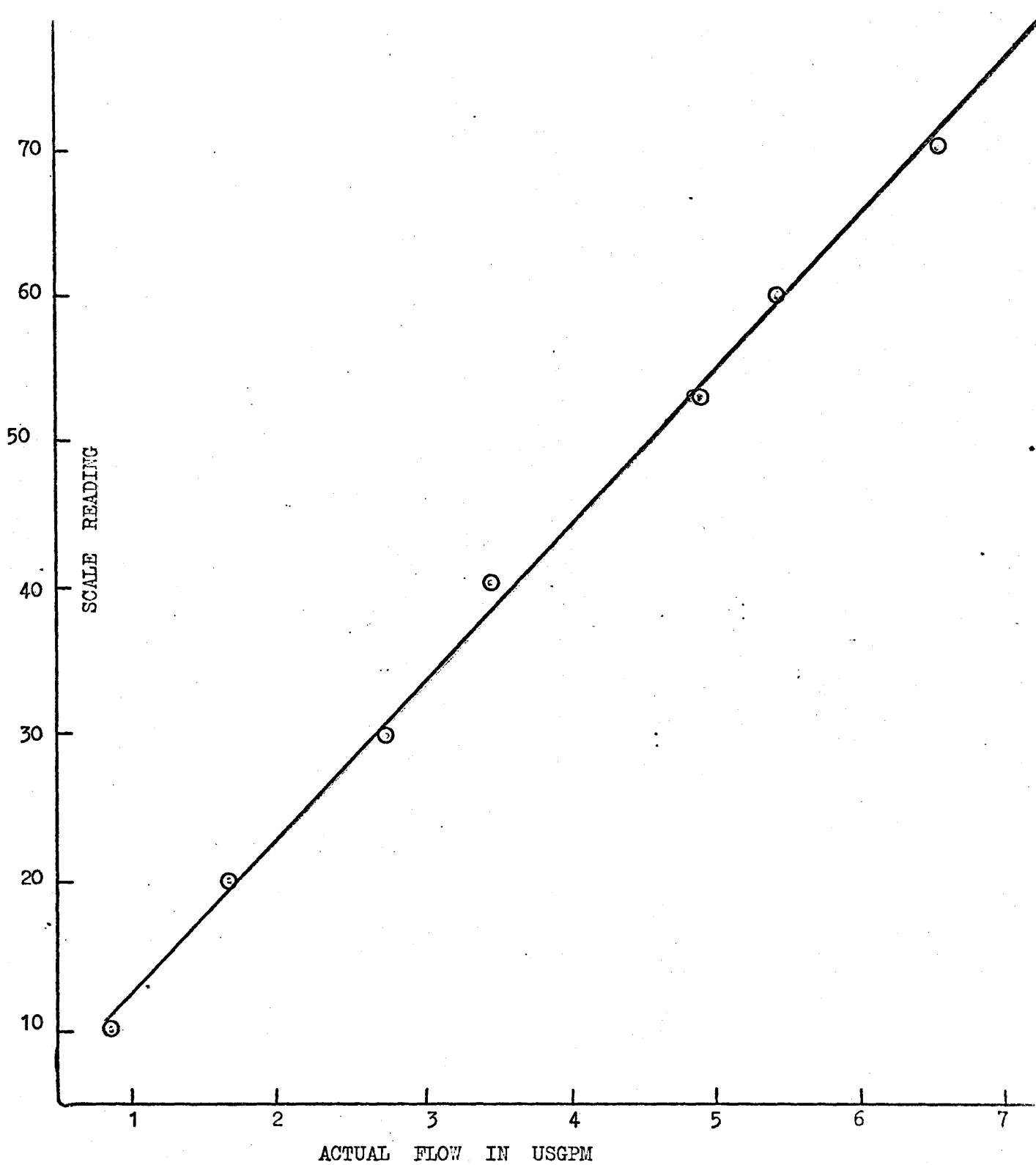
FEED ROTAMETER CALIBRATION

(water at 20°C)

A-8
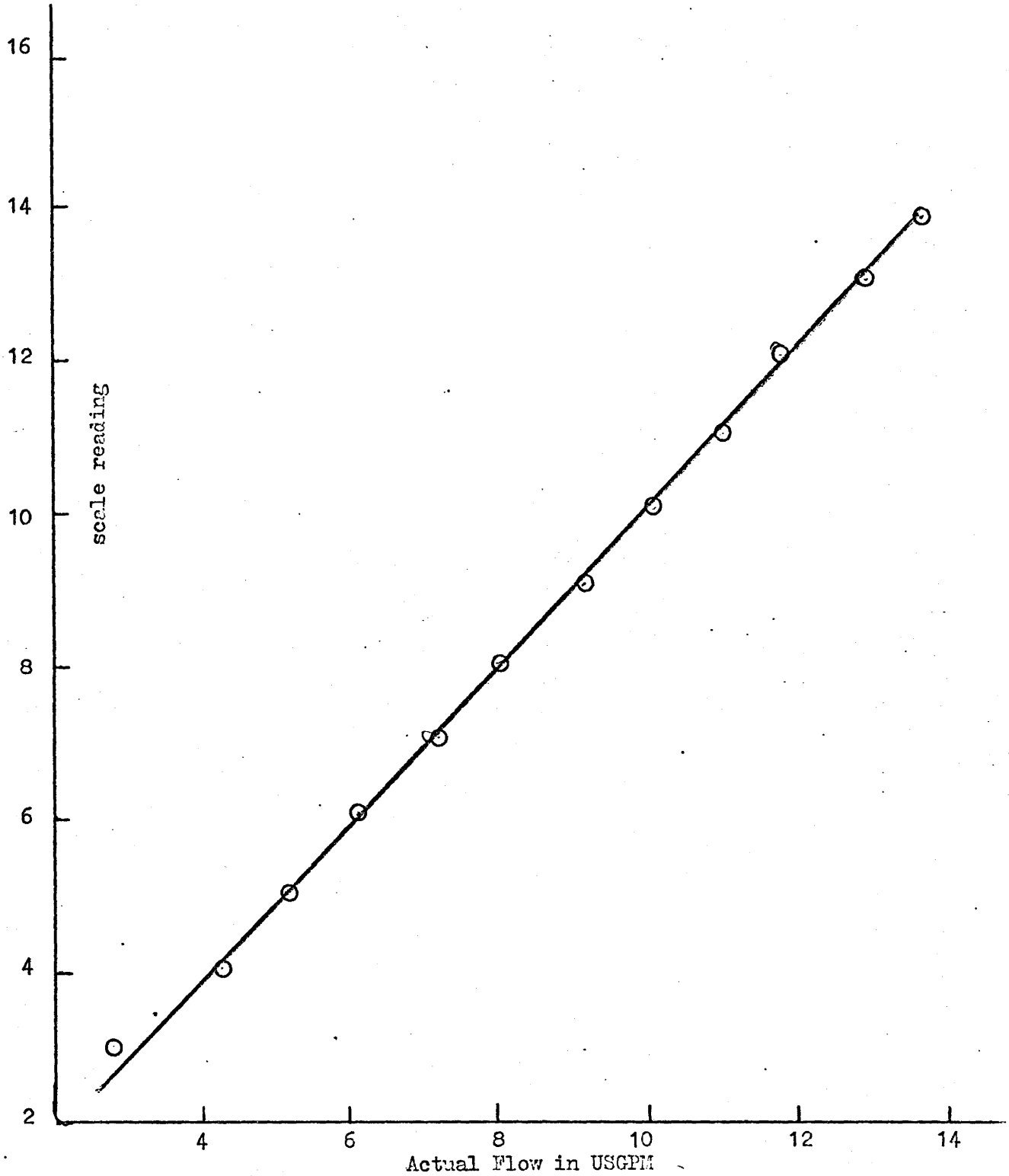
Figure A-1 .

Scale used to control overall magnification.

1 division = 10 microns
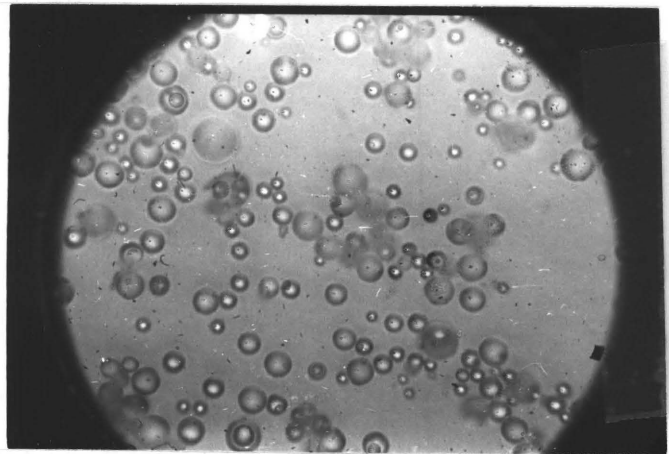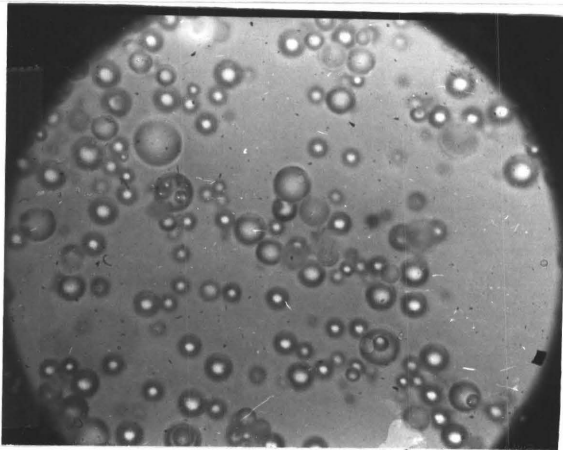
Figure A-2.

Photograph of Typical Underflow Distribution. Note the shallow depth of field indicated by comparing the two pictures.

Mass Balance on Cut Sizes

For a more detailed consistancy check, mass balances were performed on specific size ranges of particles for mass balance #8. This was done using each of two replicate feed distributions as shown below:

Mass in (of size "x to y" microns) = (Wt. % of size "x to y" in feed distribution)

    x (mass concentration of all solids in feed) x (feed flow)

Mass out (of size "x to y" microns) = the sum of underflow and overflow weights as found from a similar expression as above.

The percent error in these mass balances as expressed by

$$\frac{\text{mass out} - \text{mass in}}{\text{mass in}} \times 100$$

is given below in Table A-1.

Table A-1

Mass Balances on Cut Sizes

Cut Size microns	Percent Error Using Feed Distribution No. 2	Percent Error Using Feed Distribution No. 3
1 to 5	30	129
6 to 10	7	93
11 to 15	-13	36
16 to 20	-45	-26
21 to 25	-35	-19
26 to 30	+17	- 3
31 to 35	+6	- 8
36 to 40	+200	+25

PLOT OF CONDITIONS AT WHICH A NUMBERED

MASS BALANCE WAS PERFORMED

*indicates point at which distribution was taken

A-11
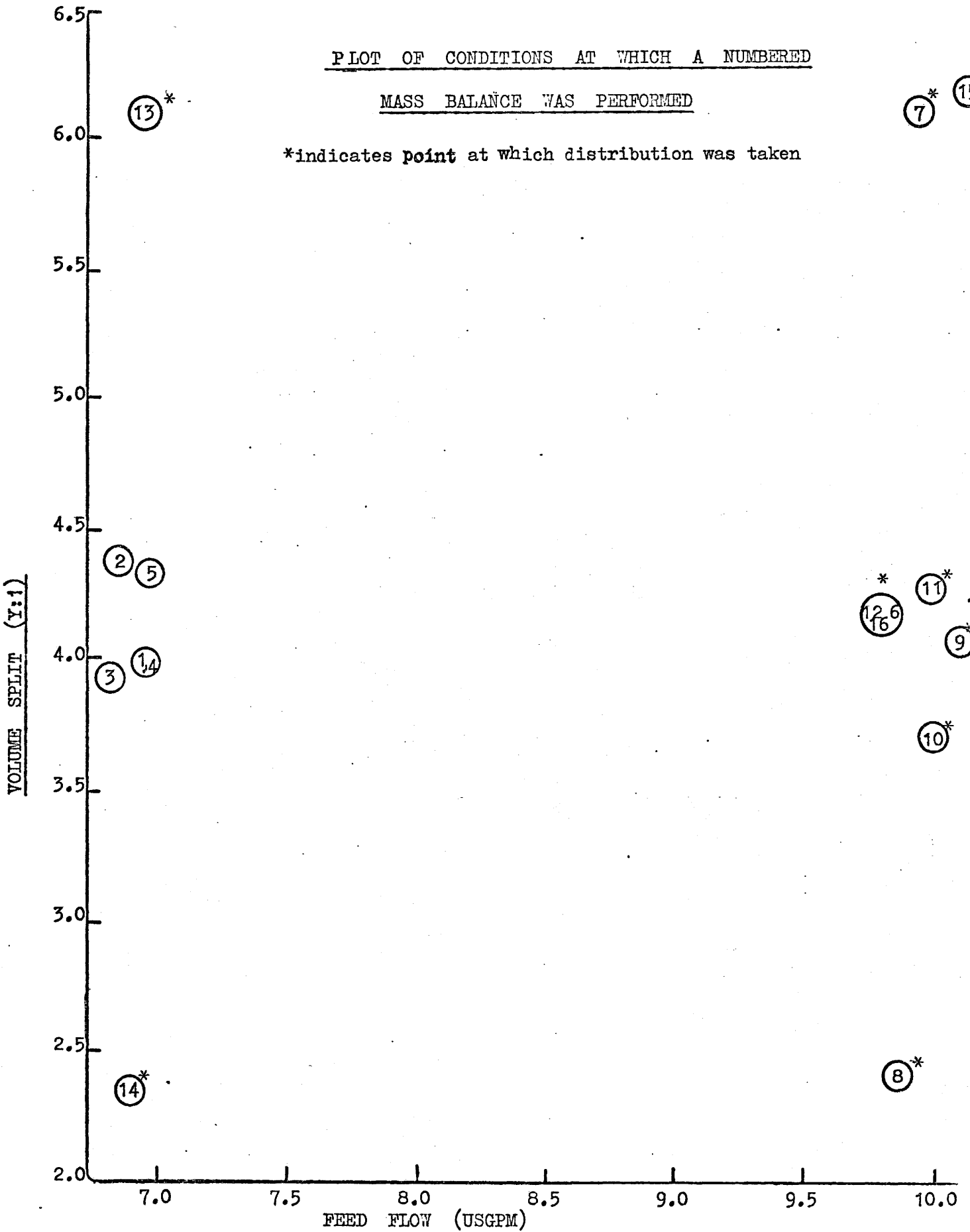
MAP OF OVERFLOW CONCENTRATIONS
UNDERFLOW

REPORTED AS P.P.M. (BY WEIGHT)

A-12

FIVE REPLICATE FEED DISTRIBUTIONS

reference line only

Dp (microns)

Cumulative Probability in %

A-13
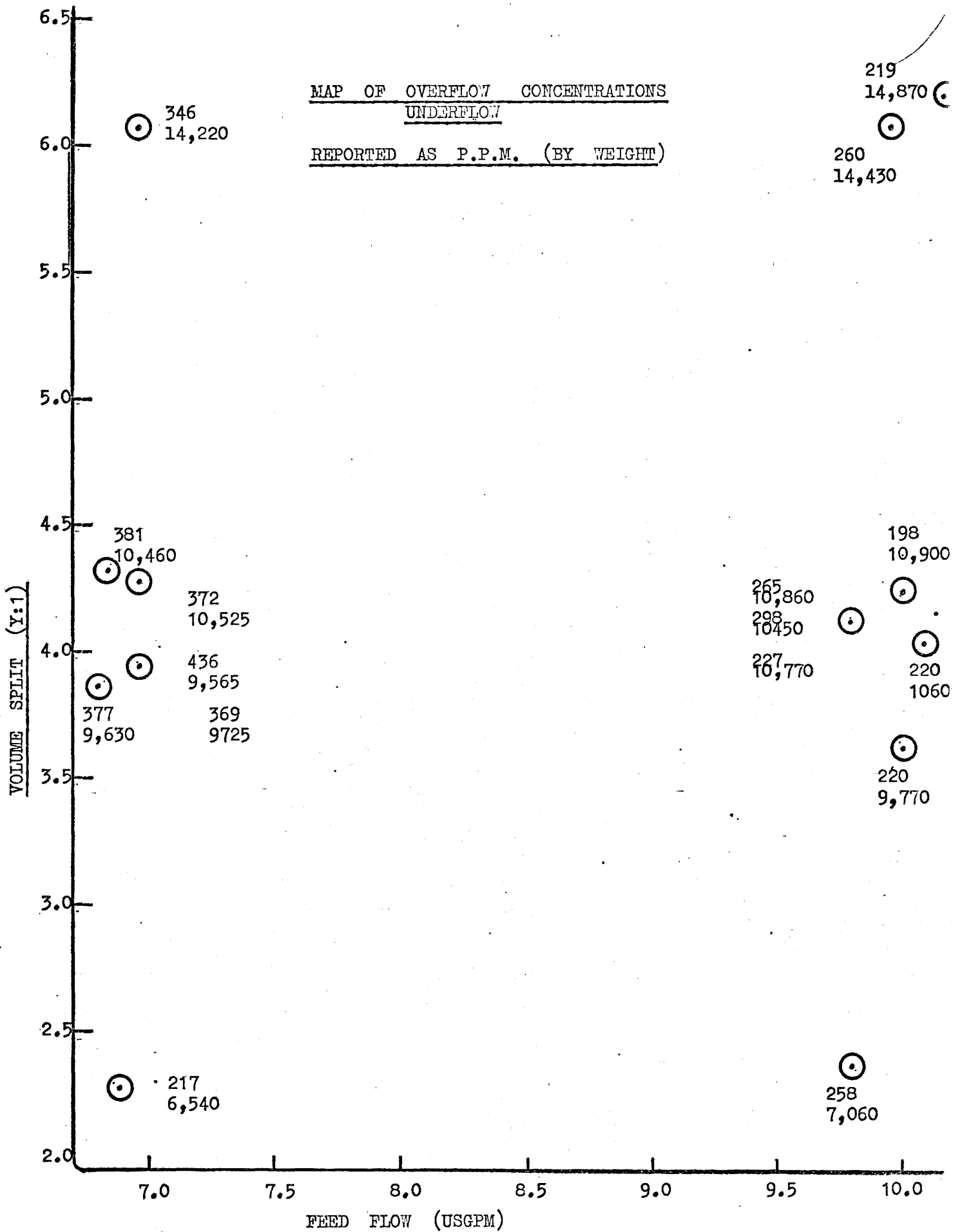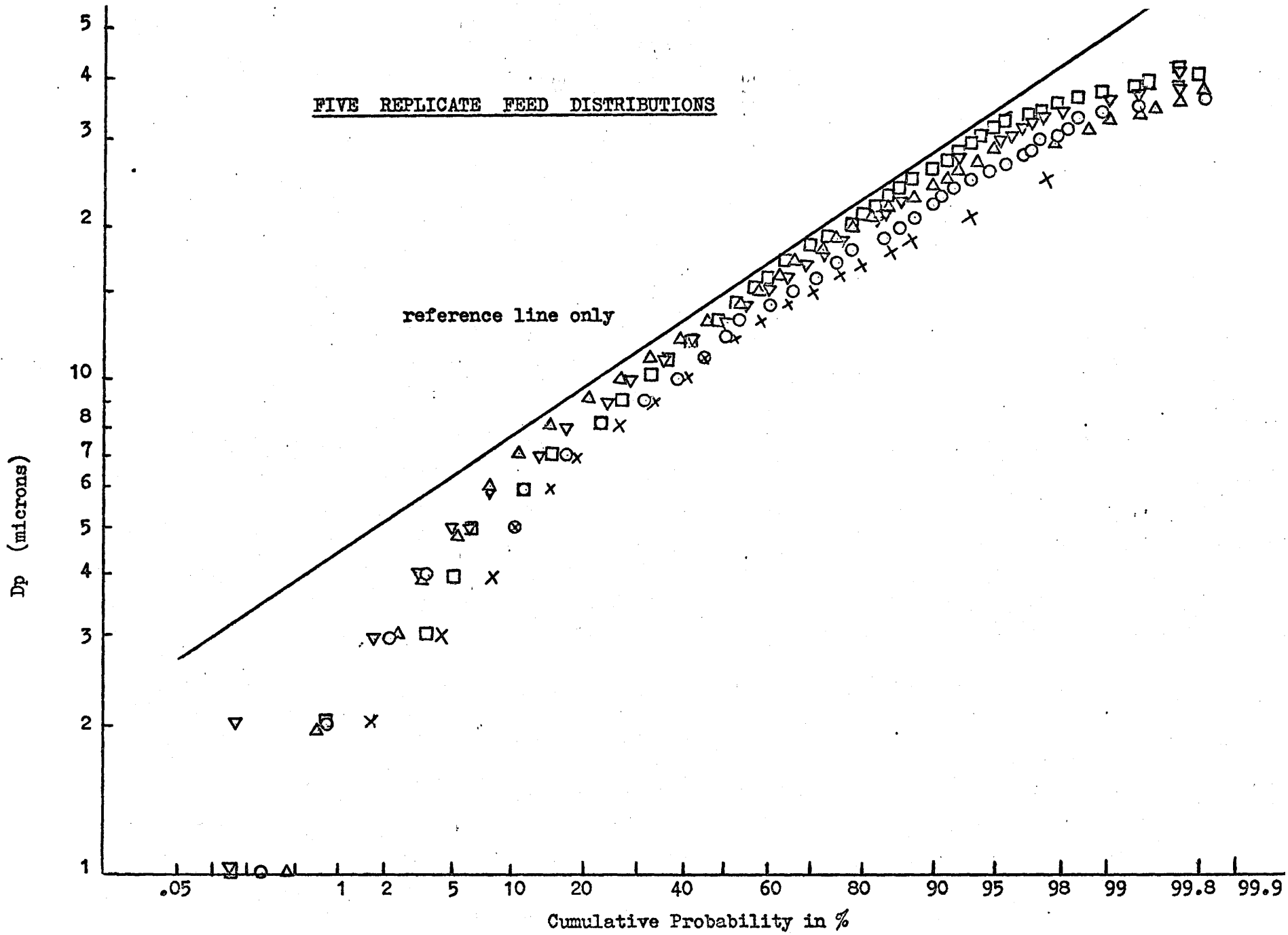
MANUFACTURERS OF MICROBEADS

Dow Chemical Company,
Sarnia, Ontario
Phone: 339-3131

Diagnostic Products — The Dow Chemical Company,
P.O. 1656, Indianapolis, Indiana 46206
Phone: 317-638-2521

Microbeads — Division of the Cataphote Corp.,
P.O. 2369, Jackson, Mississippi
Phone: 601-939-4631

Minnesota Mining and Manufacturing Company,
International Division,
St. Paul, Minnesota 55101
Phone: 612-733-2936

APPENDIX 2

COMPUTER PROGRAMS

```
FTN.
LGO.
'        6400 END OF RECORD
         PROGRAM TST (INPUT,OUTPUT,TAPE5=INPUT,TAPE6=OUTPUT)  (
C
C
C        PROGRAM FINDS MEAN AND VARIANCE FOR AN EXPERIMENTAL ZEISS DISTRIBUTION
C        THESE ARE USED TO ESTABLISH A GAUSSIAN MODEL FOR THAT DISTRIBUTION.
C        THE PROGRAM ALSO FINDS THE CONSTANT FOR THE MODEL THAT GIVES THE LOWES
C        R.M.S. BETWEEN THE MODEL AND THE EXPERIMENTAL FREQUENCIES
C
C
         DIMENSION YA(100),XA(100),XAT(100),YAC(100),YP(100)
         READ(5,1)NPTS
         FAC=SQRT(2.*3.1415)
C
         DO 100 I=1,NPTS
         XA(I)=FLOAT(I)
100      CONTINUE
C
C        CUMULATIVE VALUES READ IN YAC(I)
C
         READ(5,2) (YAC(I), I=1,NPTS)
C        YA HAS DISCRETE VALUES
         DO 101 I=2,NPTS
         YA(1)=YAC(1)
         J=I-1
         YA(I)=YAC(I)-YAC(J)
101      CONTINUE
         DO 500 LLL=1,4
C        DEGREE OF SKEWNESS CORRECTION
         DO 102 I=1,NPTS
         IF(LLL.EQ.1) XAT(I)=XA(I)
         IF(LLL.EQ.2)XAT(I)=SQRT(XA(I))
         IF(LLL.EQ.3)XAT(I)=ALOG10(XA(I))
         IF(LLL.EQ.4)XAT(I)=1./SQRT(XA(I))
102      CONTINUE
C
C        COMPUTE MEAN
         ADD=0.
         DO 103 I=1,NPTS
         ADD=ADD+YA(I)*XAT(I)
103      CONTINUF
         AMEAN=ADD/626.
C
C
C        VARIANCE CALCULATION
C
109      SS=0.
         DO 104 M=1,NPTS
         SS=SS+(ABS(XAT(M)-AMEAN))**2.
104      CONTINUE
         VAR=SS/(FLOAT(NPTS)-1.)
C
C        MODEL
C
         AINC=1.
         SSOLD=10000000000.
```

```
         F1=1.
         F3=2.*VAR**2.
400      DO300 I=1,NPTS
         F2=(ABS(XAT(I)-AMEAN))**2.
         F4=F2/F3
         YP(I)=F1/EXP(F4)
300      CONTINUE
C
C        FIND SS FOR MODEL
C
         SSM=0.
         DO 301 I=1,NPTS
         SSA=(ABS(YP(I)-YA(I)))**2.
         SSM=SSM+SSA
301      CONTINUE
         IF(SSM.LE.SSOLD) F1=F1+AINC
         IF(SSM.GT.SSOLD) GO TO 401
         SSOLD=SSM
         GO TO 400
401      F1=F1-AINC
         SSOLD=SSM
         AINC=AINC/10.
         IF(AINC.LT..01) GO TO 402
         GO TO 400
402      WRITE(6,427) AINC
         WRITE(6,25)
         DO 403 I=1,NPTS
         IF(I.EQ.1) WRITE(6,3) XA(I),XAT(I), YA(I),YP(I),AMEAN,VAR
         IF(I.GT.1) WRITE(6,3) XA(I),XAT(I), YA(I),YP(I)
403      CONTINUE
C
C        FIND SS
C
800      SUMS=0.
         DO106 I=1,NPTS
         SUMS=SUMS+(ABS(YP(I)-YA(I)))**2.
106      CONTINUE
         RMS=SUMS/(FLOAT(NPTS)-2.)
         WRITE(6,4)RMS
500      CONTINUE
         STOP
C
C
1        FORMAT(I5)
2        FORMAT(16F5.0)
3        FORMAT(1P6E15.3)
4        FORMAT(//1X,*MEAN SQ. = *,1PE10.3//)
25       FORMAT(/5X,*ACTUAL DIA.*,6X,*T. DIA*,10X,*Y ACT.*,8X,*Y PRED*,8X,*
        1D. MEAN*,8X,*VARIANCE*//)
427      FORMAT(/5X,*AINC. = *,1PE10.3)
         END
'          6400 END OF RECORD
    40
     1     5    24    32    41    73    94   142   174   211   234   272   308   336   366
   416   446   472   493   511   518   529   538   546   560   570   578   583   587   594
   606   608   612   615   618   621   622   624
'             END OF FILE
```

```
HPW2,T200.
FTN(R=3)
LGO.
.        6400 END OF RECORD
         PROGRAM TST (INPUT,OUTPUT,TAPE5=INPUT,TAPE6=OUTPUT)
C
C
C        .
C        PROGRAM CREATES DISCRETE DATA FROM CUMULATIVE  ZEISS COUNTER NOS. FOUN
C        ON LABELLED DATA CARDS - OVERFLOW AND UNDERFLOW POLYNOMIALS ARE FITTED
C        IN INCREASING ORDER FROM 1 TO M . THE FIT YIELDING THE LOWEST R.M.S. I
C        USED IN THE SOLUTOIN OF DP50. PROGRAM ALSO INTEGRATES THE TWO POLYNOMI
C        WITH THE X AXIS BEING CUBED.   THE UNDERFLOW POLY ISTHEN MODIFIED WITH
C        MASS BALANCE NOS. AND A THIRD CURVE IS FITTED (A REDUCED  OVERFLOW CUR
C        THIS REDUCED CURVE AND THE UNDERFLOW CURVE ARE SOLVED FOR INTERSECTION
C        WHOSE X AXIS VALUE IS DP50. LIMITS ON DP50 ARE FOUND BY HAVING THE PRO
C        SOLVE TWO ADDITIONAL SETS OF CURVES. THESE ARE THE UPPER AND LOWER CON
C        FIDENCE LIMIT CURVES GENERATED FROM PAR AMETERS FOUND IN ANOTHER PROGR
C
C
C        DEFINITIONS
C           NDATA=NO OF DATA SETS
C           NPTS=NO OF POIMTS IN A DATA SET
C           J=NO OF PTS USED FOR FIT
C           X=INDEPENDENT VARIABLE
C           Y=DEPENDENT VARIABLE
C           A=DUMMY ARRAY FOR SUBROUTINE
C           B=MATRIX OF COEFFICIENTS RETURNED IN ORDER B(0))....B(M)
C           JJJ=MAX ORDER POLY TO BE FIT TO N=J PTS
C           YY=FITTED VALUES OF DEP VARIABLE
C           W=DUMMY ARRAY
C           SIG=RESIDUAL SS
C           RMS=RES MEAN SQUARE
C           F=F TEST
C           DF=DEGREES OF FREEDOM =1,NN
C
         DIMENSION TITLE(10)
         DIMENSION EPO(50),EPU(50)
         DIMENSION C(200),WTFACT(5),BB(50),ERVAR(50)
         REAL MASS(5),Q(10)
         INTEGER D(200),E(200)
         DIMENSION T(200),Z(200),A(200),B(200),X(200),Y(200)
         DIMENSION YY(200),W(200)
         DIMENSION R(200)
         READ(5,1) NDATA
         READ(5,1) NPTS
         READ(5,9) (D(I), I=1,NPTS)
C
C
C        READ OVER AND UNDERFLOW PARAMETERS
C
         DO 805 K=1,11
         READ(5,801)  EPU(K)
805      CONTINUE
         DO 806 K=1,6
         READ(5,802)  EPO(K)
806      CONTINUE
         DO 200 I=1,NPTS
         C(I)=FLOAT(D(I))
         X(I)=         (C(I))
200      CONTINUE
```

```
       DO 102 KKK=1,NDATA
       READ(5,697) (TITLE(I), I=1,10)
       WRITE(6,698) (TITLE(I), I=1,10) .
       DO 302 NL=1,3
       IF(NL.FQ.3) GO TO 303
       READ(5,9) (E(I), I=1,NPTS)
       IF(NL.EQ.2) READ(5,30) (MASS(I), I=1,2)
C
C      TRANSFORM TO DISCRETE FREQ. VALUES
       Z(1)=ALOGIO(E(1))
       DO 222 L=2,NPTS
       J=L-1
       Z(L)=FLOAT(E(L)-E(J))
222    CONTINUE
C
C
C
C
       DO 100 I=1,NPTS
       Y(I)=Z(I)
  100 CONTINUE
       GO TO 304
303    DO 305 I=1,NPTS
       Y(I)=YY(I)*(WTFACT(1)/WTFACT(2))*(MASS(2)/MASS(1))
       CHANGE=(WTFACT(1)/WTFACT(2))*(MASS(2)/MASS(1))
305    CONTINUE
304    J=NPTS
       N=J
       DO 101 I=1,200
       A(I)=0.
       B(I)=0.
  101 CONTINUE
       JJJ=J-2
       WRITE(6,4)
       DO 302 M=1,7
       CALL LESQ(A,B,X,Y,M,N)
       MM=M+1
       YYY=0.
       DO 104 I=1,N
       YYY=YYY+Y(I)
       YY(I)=B(1)
       DO 104 L=2,MM
       LL=L-1
       W(I)=B(L)*(X(I))**LL
       YY(I)=YY(I)+W(I)
  104 CONTINUE
C
C      DUMMY ARRAY FOR UMDERFLOW POLY PARAMETERS
C         .
       IF(NL.EQ.1) GO TO 306
       GO TO 307
306    DO 308 I=1,8
       BB(I)=B(I)
308    CONTINUE
307    DINNY=100.
       SIG=0..
       YMEAN=YYY/FLOAT(N)
```

```
      DO 105 I=1,N
      SS=(Y(I)-YY(I))**2
      SIG=SIG+SS
  105 CONTINUE
      RMS=SIG/FLOAT(N-MM)
      R(1)=0.
      R(MM)=RMS
      NN=N-MM
      F=(R(M)*FLOAT(NN+1)-R(MM)*FLOAT(NN))/R(MM)
      WRITE(6,5) N,M,RMS,F,NN,LLL,(B(L),L=1,MM)
      IF(M.NE.7) GO TO 302
      DO 199 I=1,NPTS
      WRITE(6,198)C(I),X(I),Y(I),YY(I)
  199 CONTINUE
C
C     INTEGRATE MODEL WITH IND. VARIABLE CUBED
C
      SUM=0.
      DO 300 I=1,NPTS
      WIND=YY(I)*(C(I))**3
      SUM=SUM+WIND
  300 CONTINUE
      WTFACT(NL)=SUM
      WRITE(6,301) WTFACT(NL)
  301 FORMAT(//5X,*RELATIVE AREA OF WEIGHTED CURVE = *,1PE15.3)
      IF(NL.NE.3) GO TO 302
C
C     SOLVE FOR DP(50)
C
      CH=0.
      NN=1
      DIFFOLD=1000.
      DP501=1.
  316 AINC=1.
  315 AINC=AINC+.03333
C
      CORUN=0.
      COROV=0.
      DO 803 LNM=1,11
      LMN=LNM-1
      CORN=EPU(LNM)*AINC**LMN
      CORUN=CORUN+CORN
  803 CONTINUE
      DO 804 LNM=1,6
      LMN=LNM-1
      CORV=EPO(LNM)*AINC**LMN
      COROV=COROV+CORV
  804 CONTINUE
      IF(AINC.GT.7.9.AND.AINC.LT.8.0) WRITE(6,856) DIFF,CH,COROV,CORUN
  856 FORMAT(/5X,*DIFF = *,1PE10.3,* CH = *,1PE10.3,2X,*COROV = *,1PE10
     1.3,*CORUN = *,1PE10.3)
C
      IF(NN-2) 909,910,911
  911 COROV=-COROV
      CORUN=-CORUN
      GO TO 910
  909 COROV=0.
```

```
         CORUN=0.0
910      DIN=0.
         SUMOV=0.
         SUMUN=0.
         DO 310 I=1,8
         LA=I-1
         Y1=BB(I)*(ALOG10(AINC))**LA
         Y2=B(I)*(ALOG10(AINC))**LA
         SUMUN=SUMUN+Y1
         SUMOV=SUMOV+Y2
310      CONTINUE
         SUMOV=SUMOV-COROV*CHANGE
         SUMUN=SUMUN+CORUN
         DIFF=ABS(SUMUN-SUMOV)
         IF(DIFF.GT..5) CH=0.
         IF(DIFF.LT..5.AND.CH.EQ.0.) GO TO 319
         IF(AINC.GT.20.) GO TO 102
         DP50=AINC
         GO TO 315
319      IF(DIFFOLD-DIFF)344,320,445
445      DIFFOLD=DIFF
         GO TO 315
344      DP50=AINC-.03333
320      IF(NN-2) 321,919,922
321      WRITE(6,311) DP50
         DP501=DP50
         NN=NN+1
         GO TO 888
919      WRITE(6,980)DP50
         NN=NN+1
         GO TO 888
922      WRITE(6,920) DP50
         NN=NN+1
888      CH=1.
         DIFFOLD=1000.
         IF(NN.EQ.4) GO TO 807
         GO TO 316
807      NN=1
         AINC=DP501
         GO TO 315
302      CONTINUE
102      CONTINUE
         WRITE(6,851) DIFF,DIFFOLD,CH
851      FORMAT(/5X,*DIFF = *,1PE10.3,*DIFF = *,1PE10.3,*CH = *,1PE10.3)
852      FORMAT(/5X,1P5E15.3)
         WRITE(6,852) CHANGE,SUMUN,SUMOV,COROV,CORUN
         STOP
C
   1     FORMAT(I5)
   2     FORMAT(F9.4,F11.3)
   4     FORMAT(1H0,3X,4H PTS,1X,6H ORDER,2X,12H MEAN SQUARE,2X,16H F TEST
        1ON ORDER,4X,3H DF//)
   5     FORMAT(1H ,3X,I3,3X,I3,3X,E14.6,5X,F10.5,5X,I3,3X,I10,/1P8E14.6)
   6     FORMAT(E14.6,2I5,2E14.6)
   7     FORMAT(I1)
   8     FORMAT(5E14.6)
   9     FORMAT(16I5)
```

```
30      FORMAT(2F5.0)
198     FORMAT(  /5X,*D =*,1PE15.3,*   DT*,1PE15.3,5X,*YA*,1PE15.3,*   YP*
       1,1PE15.3,5X)
311     FORMAT(//5X,*DP(50) = *,1PE15.3)
697     FORMAT(10A8)
698     FORMAT(//20X,10A8//)
920     FORMAT(/5X,*LOWER LIMIT ON DP(50) = *,1PE10.3)
980     FORMAT(/5X,*UPPER LIMIT ON DP(50) = *,1PE10.3)
801     FORMAT(E13.6)
802     FORMAT(E13.6)
        END
'       6400 END OF RECORD
   11
   40
    1     2     3     4     5     6     7     8     9    10    11    12    13    14    15
   17    18    19    20    21    22    23    24    25    26    27    28    29    30    31
   33    34    35    36    37    38    39    40
-1.034890E+02
 1.257912E+02
-5.543615E+01
 1.214469E+01
-1.494021E+00
 1.112098E-01
-5.202629E-03
 1.539176E-04
-2.794738E-06
 2.842199E-08
-1.239425E-10
-3.970240E+00
 6.234257E+00
-7.484703E-01
 3.569067E-02
-7.681763E-04
 6.202204E-06
*********************** MASS BALANCE NO. 7 ***********************
    3     6     6    10    23    37    52    80   121   156   227   277   344   385   418
  488   514   538   558   561   570   573   581   592   595   603   607   610   613   616
  620   621   622   623   623   623   624   625
    2     3     7    21    37    70    97   171   236   318   386   439   473   496   513
  548   554   564   573   582   593   600   603   608   610   614   616   618   618   622
  622   623   623   623   624   625   625   625
19900 2195
*********************** MASS BALANCE NO. 8 ***********************
    4     7    12    17    35    57    86   121   179   234   289   339   364   393   424
  467   471   496   507   518   524   530   535   543   554   561   565   574   579   581
  591   592   600   603   608   610   611   616
    4    10    22    46    88   140   206   284   362   426   466   502   530   544   557
  580   596   596   598   602   606   612   615   616   619   621   621   622   623   623
  625   625   625   625   625   625   625   625
20800 1820
*********************** MASS BALANCE NO. 9 ***********************
    0     3     4     6    14    29    45    74   116   179   225   268   310   346   374
  423   442   473   486   506   517   533   542   558   566   572   581   590   597   603
  615   615   618   619   621   622   622   623
    8    19    53    74   121   179   241   308   368   422   454   484   506   521   534
  562   569   584   589   595   597   602   607   610   612   613   615   616   618   618
  622   622   622   623   624   624   624   625
```

21990 1620
```
*********************** MASS BALANCE NO. 10 ***********************
    1     8    16    23    34    46    66   112   145   182   214   252   294   335   376
  438   467   492   517   541   557   578   588   596   599   603   605   609   612   618
  621   622   623   624   625   625   625   625
    2     1    31    53    92   144   207   277   341   399   444   485   510   525   543
  571     8   591   597   604   607   614   616   617   620   621   622   623   623   623
  623   623   624   624   624   625   625   625
```
20920 1748
```
*********************** MASS BALANCE NO. 11 ***********************
    0     8    13    14    20    34    47    63    88   116   146   164   203   236   264
  318   354   383   411   429   457   481   496   512   528   536   557   569   575   589
  599   601   610   618   621   623   623   624
    3    15    36    59   102   157   236   319   376   430   470   504   527   549   557
  572   588   596   598   602   604   608   608   612   618   619   619   621   623   623
  623   623   624   624   625   625   625   625
```
21200 1615
```
*********************** MASS BALANCE NO. 12 ***********************
    0     3     8    12    21    26    44    69   101   129   158   192   221   249   271
  326   350   375   394   422   440   468   487   503   514   538   549   562   567   578
  597   602   611   615   618   620   621   622
    3     8    16    34    67   118   176   261   331   399   448   480   503   519   540
  569   574   581   590   595   595   602   604   607   608   612   613   615   616   617
  619   621   623   624   624   625   625   625
```
18830 1658
```
*********************** MASS BALANCE NO. 13 ***********************
    2    10    19    26    32    38    50    81   104   127   158   186   221   256   303
  364   392   420   442   466   484   506   524   536   548   555   563   570   579   586
  599   604   610   613   615   620   621   623
    0     1    10    24    49    82   132   202   267   337   374   417   451   485  ·513
  559   574   586   592   598   598   608   608   608   610   614   614   619   620   621
  622   622   622   622   625   625   625   625
```
12250 1812
```
*********************** MASS BALANCE NO. 14 ***********************
    0     6     8    13    18    35    55    91   129   165   194   233   267   290   322
  394   432   461   488   509   529   543   558   573   580   591   598   605   607   612
  616   619   621   623   623   624   624   625
    1     6    14    26    41    67   117   189   272   336   399   453   502   521   548
  592   601   606   610   613   615   618   621   623   625   628   628   632   632   632
  633   633   634   635   635   635   635   635
```
12770 1980
```
*********************** MASS BALANCE NO. 15 ***********************
          1     4     7    11    20    37    70    98   136   174   199   252   284   331
393   419   441   463   490   509   529   547   553   564   572   578   584   596   600   6
  609   610   613   615   620   623   623   625
    1     2     8    33    62   105   151   214   294   352   408   443   474   505   526
  550   560   572   577   584   588   597   599   605   607   612   615   618   619   620
  623   624   624   625   625   625   625   625
```
18400 1690
```
*********************** MASS BALANCE NO. 16 ***********************
          3     6    14    24    28    57    84   130   171   234   284   330   378   416
  477   499   512   529   544   551   560   569   575   582   591   598   601   607   611
  618   619   621   623   623   623   623   625
          2    11    29    58    99   157   228   313   374   425   469   500   519   534
  568   575   580   586   592   595   603   606   608   610   615   615   619   621   622
  624   624   624   624   625   625   625   625
```
16960 2030

```
*********************** MASS BALANCE NO. 17 ***********************
    0      5     11     18     23     33     52     71    101    138    186    226    268    305    348
  433    470    505    528    542    554    565    574    585    599    605    610    616    618    619
  623    624    625    625    625    625    625    625
    5     25     50     81    104    166    250    333    401    447    484    521    542    564    575
  594    600    602    605    608    610    614    615    616    619    621    621    622    623    624
  625    625    625    625    625    625    625    625
20000  1700
'            END OF FILE
```

CD TOT   0353